Aus dem Fachbereich Medizin

der Johann Wolfgang Goethe-Universität

Frankfurt am Main

betreut in der

Orthopädischen Universitätsklinik Friedrichsheim

Direktorin: Prof. Dr. Andrea Meurer

Functional roles of COMP and TSP-4 in articular cartilage and their relevance in osteoarthritis

Thesis

zur Erlangung des Grades Doctor of Philosophy (PhD)

des Fachbereichs Medizin

der Johann Wolfgang Goethe-Universität

Frankfurt am Main

vorgelegt von

Kathrin Maly

aus Schwarzach im Pongau

Frankfurt am Main, 2020

Dekan:	Prof. Dr. Stefan Zeuzem
Referentin:	Prof. Dr. Andrea Meurer
Korreferent:	Prof. Dr. Dirk Henrich

Tag der mündlichen Prüfung: 25.06.2021

Index

List of abbreviation

Abbreviation	Full name
°C	Degree Celsius
µl	Microlitre
µm	Micrometre
3D	Three-dimensional
ACAN	Aggrecan (gene)
ACI	Autologous chondrocyte implantation
ADAMT	a disintegrin and metalloproteinase with thrombospondin-1 domains
AEC	3-amino-9 ethylcarbazole
ALK	Activin receptor-like kinase
APS	Ammonium persulfate
BMP	Bone morphogenetic protein
bp	Base pairs
BSA	Bovine serum albumin
cDNA	Complementary deoxyribonucleic acid
Col	Collagen
COMP	Cartilage oligomeric matrix protein
CV	Column bed volume
DAPI	4’,6-diamidino-2-phenylindole
ddH2O	Double-distilled water
DMEM/F12	Dulbecco's modified eagle medium F12
DMSO	Dimethyl sulfoxide
DNA	Deoxyribonucleic acid
DPBS	Dubecco's phosphate buffered saline
e.g.	Exempli gratia (for example)
EBM	Endothelial cell basal media
EBNA	Epstein-Barr virus nuclear antigen
ECL	Enhanced chemiluminescence
ECM	Extracellular matrix
EDTA	Ethylenediaminetetraacetic acid
EdU	5-ethynyl-2’deoxyuridine
EGM	Endothelial cell growth media
ELISA	Enzyme-linked immunosorbent assay
ER	Endoplasmic reticulum
Erk	Extracellular signal-regulated kinase
EtOH	Ethanol
F	Fragment
FACIT	Fibril-associated collagens with interrupted triple helices
FBS	Fetal bovine serum
Fig	Figure
Fw	Forward
G	Grade

Abbreviation	Full name
GAG	Glycosaminoglycan
GAPDH	Glyceraldehyde-3-phosphate-dehydrogenase
GDF5	Growth differentiation factor 5
Geltrex™ matrix	Geltrex™ reduced growth factor basement membrane matrix
h	Hours
HC	Healthy control
HCl	Hydrochloric acid
HEK	Human embryonic kidney
HRP	Horseradish peroxidase
HUVEC	Human umbilical vein endothelial cells
IB	Immunoblot
IF	Immunofluorescence
Ig	Immunoglobulin
IHC	Immunohistochemistry
ka	Association rate
kd	Dissociation rate
kD	Dissociation constant
kDa	Kilo Dalton
KO	knock-out
l	Litre
LC	Loading control
LDH	Lactate dehydrogenase
M	Molar
mA	Milliampere
MACI	Matrix-associated autologous chondrocyte implantation
Matn3	Matrilin-3
max	Maximum
MED	Multiple epiphyseal dysplasia
MeOH	Methanol
mg	Milligram
min	Minimum
min	Minutes
ml	Millilitre
mM	Millimolar
mm	Millimetre
MMP	Matrix metalloproteinase
MSC	Mesenchymal stromal cell
n	Sample number
NEM	N-ethylmaleimide
ng	Nanogram
nm	Nanometre
nr	Number
OA	Osteoarthritis
OARSI	Osteoarthritis Research Society International
p	Phosphorylated

Abbreviation	Full name
P	Pentamer
Pat	Patient
PBS	Phosphate buffered saline
PBS-T	Phosphate buffered saline including Tween-20
PCR	Polymerase chain reaction
PDGF-BB	Platelet-derived growth factor-BB
pen/strep	Penicillin/streptomycin
PET	Polyethylene terephthalate
PG	Proteoglycan
PMSF	Phenylmethylsulphonyl fluoride
PSACH	Pseudoachondroplasia
PVDF	Polyvinylidene fluoride
qPCR	Quantitative polymerase chain reaction
rDNase	Recombinant deoxyribonuclease
Rev	Reverse
RNA	Ribonucleic acid
RNase	Ribonuclease
rpm	Revolutions per minute
RT	Room temperature
RU	Response units
SDS	Sodium dodecyl sulphate
SDS-PAGE	Sodium dodecyl sulphate polyacrylamide gel electrophoresis
sec	Second
SK	Skim milk
Smad	Small mothers against decapentaplegic homologs
SPR	Surface plasmon resonance
Supp	Supplement
TBE	Tris-borate-EDTA
TBS	Tris-buffered saline
TBS-T	Tris-buffered saline including Tween-20
TEMED	Tetramethylethylenediamine
Temp	Temperature
TGF-β1	Transforming growth factor β1
THBS4	Thrombospondin-4 (gene)
Tris	Tris(hydroxymethyl)aminomethane
TSP	Thrombospondin
TSP-4	Thrombospondin-4 (protein)
U	Units
UV	Ultraviolet
V	Volt
Vector Lab	Vector Laboratories
VEGF	Vascular endothelial growth factor
Vol	Volume
VWA	von Willebrand factor A-like
VWC	von Willebrand factor type C

Abstract

Osteoarthritis (OA) is a slowly progressing disease, resulting in the degradation of cartilage and the loss of joint functionality. The cartilage extracellular matrix (ECM) is degraded and undergoes remodelling in OA progression. Chondrocytes start to express degrading proteases but are also reactivated and synthesise ECM proteins. The spectrum of these newly synthesised proteins and their involvement in OA specific processes and cartilage repair is hardly investigated.

Human articular cartilage obtained from OA patients undergoing knee replacement surgery was evaluated according to the OARSI histopathology grading system. Healthy, non-OA cartilage samples were used as controls. The expression and distribution of thrombospondin-4 (TSP-4) and the closely related COMP were analysed on the gene level by PCR and on the protein level by immunohistology and immunoblot assays. The potential of TSP-4 as a diagnostic marker was evaluated by immunoblot assays, using serum samples from OA patients and healthy individuals. The functional role of both proteins was further investigated in *in vitro* studies using chondrocytes isolated from femoral condyles of healthy pigs. The effect of COMP and TSP-4 on chondrocyte migration and attachment was investigated via transwell and attachment assays, respectively. Moreover, the potential of COMP and TSP-4 to modulate the chondrocyte phenotype by inducing gene expression, ECM protein synthesis and matrix formation was investigated by immunofluorescence staining and qPCR. The activation of cartilage relevant signalling pathways was investigated by immunoblot assays.

These results showed for the first time the presence of TSP-4 in articular cartilage. Its amount dramatically increased in OA compared to healthy cartilage and correlated positively with OA severity. In healthy cartilage TSP-4 was primarily found in the superficial zone while it was wider distributed in the middle and deeper zones of OA cartilage. The amount of specific TSP-4 fragments was increased in sera of OA patients compared to healthy controls, indicating a potential to serve as an OA biomarker. COMP was ubiquitously expressed in healthy cartilage but degraded in early as well as re-expressed in late-stage OA. The overall protein levels between OA severity grades were comparable. Contrary to TSP-4, COMP was localised primarily in the upper zone of OA cartilage, in particular in areas with severe damage. COMP could attract chondrocytes

and facilitated their attachment, while TSP-4 did not affect these processes. COMP and TSP-4 were generally weak inducers of gene expression, although both could induce *COL2A1* and TSP-4 additionally *COL12A1* and *ACAN* after 6 h. Correlating data were obtained on the protein level: COMP and TSP-4 promoted the synthesis and matrix formation of collagen II, collagen IX, collagen XII and proteoglycans. In parallel, both proteins suppressed chondrocyte hypertrophy and dedifferentiation by reducing collagen X and collagen I. By analysing the effect of COMP and TSP-4 on intracellular signalling, both proteins induced Erk1/2 phosphorylation and TSP-4 could further promote Smad2/3 signalling induced by TGF-β1. None of the two proteins had a direct or modulatory effect on Smad1/5/9 dependent signalling.

In summary, COMP and TSP-4 contribute to ECM maintenance and repair by inducing the expression of essential ECM proteins and suppressing chondrocyte dedifferentiation. These effects might be mediated by Erk1/2 phosphorylation. The presented data demonstrate an important functional role of COMP and TSP-4 in both healthy and OA cartilage and provide a basis for further studies on their potential in clinical applications for OA diagnosis and treatment.

Zusammenfassung

Osteoarthrose (OA) ist eine langsam fortschreitende Krankheit, die zum Abbau des artikulären Knorpels und somit zum Verlust der Gelenkfunktionalität führt. Die extrazelluläre Matrix (ECM) des Knorpels wird abgebaut und im Verlauf der OA neu organisiert. Chondrozyten beginnen abbauende Proteasen zu exprimieren, werden aber auch reaktiviert und synthetisieren ECM-Proteine. Das Spektrum dieser neu synthetisierten Proteine und ihre Beteiligung an OA spezifischen Prozessen und an der Knorpelreparatur ist jedoch kaum untersucht.

Humaner Gelenkknorpel von OA-Patienten, die sich einer Kniegelenkersatzoperation unterzogen haben, wurde gesammelt und nach dem histopathologischen Bewertungssystem der OARSI eingestuft. Gesunder Nicht-OA-Knorpel wurde als Kontrolle verwendet. Die Expression und Verteilung von Thrombospondin-4 (TSP-4) und des eng verwandten Proteins COMP wurden auf Genebene mittels PCR und auf Proteinebene mittels immunhistologischer Färbungen und Immunoblots analysiert. Das Potenzial von TSP-4 als diagnostischer Marker wurde mittels Immunoblots unter Verwendung von Serumproben von OA-Patienten und gesunden Personen evaluiert. Die funktionelle Rolle beider Proteine wurde in *in-vitro* Studien mit Chondrozyten, welche aus den Femurkondylen gesunder Schweine isolierten wurden im Detail untersucht. Die Wirkung von COMP und TSP-4 auf die Migration und Adhäsion von Chondrozyten wurde mittels Transwell- bzw. Attachment-Assays untersucht. Darüber hinaus wurde die Wirkung von COMP und TSP-4 auf den Phänotyp der Chondrozyten untersucht, indem die Induktion der Genexpression, die Synthese von ECM-Proteinen und die Matrixbildung mittels Immunfluoreszenzfärbung und qPCR analysiert wurden. Die Aktivierung knorpelrelevanter Signalwege wurde mittels Immunoblots untersucht.

Diese Ergebnisse zeigen zum ersten Mal die Expression und Verteilung von TSP-4 im Gelenkknorpel. Im Vergleich zu gesundem Knorpel nahm die Menge an TSP-4 in OA dramatisch zu und korrelierte positiv mit dem OA-Schweregrad. TSP-4 wurde im gesunden Knorpel vor allem in der oberflächlichen Zone gefunden, während es bei OA überwiegend in den mittleren und tieferen Zonen des Knorpels lokalisiert war. Die Menge an spezifischen TSP-4 Fragmenten war in den Seren von OA-Patienten erhöht im

Vergleich zu gesunden Kontrollen, was auf ein Potenzial als OA Biomarker hinweist. COMP war im gesunden Knorpel ubiquitär exprimiert, wurde aber im Frühstadium der OA abgebaut und im Spätstadium neu synthetisiert. Der Gesamtproteingehalt zwischen den einzelnen OA-Schweregraden war allerdings vergleichbar. Im Gegensatz zu TSP-4 wurde COMP vor allem in der oberen Zone des OA-Knorpels lokalisiert, insbesondere in schwer geschädigten Bereichen. COMP konnte Chondrozyten anlocken und ihre Adhäsion unterstützen, während TSP-4 diese Prozesse nicht beeinflusste. COMP und TSP-4 waren generell schwache Induktoren der Genexpression, trotzdem konnten beide nach 6 h *COL2A1*, und TSP-4 zusätzlich *COL12A1* und *ACAN* induzieren. Des Weiteren verstärkten beide Proteine die Synthese und Matrixbildung von Kollagen II, Kollagen IX, Kollagen XII und Proteoglykanen. Gleichzeitig inhibierten beide Proteine die Hypertrophie und Chondrozyten Dedifferenzierung durch Reduktion von Kollagen X und Kollagen I. Die Analyse der intrazellulären Signalwege ergab, dass COMP und TSP-4 direkt die Erk1/2 Phosphorylierung induzieren konnten und TSP-4 zusätzlich das durch TGF-β1 induzierte Smad2/3 Signal verstärkte. Keines der beiden Proteine hatte eine direkte oder modulierende Wirkung auf den Smad1/5/9 Signalweg.

Zusammenfassend lässt sich feststellen, dass COMP und TSP-4 zur Erhaltung und Reparatur der ECM beitragen, indem sie die Expression essenzieller ECM-Proteine induzieren und die Chondrozyten Dedifferenzierung unterdrücken. Diese Effekte könnten durch Erk1/2 Phosphorylierung vermittelt werden. Die vorliegenden Daten zeigen eine wichtige funktionelle Rolle von COMP und TSP-4 sowohl in gesundem als auch in OA-Knorpel. Zudem liefern die Daten eine Grundlage für weitere Studien über das Potenzial von COMP und TSP-4 in der klinischen Anwendung, speziell im Bereich OA Diagnose und Therapie.

1. Introduction

1.1. Knee joint

Walking, standing or sitting are natural daily activities, depending on the functionality of joints. The human knee joint (**Fig.1.1**) is formed, by two long-bones: femur and tibia. The joint forming surfaces of these bones are covered, with articular cartilage, a connective tissue with specific biomechanical properties providing a smooth and lubricated surface. Two menisci are placed, between the tibia and femur acting as a shock absorber. The joint is surrounded by a capsule and the ligaments, supporting the stability and proper alignment. The joint capsule seals the joint and its inner surface is lined with the synovial membrane, which produces the synovial fluid, an oily substance, filling the joint cavity and acting as a lubricant as well as a nutrition source. The knee joint is a complex biological and mechanical system requiring a functional interplay of all components. Although, it is the integrity of articular cartilage, which provides the biomechanical properties, crucial for an unrestricted movement. (1, 2)

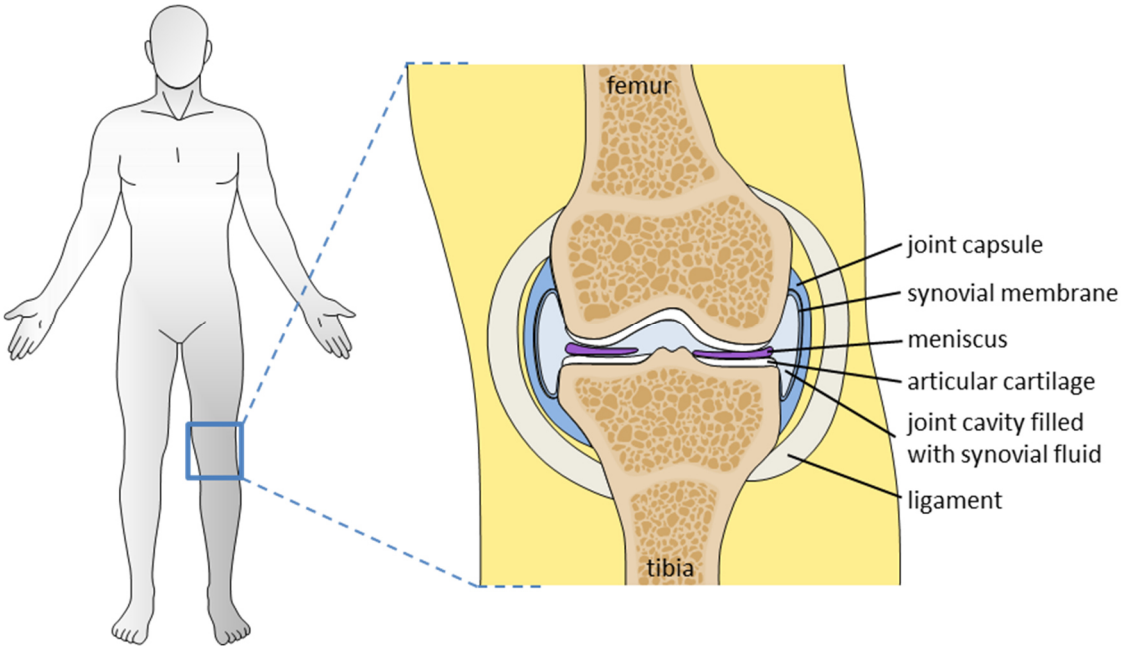

Figure 1.1. Anatomy of the knee joint
Schematic drawing of the knee joint. Tibia and femur are covered with articular cartilage and separated by the meniscus. A capsule, lined with the synovial membrane at its inner surface, is sealing the joint, which cavity is filled with the synovial fluid. Ligaments are connecting the bones and support the stability of the joint.

1.2. Articular cartilage

Depending on the biochemical composition, three cartilage types can be distinguished: (I) elastic cartilage, containing high amounts of elastin and is present in tissues requiring high flexibility, as the outer ear. (II) fibrocartilage, such as in the meniscus and (III) articular cartilage in knee joints. All types are similar in their architecture and mainly differ in the composition of their extracellular matrix (ECM). Fibrocartilage is sometimes naturally formed as repair tissue, replacing damaged articular cartilage, but lacks its mechanical qualities and cannot properly fulfil its functions. (1)

Healthy articular cartilage is a thin layer covering the ends of long-bones and absorbs the mechanical force during movement to allow a painless and frictionless motion. It consists of one cell type called chondrocyte which is surrounded by an extremely dense ECM. Chondrocytes represent only 1-5 % of the cartilage volume (3), meaning the other ~95 % are ECM. Four zones, hierarchically organised, form the complex cartilage tissue from the surface to the bone: the superficial zone, the transitional zone, the deep zone and the calcified zone (**Fig.1.2.A, B**). The deep and the calcified zone are separated by the tidemark, a faint line, dividing non-mineralised (deep zone) and mineralised (calcified zone) cartilage. The deep zone also serves as a barrier of vascularisation, separating cartilage from bone (4). The calcified zone is a transitional tissue of moderate stiffness, connecting the flexible cartilage with the stiff bone (5). Besides the cartilage zones, also the ECM can be subdivided, depending on the localisation around chondrocytes. The area directly surrounding the chondrocyte is called the pericellular matrix, which is directly surrounded by the territorial matrix. The area between the territorial matrices of chondrocytes is named the interterritorial matrix (**Fig.1.2.C**). (3, 5)

Depending on the cartilage zone the chondrocyte shape as well as the orientation of collagen fibrils, one of the main components of the ECM, are changing (**Fig.1.2.B**). In the superficial zone, chondrocytes are flattened and collagens aligned in parallel to the cartilage surface, resisting the enormous pressure resulting from articulation to protect the underlying cartilage layers. Due to the parallel orientation of collagen fibrils the superficial zone is the stiffest (6). The chondrocyte shape becomes more spherical and

the orientation changes from obliquely in the intermediate zone to a column alignment, perpendicularly to the cartilage surface in the deep zone (5). The collagen fibrils in the underlying zones are randomly oriented in the intermediate zone and aligned perpendicularly to the cartilage surface in the deep zone to provide a less stiff matrix (6).

Articular cartilage in a healthy state is not vascularised, has no neural or lymphatic tissue and chondrocytes depend on the nutrition diffusing from the synovial fluid (5). Due to these limitations, articular cartilage has a poor regeneration capacity and is made to last a life long compared to other self-repairing tissues, such as bone (7).

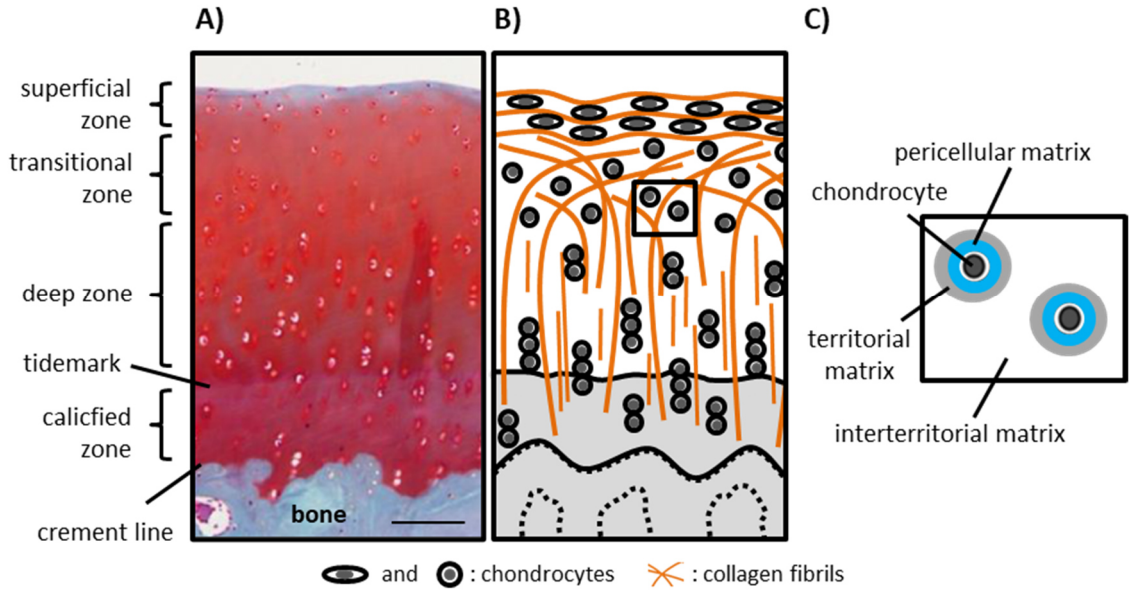

Figure 1.2. Structure and organisation of articular cartilage
A) Safranin-O staining of proteoglycans in bovine articular cartilage. Schematic drawing hierarchical zones (**B**) and the ECM areas around the chondrocytes **(C**) in articular cartilage, with indicated chondrocytes and collagens. (modified from (8, 9)).

1.3. Chondrocytes

Chondrocytes origin from mesenchymal stromal cells, which condensate, proliferate and differentiate during cartilage development, first to prechondrogenic cells and then into mature chondrocytes forming the articular cartilage ECM. (10)

Chondrocytes are very specialised cells, varying in size and shape depending on the cartilage zone they are residing in (**Fig.1.2.B**). The superficial zone consists of a high density of flattened chondrocytes, while the number decreases in deeper zones. Chondrocytes in the calcified zone are distinguishable from the ones in the other

cartilage zones by its hypertrophic phenotype. These hypertrophic chondrocytes are low in number and produce specific ECM molecules to provide moderate stiffness and enable an anchorage of the cartilage to the subchondral bone (5). After articular cartilage formation, chondrocytes become quiescent and mediate ECM maintenance in a low turnover state (11) by modulating the balance between catabolic and anabolic processes. Intracellular signalling pathways can be induced by ECM components, by a so-called cell-matrix interaction. Growth factors are polypeptides, stored in the ECM and released under certain conditions to interact with the cell surface, regulating processes like cell proliferation, growth, differentiation and survival. (12, 13)

An altered interaction with ECM components or the response to unusual mechanical forces can affect the chondrocyte phenotype, which becomes unstable (14). In this manner, chondrocytes might become dedifferentiated (15), implicating an elongated fibroblast-like shape (16) and the production of ECM proteins, characteristic for fibrocartilage. Chondrocytes can also differentiate to a hypertrophic phenotype (17), contributing to the extension of the calcified zone. The integrity of the ECM as well as its functionality is depending on the stability of the chondrocyte phenotype. Despite, the severe consequences of abnormal chondrocyte interactions, it is not known which ECM components can influence the phenotype stability.

1.4. Extracellular matrix

The ECM is a highly complex network composed of water (65-80 % of the wet weight), collagens (10-20 % of the wet weight), proteoglycans (10-20 % of the wet weight), hyaluronic acid and to a minor part of non-collagenous proteins (3) (**Fig.1.3**). The water is the source of several inorganic ions, is involved in the distribution of nutrients and lubrication while the solid components provide stiffness (collagens), elasticity (proteoglycan) and stability of the network (5).

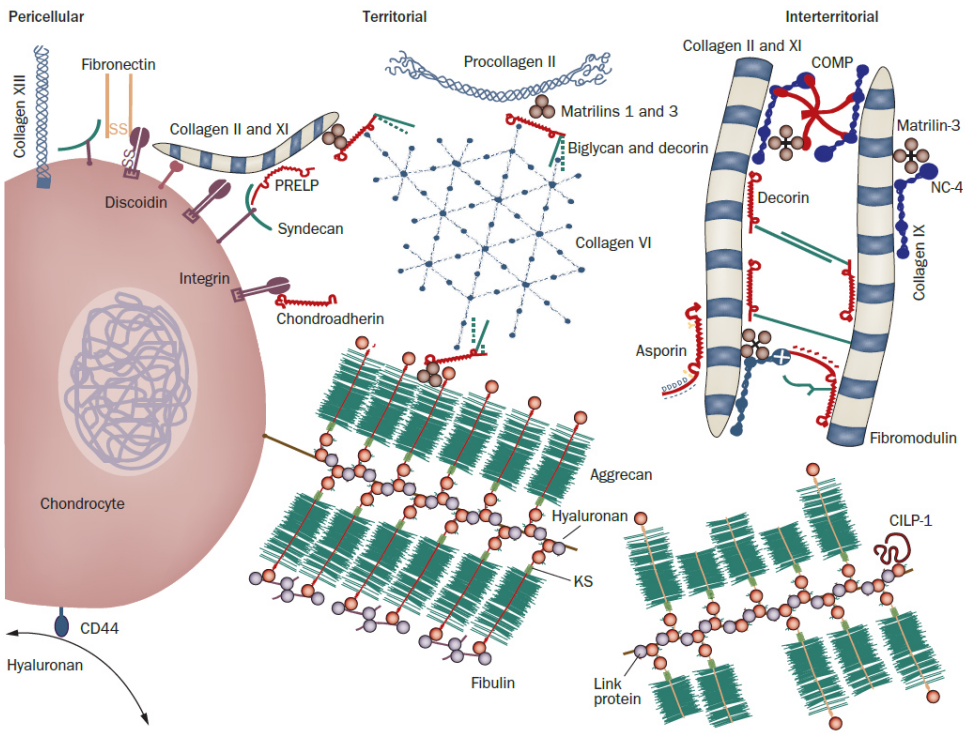

Figure 1.3. The extracellular matrix of articular cartilage
Schematic drawing, showing the composition and organisation of the extracellular matrix in the pericellular, territorial and interterritorial matrix. The figure was modified from (18).

The collagen superfamily consists of 28 members (19) distributed in different tissues of the body. Collagen II, III, IV, VI, IX, X, XI, XII, XIV, XVI and XXII (20, 21) could be detected in healthy articular cartilage, whereas collagen II is with 90-95 % the most abundant collagen, essential for the physical properties of the collagen network. The collagen family can be subdivided into fibril forming collagens, like collagen II, III and XI as well as fibril-associated collagens with interrupted triple helices (FACIT), like collagen IX, XII, XIV, XVI and XXII (20, 22). The FACIT-collagens are located on the surface of fibrillar collagens, connecting collagens and other matrix components with each other. Furthermore, network forming collagen IV, VI and X can be distinguished (20). In the following paragraphs only collagens with relevance for this project are discussed in more detail. The characteristic collagen II fibril in articular cartilage is a heteropolymer, consisting of collagen XI, forming the core and collagen IX, covalently bound to the surface (22). These fibrils can further fuse to thicker and stronger collagen fibrils, located in the interterritorial region, although without collagen IX (23, 24). This structure makes collagens less flexible but provides tensile strength, to sustain the forces during articulation (3) and protection from degrading enzymes. Collagens in the articular

cartilage are stable proteins (25) with a half-life of more than 100 years (26, 27), indicating their enormous resilience.

The expression and distribution of different collagen types in the ECM varies, depending on the cartilage zone and their function. The tightly packed collagen fibrils in articular cartilage mainly consist of collagen II and IX (6), especially in the territorial matrix (23). Collagen IX is covalently crosslinked with collagen II and resides on its surface. Studies on mice with inactivated *Col9a1* gene developed joint diseases, with cartilage degradation in their life (28, 29), indicating a matrix stabilising role. A closer look on newborns revealed an abnormal growth plate morphology with shortened and broader long-bones, which could be attenuated in adult mice (30). The absence of collagen IX resulted in collagen II fibrils, larger in diameter and altered in composition (31, 32). Due to its presence in thin collagen fibrils and its binding capacity to other matrix proteins, like matrilin-3 (31), collagen IX has an important role in collagen fibril organisation and matrix stabilisation. In human articular cartilage, the amount of collagen IX reduces with age (33), which might be associated with age depending cartilage degradation.

Structurally similar to collagen IX is collagen XII (34), which is non-covalently linked to fibrillar collagens (21). Collagen XII is predominantly expressed in the superficial layer of articular cartilage and associated with collagen II fibrils, indicating a zonal specific distribution (35). Collagen XII can interact with other ECM components, like fibromodulin, decorin (36), the cartilage oligomeric matrix protein (COMP) (37) and collagen I (38). Its function in articular cartilage is still not fully elucidated, although studies demonstrate a possible involvement in articular cartilage formation and suggest a contribution in matrix stabilisation and organisation (35, 39).

Collagen X is involved in calcification processes, matrix stiffness and associated with vascular invasion (40-43). It is the characteristic marker of hypertrophic chondrocytes and is only expressed, in the calcified zone of the cartilage (44).

Collagen I is usually not expressed in healthy articular cartilage but can be synthesised as an attempt of repair. The generated fibrocartilage has high amounts of collagen I but contains barely collagen II. In contrast to collagen II, collagen I is less glycosylated and has fewer hydroxylysyl residues, resulting in a weaker interaction with proteoglycans and altered biomechanical properties (45).

Proteoglycans are a family of glycoconjugates and all members have a similar structure, composed of a core protein with at least one glycosaminoglycan (GAG) side chain (46, 47). Two groups of proteoglycans can be distinguished: the large aggregating hyaluronic acid binding proteoglycans, like aggrecan and small proteoglycans with a core composed of leucine-rich repeats (48). The cartilage ECM contains both, with aggrecan as the most abundant proteoglycan, which is still synthesised in the mature ECM (49). The GAGs give the aggrecan its negative charge and the ability to bind water molecules, leading to hydration and swelling pressure to resist compressive forces (46). Proteoglycans can also interact with collagens and non-collagenous matrix proteins to crosslink and stabilise the ECM (50-52). The smaller proteoglycan decorin is interacting with collagen II and is assumed to be involved in fibril organisation (49). In that manner decorin is mainly found in the interterritorial matrix (53) associated with thicker fibrils lacking collagen IX (24), indicating a role in the regulation of the fibril thickness.

Besides the two main components of the ECM, the cartilage contains plenty of non-collagenous proteins with varying structure and function. They are supporting the matrix stabilisation, but most of them are hardly investigated and their functional role in articular cartilage is mainly unknown. The best-studied proteins belong to the matrilin and thrombospondin families. They have primarily an adaptor function to further crosslink matrix components and influence the maintenance of the ECM by providing stability (31, 54, 55). Adaptor proteins usually have a polymeric structure by forming either homo- or hetero-polymers, providing an increased potential to crosslink more than one protein with others. Matrilin-1 and -3 are predominantly expressed in cartilage, while matrilin-2 and -4 expressions are more widely spread (54). Matrilin-3 can interact with plenty of matrix components, including collagens or COMP (31, 56). The function of matrilin-3 depends on its localisation, while immobilised matrilin-3 has ECM protective properties by inducing ECM protein expression and inhibiting degrading proteases, soluble matrilin-3 leads to ECM degradation by activating proteases and inducing the expression of pro-inflammatory cytokines (57-59). The knock-out (KO) of matrilin-3 has only a minor effect on overall skeletal phenotype but shows the involvement of the protein in chondrocyte differentiation and matrix stabilisation (60, 61). Besides, its adaptor function, the role of matrilin-3 (Matn-3) in mature articular

cartilage is not fully understood. A similar adaptor function is also known for members of the thrombospondin family.

1.4.1. Thrombospondins

The thrombospondin (TSP) family consists of five members, termed 1-5, with TSP-5, also known as COMP (55). All thrombospondins have low tissue specificity and are present in almost all parts of the body. TSP-1 and TSP-2 are the best-studied members of this family, especially in the context of their antiangiogenic characteristics (62-66). TSP-3 is mainly expressed in lung, cartilage and brain (67); and TSP-4 predominantly investigated in neural and vascular tissues (68) as well as COMP in cartilage (55), tendon and bone (69). The thrombospondin family consists of two subgroups, accordingly to their oligomerisation status and structural domains. Group A consists of the homotrimers TSP-1 and -2, while TSP-3, -4 and COMP are homopentamers, belonging to group B. They are structurally different to group A by lacking the procollagen and type I domains. Despite the differences, all thrombospondins have a highly conserved C-terminal domain. **Figure 1.4** shows a schematic illustration of the domain organisation and the oligomeric structures of TSPs. (55, 70, 71)

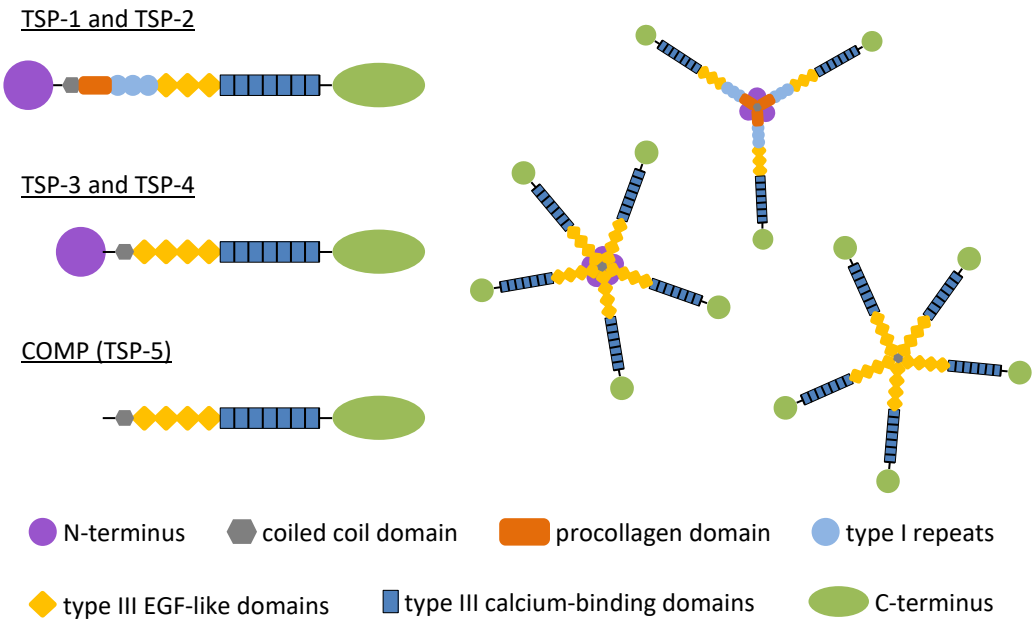

Figure 1.4. Structure of the thrombospondins
Schematic illustration, showing the monomeric and polymeric structures of all thrombospondin family members.

All five TSPs are present in human cartilage. TSP-1 is predominantly expressed in the transitional and upper deep zone of cartilage (72) and chondrocytes are not able to attach to the protein, in contrast to COMP (73). TSP-1 as well as TSP-2 are also present during cartilage formation and suggested to have an antiangiogenic effect, preventing ossification (62, 74, 75). TSP-3, which is present in the developing cartilage, is involved in endochondral ossification as well as bone maturation (74, 76) and is the target of fewer investigations.

1.4.1.1. COMP

The cartilage oligomeric matrix protein (COMP) is one of the most intensively studied non-collagenous proteins in the cartilage ECM. COMP is a large disulfide-bounded pentameric and glycosylated matrix protein with a size of approximately 524 kDa (77). COMP and TSP-4 are structurally very similar, but COMP lacks the N-terminal heparin-binding domain (67). The oligomerisation of the five COMP monomers occurs in the coiled-coil domain at the N-terminus (55, 78). It is synthesised during bone and joint development and its expression by chondrocytes continuous even in the mature, adult cartilage (79). There, it is ubiquitously expressed and located in the interterritorial, territorial as well as in the pericellular matrix (79). COMP stabilises the ECM by crosslinking plenty of molecules by binding to collagen I, II (80), IX (81, 82), XII, XIV (37), fibronectin (83), aggrecan (51) and matrilins (56), mainly via the C-terminal domain. Besides its adaptor function, COMP regulates intracellularly, the collagen secretion (84) as well as extracellularly, the fibril formation and organisation. The latter functions depend on COMP's pentameric structure, most likely by bringing several proteins closer together for an enhanced assembly (85). The distribution of COMP in the pericellular matrix enables interactions with cell surface receptors, so-called integrins, and facilitates chondrocyte (73, 86) attachment. COMP also interacts with growth factors of the TGF-β superfamily (87, 88). TGF-β1 regulates plenty of processes within the articular cartilage, including chondrocyte differentiation as well as the induction of proliferation (89). It can further induce the synthesis of various matrix proteins, like collagen II, aggrecan (90) and COMP itself (91). Haudenschild et al. (87) could show that monomeric COMP has at least two binding sites for TGF-β1, which are simultaneously accessible, demonstrating that pentameric COMP can bind several TGF-β1 molecules.

Interestingly, COMP could not only interact with TGF-β1 but also enhance its transcriptional capacity, most likely by increasing its local concentration in proximity to cell surface receptors. COMP expression itself is also regulated by TGF-β1, suggesting that the interaction between these molecules, leads in a positive feedback loop, to an increased expression of COMP. All these data indicate a relevant role of COMP in the development and maintenance of the cartilage architecture and biomechanical properties. However, COMP-KO mice show no altered skeletal phenotype (92). Also, other thrombospondin family members were not increased in the absence of COMP, suggesting that none of them is compensating for the loss (92). In contrast to the unaffected phenotype of mice lacking COMP, mutations in the COMP gene have severe consequences for cartilage and bone development.

Mutations in the COMP gene are associated with skeletal diseases named multiple epiphyseal dysplasia (MED) and pseudoachondroplasia (PSACH) (93-95). MED and PSACH can occur in a mild to severe form causing dwarfism, ligamentous laxity and early onset of degenerative joint disease (96). An altered protein folding causes retention of COMP in the rough endoplasmic reticulum (ER) (97) and induces an ER stress response, consequently resulting in chondrocyte cell death (98, 99). COMP retention leads to a co-retention of other proteins and results in a reduction of collagen IX and Matn-3 in the ECM, causing a disorganised matrix and point to the importance of these three proteins in ECM assembly (100). Other COMP mutations do not interfere with COMP trafficking but still causing the PSACH phenotype, indicating that other mechanisms than COMP retention are involved in disease-onset (101). A less efficient chondrocyte attachment to mutated COMP could influence matrix-cell interactions (101) or alterations in the binding capacity to other matrix proteins or growth factors, affecting the ECM integrity. The impact of altered binding properties to chondrocytes or growth factors, such as TGF-β1 on ECM homeostasis is hardly investigated.

1.4.1.2. TSP-4

Thrombospondin-4 (TSP-4) shows the highest structural similarities to TSP-3 and contains an N-terminus, a coiled coil domain for oligomerisation of five monomers by disulfide bridges, four EGF-like domains, seven type III calcium-binding domains and a C-terminus (102) (**Fig.1.4**). With a size of approximately 700 kDa, TSP-4 is larger than COMP (102). The N-terminus contributes to a certain degree to the ligand interaction (103) and consists of a heparin-binding domain, which might be involved in cell surface binding (104) and therefore, also in matrix-cell interactions. The C-terminal domain of TSP-4 is the main binding site for various extracellular matrix proteins, including collagen I, II, III, V, laminin-1, fibronectin and matrilin-2 (103), indicating an adaptor function of TSP-4 in the ECM. Often, TSPs are expressed in the same tissues. Nevertheless, they are supposed to have different functional roles. So far, the most obvious difference to other TSPs, is the proangiogenic character of TSP-4 (105, 106), compared to the antiangiogenic TSP-1 and TSP-2 (62). In the vascular system, TSP-4 promotes endothelial cell adhesion, proliferation and migration (106). Furthermore, TSP-4 supports myoblast adhesion (107) and a KO leads to an increased expression of ECM proteins and heart size (108). In tendon and skeletal muscle, TSP-4 distribution is abundantly and ablation in tendons reveal a modulating role in fibril assembly and maintenance of the ECM (109). Contrary to the heart, a TSP-4-KO decreases the production of ECM proteins in red muscles, indicating a tissue specific effect of TSP-4 (109). Hardly any data are reported about TSP-4 in articular cartilage. So far, its presence is only confirmed, on gene level and no information about its protein content or distribution are available. Although, the absence of TSP-4 results in a temporarily thinning of articular cartilage in a mouse model, suggesting a role in cartilage integrity (110). Furthermore, pig chondrocytes stimulated with human TSP-4 show no aberrant effects on cell metabolic activity, proliferation, apoptosis and gene expression (110).

The effects of TSP-4 are very heterogeneous. However, a general and tissue independent association with tissue remodelling, especially in injury and diseases, like atherosclerosis (111), failing hearts (112-115), hypertrophic scar formation (116), muscle dystrophy (117), neuropathic pain (118, 119) and several types of cancer (120-123), are reported. Antibodies against TSP-4 are detected in sera of osteoarthritic

patients, indicating an involvement in the disease (124). Another research group found increased gene expression levels in osteoarthritic bone marrow lesions (125) but did not investigate its disease-associated role. The results of these studies suggest an involvement of TSP-4, also in articular cartilage ECM remodelling in osteoarthritis. However, no data are provided to confirm this hypothesis.

1.5. Chondrocyte signalling

The maintenance of the cartilage ECM requires a delicate balance of catabolic and anabolic processes, which are regulated among others by growth factors. TGF-β1 has a pivotal role in this homeostasis by activating the necessary signalling cascades (**Fig.1.5**). One of the most relevant pathways to maintain cartilage homeostasis is the Smad (small mothers against decapentaplegic homologs) signalling. The counteracting Smad2/3 and Smad1/5/9 can be distinguished and activated by ligand-receptor binding on the chondrocyte surface (9, 126). The activin receptor-like kinase (ALK) 5 is the classical TGF-β1 receptor to directly phosphorylate Smad2/3, while in non-classical ways, TGF-β1 can also induce the phosphorylation of Smad1/5/9 via ALK 1 (127). Activation of Smads depends on TGF-β1 concentration, favouring the activation of Smad2/3 at low concentrations and Smad1/5/9 at high concentrations (9). After Smad phosphorylation, Smad2/3 or Smad1/5/9 build a complex with the co-Smad4, which promotes nuclear entry and accumulation. Smad2/3 and Smad1/5/9 have different Smad-binding motifs in the DNA sequence, resulting in the downstream transcription of differential genes. TGF-β1 typically induce Smad2/3 signalling, promoting the matrix maintenance by inhibiting chondrocyte hypertrophy (128, 129) and inducing the expression of matrix proteins like aggrecan and collagen II (90). Smad1/5/9 phosphorylation results in the opposite, the expression of collagen X and MMP-13, causing chondrocyte hypertrophy and matrix degradation (127).

TGF-β1 can also activate another pathway important in matrix maintenance, the extracellular signal-regulated kinase (Erk) 1/2 signalling. In chondrocytes, Erk1/2 phosphorylation by TGF-β1 via ALK 5 induces the synthesis of aggrecan and collagen II as well as the suppression of hypertrophy (90, 130), comparable to Smad2/3 signalling. Erk1/2 can further facilitate the phosphorylation of Smad2/3 by an Erk1 dependent interaction (131, 132), indicating a synergistic effect of these pathways. A cross-talk

between Smad and Erk is necessary, regarding the finding that Smad2/3 can induce aggrecan expression relatively fast, while Erk1/2 is important for maintaining this high expression level (133). In ageing, the amount of ALK 5 decreases more dramatically than ALK 1, causing a shift to Smad1/5/9 signalling, making the cartilage more prone to degradation (127). The balance between Smad, as well as Erk signalling pathways, is a requirement for cartilage homeostasis and pointed out, by studies in KO-mice. Dysfunctional Smad3 causes severe joint diseases, characterised by ECM degradation, affecting proteoglycans and an increased number of hypertrophic chondrocytes, producing collagen X (134). Mice with a Smad1/5 ablation develop severe chondrodysplasia as a result of lacking hypertrophic chondrocytes (135). The ablation of Erk1/2 in hypertrophic chondrocytes, cause enchondroma-like lesions in the bone marrow (136) and the inhibition of Erk1/2 signalling in human chondrocytes lead to chondrocyte cell death, demonstrating the involvement of Erk1/2 not only in chondrocyte differentiation but also in survival (137). If ECM proteins contribute to cartilage homeostasis by inducing or modulating Smad and Erk signalling in chondrocytes is not investigated so far.

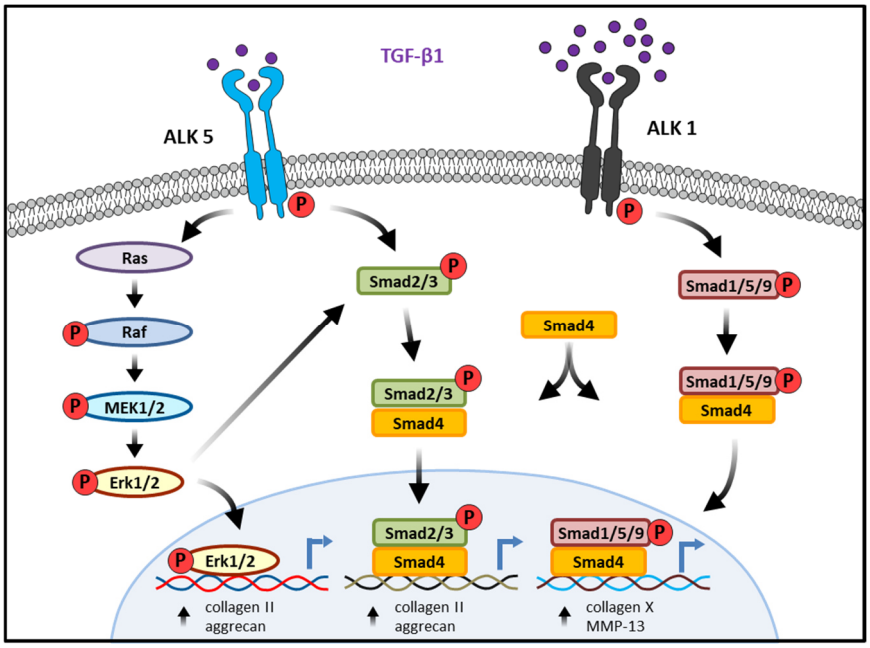

Figure 1.5. Schematic overview of Smad and Erk signalling pathways
TGF-β1 induces Smad2/3 and Erk1/2 signalling via ALK 5 and the phosphorylation of Smad1/5/9 via ALK 1. Smad phosphorylation results in a complex formation with co-Smad4. Erk1/2 phosphorylation occurs via Ras-Raf-MEK1/2 signalling, leading to the transcription of target genes. ALK = activin receptor-like kinase; Erk = extracellular signal-regulated kinase; Smad = small mothers against decapentaplegic homologs

1.6. Cartilage damage

Cartilage damage was already described 1743 by William Hunter, who mentioned the problematic of cartilage ulceration and that once destroyed cartilage is not able to regenerate anymore. As a consequence, he concluded, that a more complex therapy, than that used for bone, will be needed. Centuries later, there are still open questions and no solution for a successful cure for cartilage degradation. (138)

1.6.1. Osteoarthritis

Several reasons are leading to cartilage damage, including age, trauma or degenerative joint diseases, like arthritis. The most common type of arthritis is osteoarthritis (OA), which affects predominantly, knee, hip, hand and spine but may generally affect any joint of the human body (139). Of all OA affected joints, the knee is with 85 % worldwide the most affected one and the leading cause of immobility (140).

OA is a slowly progressing multifactorial disease, involving every compartment of the joint, including the articular cartilage, subchondral bone, synovium, meniscus and ligament (141). The hallmarks of this disease are articular cartilage degradation, remodelling of the subchondral bone and formation of osteophytes, as well as inflammation of synovial tissue and degradation of the menisci (142), leading to stiffness and pain. **Figure 1.6** shows a schematic comparison of a healthy and OA knee joint.

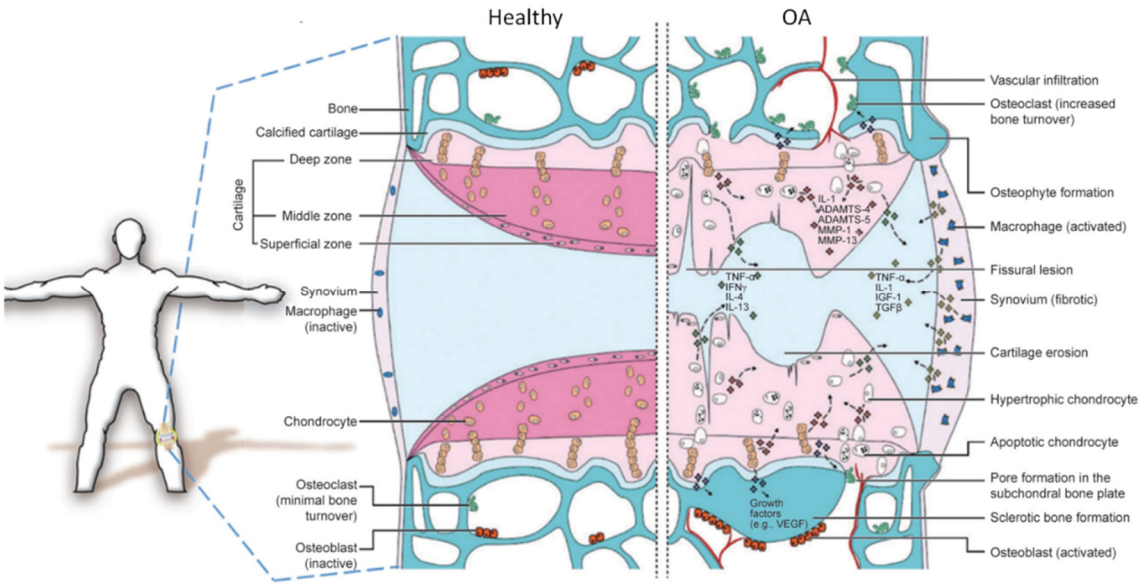

Figure 1.6. Knee joint in health and OA
Comparison of a healthy and OA knee joint. OA dependent alterations are observable in every compartment of the joint. The figure was modified from (143).

Current data reveal that women are more prone to knee OA than men (144, 145) but the reasons, are not fully understood but anatomical and mechanical differences, as well as hormones, might be considered (146). Other risk factors are age, obesity, joint injury/trauma, genetic predisposition (e.g. a polymorphism in the GDF5 (147) or matrix Gla protein gene (148)) and mechanical alterations resulting from malalignments or abnormal joint shape (142, 149).

The mechanisms, responsible for OA-onset are still not completely understood, but involve the failing regulation of metabolic processes by chondrocytes, leading to an imbalance of anabolic and catabolic reactions/processes. For yet unknown reasons chondrocyte favours Smad1/5/9 signalling, in OA, leading to an unstable chondrocyte phenotype (150). The level of activated TGF-β1 is increased in the synovial fluid of OA patients (151), suggesting an enhanced interaction with chondrocytes, leading to an ALK 1 binding due to the high TGF-β1 concentration. Reactivated chondrocytes accumulate in cell clusters, proliferate, become hypertrophic and intensively produce ECM proteins, but also ECM degrading enzymes (142). In the course of OA, collagen II but also collagen I is extensively synthesised in late stages (152), especially in areas where fibrocartilage is formed (153). Also, the adaptor protein Matn-3 is increased in OA cartilage and its expression correlates with severity grades (154). In late-stage OA, several ECM proteins, such as collagens, COMP, fibronectin and fibromodulin, are re-expressed (79, 155-157). Hypertrophic chondrocytes produce collagen X, alkaline phosphatase, annexin II and annexin V, resulting in matrix mineralisation (158, 159) and extension of the calcified zone (160). ECM synthesis is accompanied by degradation caused by matrix degenerating enzymes (142), like matrix metalloproteinases (MMPs) and ADAMTSs (a disintegrin and metalloproteinase with thrombospondin-1 domains) (161). The expression of MMP-3, which performs matrix protein degradation in healthy cartilage, is also detectable in early but decreases in more severe OA stages (162). MMP-13 is highly expressed in late-stage OA, suggesting degradation of proteoglycans and non-collagenous matrix proteins in early and collagens at a later time point (162). ADAMTSs are the predominant degradation source for aggrecan in late-stage OA, although the degradation profile, including the combination of involved ADAMTSs and MMPs, is divergent between patients and no general statement can be made (163). With the loss of aggrecan, the collagens are accessible for degradation at a later stage, for

example by MMP-13, indicating a damaged state of no return (142, 164). During OA progression, also other ECM proteins, like COMP, fibronectin, fibromodulin (79, 155) and collagen IX, are degraded (165). Some degradation products, like from collagen II and fibronectin, have chondrolytic effects on chondrocytes, inducing the synthesis of MMPs and pro-inflammatory cytokines (166-168), leading to further matrix degradation. Inflammatory cytokines and degradation products can induce these matrix degrading effects by activating the Erk1/2 signalling pathway (169), indicating a shift from anabolic, induced by TGF-β1 to catabolic properties. The detection of COMP but also TSP-4 antibodies in sera of OA patients proofs the involvement of the immune system, which induces the production of auto-antibodies in response to degradation products (124). The matrix composition is changing and becomes susceptible to physical forces. Initially, erosions and fissures occur in the superficial zone but expand during progression also to the deeper zones (140) until the subchondral bone becomes exposed. Beneath the calcified cartilage, the subchondral bone also undergoes structural and organisational changes (170). It is suggested that vascularisation is the initiating process of cartilage invasion and associated with osteophyte formation (170, 171). The precise mechanism leading to cartilage vascularisation is not known, although, the enhanced expression of the vascular endothelial growth factor (VEGF) in the OA matrix (172, 173) might be a promoter. Vascular invasion occurs in areas where collagens are already degraded (174) and hypertrophic chondrocytes undergo apoptosis to be replaced by bone (175). All these changes in the ECM lead to joint failure, resulting in pain and immobility. Currently, the mechanisms leading to an aberrant chondrocyte phenotype and dysregulated signalling cascades are still elusive. Also, to what extend newly synthesised ECM proteins contribute to ECM maintenance or cartilage repair processes are still poorly understood and need further investigations.

1.6.2. Diagnosis and treatment

The most common and cheapest way to diagnose OA is by radiographic images (176-178). Although, if OA is visible via x-ray, the cartilage damage progressed already to an irreparable stage. Therefore, diagnostic tools detecting OA already at a time point before severe damage occur are needed. For that reason, researchers tried to identify OA specific biomarkers, which are detectable in body fluids, like synovial fluid, serum or

urine. These proteins and fragments are soluble in the ECM, diffuse to the synovial fluid (179) and from there to the circulatory system, where detection in the serum via non-invasive methods, is possible. Antibodies, detecting COMP (180), the C-terminal telopeptide of collagen II (181-183) as well as fragments of aggrecan (184-188) are available. Hunter D.J. et al. (189) showed that COMP but not collagen II or aggrecan levels correlate with OA associated cartilage loss. COMP also increases with age (180), motion (190, 191), systemic sclerosis (192), liver diseases (193, 194) and cancer (193, 195-197) leading to a loss of credibility as OA-specific biomarker. Therefore, specific antibodies against COMP fragments (198, 199) detected in OA are developed; allowing a disease-specific diagnosis but also here further investigations will be necessary before a clinical application will be possible. Therefore, it is essential to identify additional ECM proteins or derived fragments, which are upregulated in OA and can be used as specific biomarkers to detect OA, especially in an early stage.

The higher sensitivity of diagnostic tools will enable follow up studies on OA progression and further help to develop disease-modifying therapies. Total knee replacement improves the life quality of most of the patients by causing pain relief and enhanced mobility. However, studies reveal that more and more young people (187) suffer from OA and the shelf-life of knee prostheses is restricted, especially due to the increased activity of young patients, there is a need for alternative therapies.

Autologous chondrocyte implantation (ACI) is a procedure carried out in two steps, starting with the isolation of chondrocytes from a healthy biopsy and an *in vitro* expansion for four to six weeks, following step two, the transplantation into the damaged area. In the next generation of this procedure, the matrix-associated autologous chondrocyte implantation (MACI), chondrocyte seeding and expansion on collagen scaffold are performed, before transplantation into the damaged area. Both techniques enable articular cartilage-like tissue development and show a graft survival of 78 % after 5 years and 51 % after 10 years. (200)

Follow up studies of OA patients undergo MACI of the knee show production of articular-like cartilage but also fibrocartilage (201, 202), reducing the functional properties of the tissue. The *in vitro* chondrocyte expansion leads to a dedifferentiated phenotype and the production of collagen I, changing the biomechanical properties of the cartilage (203). Therefore, new techniques to overcome these limitations and

suppress chondrocyte dedifferentiation are needed for a successful resembling of articular cartilage and a prolonged graft survival.

1.7. Aim of this project

Osteoarthritis is a slowly progressing joint disease, leading to the degradation of the articular cartilage. At disease onset, the quiescent chondrocytes become reactivated and start to proliferate, form cell clusters and undergo differentiation. These changes lead to a dysregulation of anabolic and catabolic cell signalling pathways, especially of Smad and Erk. Thereby, ECM proteins are not only degraded but also re-expressed and newly synthesised, resulting in an ECM remodelling. The spectra of ECM molecules, involved in OA onset and disease specific processes are still poorly understood.

Therefore, this project focuses on the investigation of ECM proteins, which are regulated in OA, to gain knowledge about the complex protein network and ongoing processes in cartilage remodelling. While COMP is ubiquitously expressed in healthy cartilage and degraded as well as re-expressed in OA, no data about the regulation of its family member, TSP-4 are available. TSP-4 is upregulated in several pathological conditions but its distribution in articular cartilage as well as its involvement in OA associated ECM remodelling was not investigated, so far.

In the first part of this project, the expression and distribution of TSP-4 and other ECM proteins in healthy and OA cartilage are characterised. A quantitative investigation of these proteins will further confirm a regulation in OA and identify potential candidates, tested as OA biomarker.

The second part focuses on the functional role of regulated ECM proteins in articular cartilage and their contribution to OA typical processes. Therefore, their effects on chondrocyte migration, proliferation, differentiation and ECM synthesis are determined. Involvement in cell signalling processes is investigated in more detail by analysing their potential to induce and modulate Smad and Erk signalling pathways.

The obtained data will contribute to a better understanding of the complex ECM network and the ongoing processes in health and pathologic conditions. Furthermore, the data might help to improve and develop effective diagnostic tools and therapeutic applications.

2. Material and Methods

All solutions, buffers and reactions were prepared with distilled water, except mentioned otherwise. All indicated pH values are referred to the ready to use solutions or buffers at room temperature (RT). Glass and plastic equipment was sterilised by autoclaving at 121 °C before usage.

2.1. Materials

All chemicals and reagents used in this project are listed in **table 2.1**.

Table 2.1: Used chemicals and reagents

Chemicals and reagents	Company
Acetic acid	Carl Roth
Acetic alcohol	ScyTec Laboratories
Acrylamide-bis ready-to-use solution 40% (37.5:1)	Merck
Agarose	Carl Roth
Albumin faction V (pH 7.0) (BSA)	PanReac, AppliChem
Ammonium persulfate (APS)	Sigma-Aldrich
β-mercaptoethanol	Sigma-Aldrich
Biacore running buffer	Biacore AB
Biotin	Sigma-Aldrich
Boric acid	Sigma-Aldrich
Bromophenol blue	Serva
Collagenase CLS II	Biochrom
DAPI (4',6-diamidino-2-phenylindole)	Sigma-Aldrich
DAPI fluoroshield mounting medium	Abcam
Dimethyl sulofixe (DMSO)	Sigma-Aldrich
Disodium hydrogen phosphate (Na_2HPO_4)	Sigma-Aldrich
Dubecco's phosphate buffered saline (DPBS), sterile	ThermoFisher Scientific
Dulbecco's modified eagle medium F12- (DMEM/F12)	Gibco
Endothelial cell basal media-2 (EBM-2)	Lonza
Endothelial cell growth media-2 (EGM-2)	PromoCell
Entellan	Sigma-Aldrich
Ethanol 96 % (EtOH)	Carl Roth
Ethanolamine solution (1 M), pH 8.5	Biacore AB
Ethylenediamine tetraacetic acid (EDTA)	VWR
Fast-green	Sigma-Aldrich
Fetal bovine serum (FBS)	Gibco
FuGENE® 6 transfection reagent	Roche Diagnostics
GelRed nucleic acid gel stain	Biotium Inc
Geltrex™ reduced growth factor basement membrane matrix	ThermoFisher Scientific
GeneRulerTM 1 kb DNA ladder	ThermoFisher Scientific
Glycerol	Sigma-Aldrich

Chemicals and reagents	Company
Goat serum	Abcam
Guanidine hydrochloride	Sigma-Aldrich
Hyaluronidase	Sigma-Aldrich
Hydrogen peroxide	Sigma-Aldrich
Isopropanol	VWR
Kaiser's glycerol gelatine	Carl Roth
L-ascorbic acid 2-phosphate (ascorbic acid)	Sigma-Aldrich
Luminol	Sigma-Aldrich
Methanol 99 % (MeOH)	ThermoFisher Scientific
N-ethylmaleimide (NEM)	Sigma-Aldrich
NHS (0.05 M)/EDC (0.2 M) solution	Biacore AB
Orange G	Carl Roth
PageBlue™	ThermoFisher Scientific
Paraffin	ThermoFisher Scientific
Paraformaldehyde	Sigma-Aldrich
p-Coumaric acid	Sigma-Aldrich
Penicillin/streptomycin (Pen/strep)	Gibco
Phenylmethylsulphonyl fluoride (PMSF)	Sigma-Aldrich
Phosphate buffered saline tablets (PBS)	ThermoFisher Scientific
PhosphoSafe™	Merck
Platelet-derived growth factor-BB (PDGF-BB)	Miltenyi Biotec
Potassium chloride (KCl)	Sigma-Aldrich
Potassium dihydrogen phosphate (KH2PO4)	Sigma-Aldrich
Precision plus protein™ dual color standard	Bio-Rad
Prestained protein ladder	Abcam
Pronase from streptomyces griseus	Roche Diagnostics
Proteinase K	Qiagen
Puromycin	Gibco
RNase-free H_2O	Macherey-Nagel
Roti®Blue	Carl Roth
Safranin-O	Carl Roth
Shandon™ zinc formal-fixx™	ThermoFisher Scientific
Skim milk	Carl Roth
Sodium acetate	Sigma-Aldrich
Sodium chloride (NaCl)	Merck
Sodium dodecyl sulfate (SDS)	VWR
Tetramethylethylenediamine (TEMED)	Sigma-Aldrich
TGF-β1	R&D
Tris base	Sigma-Aldrich
Tris hydrochloride (Tris-HCl)	PanReac AppliChem
Triton X-100	Merck
Trypan blue (0.4 %)	Bio-Rad
Trypsin	Biochrom
Tween-20	Sigma-Aldrich
Weigert’s iron haematoxylin	Carl Roth
Xylene	Carl Roth

All kits used in this project are listed in **table 2.2**.

Table 2.2: Used kits

Kits	Company
AEC-2-component kit	DCS
EdU cell proliferation kit	baseclick GmbH
ImmPRESS® HRP horse anti-rabbit IgG polymer detection kit	Vector Laboratories
LDH cytotoxicity detection kit	TAKARA BIO INC
PerfeCTa SYBR® green supermix	Quantabio
qScript cDNA supermix	Quanta BioSciences
Qubit protein assay kit	ThermoFisher Scientific
Taq PCR master mix	Qiagen
NucleoSpin®RNA/protein purification kit	Macherey-Nagel

A list of the used equipment and devices is provided in **table 2.3**.

Table 2.3: Used equipment and devices

Equipment and material	Company
Analog vortex mixer	VWR
Analog shaker, standard	VWR
Biacore 2000	Biacore AB
Biological safety cabinet, safe 2020	ThermoFisher Scientific
Cell culture inserts; ThinCert™	Greiner Bio-One
Cell scraper	Corning
Cell strainer (nylon, 70 µm)	Corning
Centrifuges: Mega Star 3.0 and Micro Star 17 (R)	VWR
Chamber slides; Nunc™ Lab-TekTM II, 4 well	ThermoFisher Scientific
Chemi DocTM XRS+	Bio-Rad
CO_2-incubator; HERAcell vios 250	ThermoFisher Scientific
CoolCell® cell freezing container	Corning
Excelsior AS tissue processor	Thermo Scientific
Freezer -80°C; HERAfreeze HFU T-series	ThermoFisher Scientific
HistoStar embedding workstation	Thermo Scientific
Horizontal electrophoresis system; Sub-Cell GT cell	Bio-Rad
Incubation shaker; Minitron	Infors HAT
Light and fluorescence microscope; Nikon Eclipse Ti	Nikon
Light microscope, CKX41	Olympus
Magnetic stirrer	IKA
Microtome RM2235	Leica
MilliQ water purification system	Sartorius
Mini Trans-blot® electrophoretic transfer cell	Bio-Rad
Mini-PROTEAN® tetra-cell system	Bio-Rad
NanoDrop One^C	ThermoFisher Scientific
Neubauer improved counting chamber	BRAND
Nitrocellulose membrane (0.45 µm)	GE Healthcare
Object slides; superfrost plus object slides	ThermoFisher Scientific
pH calibrator	Mettler Toledo
Plate reader; Infinite® 200 pro	Tecan Group Ltd.
Power supply	Life Technologies
PVDF membrane (0.45 µm)	GE healthcare

Equipment and material	Company
Qubit 2.0 fluorometer	ThermoFisher Scientific
qTOWER3G real-time PCR thermal cycler	Analytik Jena
Scale, BP221 S	Sartorius
Thermal shaker	VWR
Tube roller	Fisher Scientific
Vacuum pump, BVC professional	Vacuubrand
Water bath WNB 14	Memmert
WET FRED device	IBA

A list of the software used in this project is shown in **table 2.4**.

Table 2.4: Used software

Software	Company or Source
BIAevaluation software	Biacore AB
cellSens Entry software	Olympus
CorelDraw	Corel Corporation
ImageJ version 1.5 software	(http://imagej.nih.gov/ij)
ImageLab™ software	Bio-Rad
Microsoft Office	Microsoft
NIS Elements BR 4.40.00 software	Nikon
Photoshop	Adobe
SigmaPlot version 13.0 software	Systat Software, Inc

The list of used standard buffers and their recipes is provided in **table 2.5**.

Table 2.5: Composition of standard buffers

Buffer		Ingredients
Basic medium	0.1 %	BSA
	25 µg	Ascorbic acid
		in DMEM/F12
Laemmli buffer (4x)	250 mM	Tris-HCl, pH 6.8
	40 %	Glycerol
	0.04 %	Bromophenol blue
	8 %	SDS
		in ddH_2O
PBS (1x)	140 mM	NaCl
	10 mM	KCl
	8 mM	Na_2HPO_4
	2 mM	KH_2PO_4
		pH 7.4, in ddH_2O
PBS-T (1x)		PBS (1x)
	0.1 %	Tween-20

TBE (10x)	1 M	Tris base
	1 M	Boric acid
	0.02 M	EDTA
		in ddH_2O
TBS (10x)	0.1 M	Tris base
	1.5 M	NaCl
		in ddH_2O
TBS-T (10x)		TBS (10x)
	1 %	Tween-20
Trypsin-EDTA	50 mg/ml	Trypsin
	20 mg/ml	EDTA
		in PBS

All antibodies used in this project are listed in **table 2.6** (primary antibodies, unconjugated), **table 2.7** (labelled conjugate) and **table 2.8** (secondary antibodies).

Table 2.6: List of unconjugated primary antibodies

Antigen	Host	Dilution	Reference or supplier
COMP	rabbit	1:100 (IF), 1:500 (IHC), 1:1000 (IB)	(73)
Collagen I	rabbit	1:200 (IF)	Abcam (ab34710)
Collagen II	mouse	1:200 (IF)	Merck (Ab-1) (II-4C11)
Collagen IX	guinea pig	1:200 (IF)	(31)
Collagen X	mouse	1:50 (IF)	Mengjie Zhou
Collagen XII	rabbit	1:200 (IF)	Manuel Koch
Matrilin-3	rabbit	1:100 (IF), 1:500 (IHC)	(204)
TSP-4	rabbit	1:100 (IF), 1:500 (IHC)	AG Zaucke and (205)
TSP-4	guinea pig	1:100 (IF)	(103, 206)
VEGF	mouse	1:50 (IF)	Santa Cruz (sc-7269)
Smad2	rabbit	1:1000 (IB)	Cell Signalling (#5339)
pSmad2 E8F3R	rabbit	1:2000 (IB)	Cell Signalling (#3108)
Smad1/5/9	rabbit	1:500 (IB)	Santa Cruz (sc-6031-R)
pSmad1/5/9	rabbit	1:1000 (IB)	Cell Signalling (#13820)
Erk1/2	mouse	1:2500 (IB)	Cell Signalling (#9107)
pErk1/2	rabbit	1:2000 (IB)	Cell Signalling (#4370)
GAPDH	mouse	1:2000 (IB)	Thermo Fisher Scientific (#MA5-15738)

Table 2.7: Labelled conjugate

Target	Conjugate	Dilution	Reference or producer	Conjugated
Strep-Tag II	Strep-Tactin	1:100 000	IBA (2-1502-001)	HRP

Table 2.8: List of secondary antibodies

Antigen	Host	Dilution	Reference or producer	Conjugated
Rabbit IgG	goat	1:1000 (IB, IHC)	Agilent (#P0448)	HRP
Guinea pig IgG	rabbit	1:1000 (IB, IHC)	Agilent (#P014102-2)	HRP
Mouse IgG	goat	1:1000 (IB, IHC)	Agilent (#P0447)	HRP
Rabbit IgG	horse	Ready to use	Vector Lab.(#MP-7401)	HRP
Rabbit IgG	goat	1:500 (IF)	Invitrogen (#A-11037)	AlexaFluor 594
Guinea pig IgG	goat	1:500 (IF)	Invitrogen (#A-11073)	AlexaFluor 488
Mouse IgG	goat	1:500 (IF)	Invitrogen (#A-11029)	AlexaFluor 488

All primers used in this project, for PCR and qPCR analyses, were received from ThermoFisher Scientific. The gene name, the oligonucleotide sequences of forward (fw), reverse (rev) primer and the size of the expected amplicon are shown in **table 2.9**.

Table 2.9: List of used primer pairs

Human genes	Primer	Sequence (5' → 3')	Product length
COMP	Fw	AGGGAGATCGTGCAGACAA	
	Rev	AGCTGGAGCTGTCCTGGTAG	154 bp
THBS4	Fw	ATGAAGGCTCTGAGTTGGTG	
	Rev	CTTGGAAGTCCTCAGGGATG	153 bp
GAPDH	Fw	CTCCTGTTCGACAGTCAGCC	
	Rev	TTCCCGTTCTCAGCCTTGAC	262 bp
Pig genes	**Primer**	**Sequence** (5' → 3')	**Product length**
ACAN	Fw	ACCTAGTTTCGAGTGCCACG	
	Rev	TCTTCTTTCCGGGTCGTTGG	100 bp
COMP	Fw	CGCGTTCTCTTGATCACCCT	
	Rev	CGCGTTGGTCTCCTGTAGTT	111 bp
COL1A1	Fw	CCAAGAAGAAGACATCCCACC	
	Rev	ATCGCACAACACATTGCC	124 bp
COL2A1	Fw	GAGAGGGGACTGAAGGGACA	
	Rev	TCTTTGCCTGAAGGACCGAC	149 bp
COL9A1	Fw	CCCCCACTGCAGGCAATAAA	
	Rev	AACCCCCATGTGCTGTAAGG	127 bp
COL10A1	Fw	GTGCCAACCAGGGAGTAACA	
	Rev	TCATAGTGCTGTTGCCCGTT	127 bp
COL12A1	Fw	TCCTCCTGGATACTGCGACT	
	Rev	TTTGTTAGCCGGAACCTGGA	80 bp
MATN3	Fw	GACCCACTCGGATAAGCAGG	
	Rev	GTGAAGGCTTTGTCCATCGC	111 bp
MMP3	Fw	CCCTTTTGACGGACCTGGAA	
	Rev	TCATGGGCAGCAACAAGGAA	141 bp
MMP13	Fw	GCCTAACAACTGAGGAGTCAA	
	Rev	GTGACCCTGACACAGCAAGT	89 bp
THBS4	Fw	ATGAGGGGCTGCAAAATGGA	
	Rev	GATACACTGCGCGTTCACAC	75 bp
VEGF	Fw	AGCGAGGCAAGAAAATCCCT	
	Rev	CGAGTCTGTGTTTTTGCAGGA	103 bp
GAPDH	Fw	GAACATCATCCCTGCTTCTAC	
	Rev	TCAGATCCACAACCGACAC	125 bp

2.2. Collection of samples

2.2.1. Human samples

Adult, human, anonymised cartilage samples were obtained from 21 patients undergoing endoprosthetic knee replacement surgery at the Orthopaedic University Hospital Friedrichsheim, Frankfurt/Main, Germany. The mean age of patients was 69 years (min. = 45 years; max. = 87 years) and 6 males and 15 females were included. Two healthy, non-OA control cartilage samples for (immuno-) histological staining were a gift from Gerjo van Osch (Erasmus MC University Rotterdam, Rotterdam, Netherlands) and one cartilage sample was obtained from a trauma patient treated at the Orthopaedic University Hospital Friedrichsheim (Frankfurt/Main, Germany). The mean age of control samples was 39 years (min. = 17 years; max. = 52 years).

Serum samples were used from a previous study (207). In total, 18 serum samples from healthy controls (n: 5; age: min. = 39 years; max. = 64 years; gender: 4 males and 1 female) and knee OA patients (n: 13; age: min. = 54 years; max. = 65 years; gender: 8 males and 5 females) were used for analysis.

2.2.2. Animal samples

Pig legs were obtained from the animal house at Goethe University Frankfurt, Frankfurt/Main, Germany from animals, sacrificed within the scope of other scientific projects. Legs from 13 female, healthy pigs (3 to 6 month) and from 1 female, old mini-pig (9 years) were received immediately after sacrificing the animal.

2.3. Grading of human cartilage samples

First, all femoral cartilage condyles from OA patients were visually scored according to the following criteria based on the OARSI grading system (208): Intact cartilage areas with a smooth and shiny surface were scored as grade 1 (G1), cartilage areas with superficial fissures and a rough surface were scored as grade 2, and areas with deeper fissures and/or exposure of subchondral bone as grade 3 to 4 (G3/4). To confirm the severity grade histologically, paraffin-embedded cartilage sections were stained with Safranin-O and Fast-green (**2.7.3. Histological staining of cartilage tissue sections**) and

scored again based the OARSI grading system (208). Healthy, non-OA cartilage were always categorised as grade 0 (G0).

2.4. Cell culture

2.4.1. Isolation and culture of primary chondrocytes

Articular cartilage of human knee femoral condyles was scraped off with a scalpel from areas with specific OA severity grades (G1, G2, and G3/4). Only patients showing all three severity grades were included. Cartilage of each severity grade was separately washed with PBS and cut into pieces (2–3 mm^3) to isolate chondrocytes under sterile conditions, for further RNA isolation.

Pig legs were processed to expose the knee and the knee joint opened to scrape off the articular cartilage from the femoral condyles under sterile conditions. The cartilage was washed with PBS and cut into small pieces (2–3 mm^3) to isolate chondrocytes.

The cartilage pieces of human and pig knee joints were weighted, transferred into a sterile tube and digested with 0.2 % pronase in DMEM/F12 medium (containing 5 % FBS and 5 % pen/strep) for 2 h at 37 °C with the agitation of 60 rpm. The volume was adjusted to the cartilage weight, 10 ml DMEM/F12 was used per g tissue. After incubation, cells and cartilage pieces were pelleted by centrifugation at 300 × g, 5 min at RT and the supernatant decanted. Cells and cartilage pieces were washed 3× with PBS and digested with 200 U/ml collagenase type II solution in DMEM/F12 medium (containing 5 % FBS and 5 % pen/strep) overnight at 37 °C with the agitation of 60 rpm. The chondrocyte suspension was filtered through a 70 µm nylon cell strainer and centrifuged at 300 x g for 5 min at RT. The pelleted cells were resuspended, counted with a Neubauer chamber (**2.5. Cell counting**) and seeded either in DMEM/F12 containing 5 % FBS or resuspended in medium containing 0.1 % BSA for direct use in downstream procedures. All cells were cultured at 37 °C, 5 % CO_2 and 20 % O_2 in a CO_2-incubator.

Pig chondrocytes were used in *in vitro* experiments to test the effect of COMP and TSP-4. Therefore, different cell densities, culture vessels and stimulation times were used (**table 2.10**). Chondrocytes used for immunoblot and gene expression studies were

seeded in 6-well plates in a density of 300 000 cells per well in 2 ml DMEM/F12 containing 5 % FBS.

To analyse the production of matrix proteins and matrix formation 40 000 cells in 400 µl DMEM/F12 containing 5 % FBS were seeded in each chamber of a Nunc™ Lab-Tek™ II 4 well chamber slide.

The cells were allowed to attach to the bottom overnight. The following day, the cells were washed twice with PBS and starved in basic medium (**table 2.5**) for 24 h. Then, the cells were stimulated with recombinant proteins. Different concentrations of TGF-β1 were used, depending on the downstream assay. In all assays, 10 µg/ml COMP (homemade) and 10 µg/ml TSP-4 (homemade) were used. The chondrocytes were treated with TGF-β1, COMP or TSP-4 alone and in the combination of TGF-β1 with COMP or TSP-4 in basic medium. When cells were stimulated in the combination of TGF-β1 with COMP or TSP-4, the two components were mixed in a tube and pre-incubated for 20 min at RT, before applying to the cells.

For immunoblot analyses, chondrocytes were stimulated with 0.1 ng/ml, 0.25 ng/ml, 0.5 ng/ml, 1 ng/ml and 10 ng/ml of TGF-β1, 10 µg/ml COMP, 10 µg/ml TSP 4 or a combination of all TGF-β1 concentrations with COMP or TSP-4 for 30 min at 37 °C.

In a pilot experiment, the effect of several concentrations of TGF-β1 (0.01 ng/ml, 0.1 ng/ml, 0.5 ng/ml, 1 ng/ml, 10 ng/ml, 30 ng/ml) on proteoglycan synthesis was investigated by Safranin-O staining and a concentration of 0.5 ng/ml considered as the most conclusive concentration to observe modifying effects of COMP and TSP-4.

Chondrocytes used in gene expression analyses were stimulated with 0.5 ng/ml TGF-β1, 10 µg/ml COMP, 10 µg/ml TSP-4 alone and in the combination of TGF-β1 with COMP or TSP-4 for 6 h and 24 h at 37 °C.

Chondrocytes seeded in chamber slides were stimulated with 0.5 ng/ml TGF-β1, 10 µg/ml COMP, 10 µg/ml TSP-4 and in the combination of TGF-β1 with COMP or TSP-4 for a period of 7 days. The chondrocytes were first stimulated with recombinant protein in the basic medium for 4 days. The medium was changed at day 4 and recombinant proteins applied in a basic medium containing 5 % FBS. At day 7, the medium was replaced by a basic medium containing only 5 % FBS and chondrocytes cultured until day 10. The supernatants were collected after each medium change.

Table 2.10: Experimental cell culture set-up for downstream *in vitro* experiments

Application	Cell density	Culture vessel	Vol	Stimulation time
Immunoblot	300 000 cells/well	6-well plate	2 ml	30 min
qPCR	300 000 cells/well	6-well plate	2 ml	6 h and 24 h
IF staining	40 000 cells/chamber	4-chamber slide	400 µl	7 days

IF = immunofluorescence; vol = amount of medium/well or chamber

2.4.2. Culture of HEK-293 EBNA cells

Human embryonic kidney (HEK) -293 EBNA cells (received from the University of Cologne) were used for the production of recombinant proteins. The cells were transfected with the pCEP-Pu V162 expression vector (generated by Prof. Manuel Koch, University of Cologne) carrying the sequence of full-length rat COMP and TSP-4 (**Fig.2.1**). The cells and the expression vector contain the *Epstein-Barr virus nuclear antigen* (EBNA-1), which binds directly to the oriP of the expression vector, supporting the replication of extrachromosomal DNA-constructs (209, 210). The contained BM40 signal peptide sequence is directing the recombinant protein to the ER and supports its secretion into the cell culture supernatant (211, 212). Utilizing the N-terminal Strep-Tag II, recombinant proteins can be easily purified from the supernatant by affinity chromatography. The expression vector also contains the *pac* gene, coding for the puromycin N-acetyltransferase, causing resistance to puromycin and allows a positive selection of transfected cells.

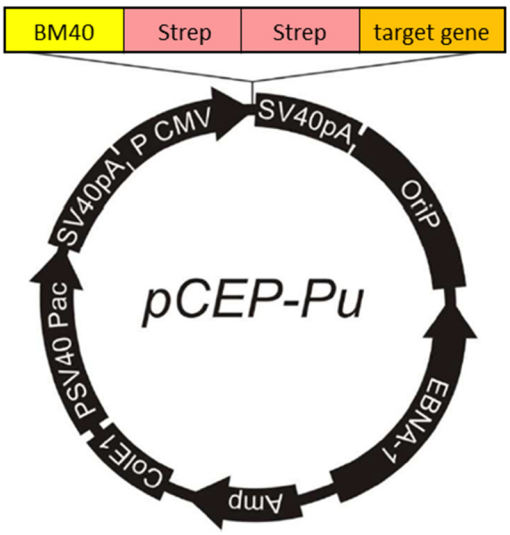

Figure 2.1: pCEP-PU expression vector map
Illustration of pCEP-PU expression vector with highlighted target gene, Strep-Tag II motif and BM40 signal peptide sequence. Modified from (213)

HEK-293 EBNA cells were cultured in DMEM/F12 medium containing 10 % FBS and 1 % pen/strep. The medium was changed every two days and when confluency was reached, cells were split by using trypsin-EDTA (**table 2.5**). The volume of trypsin-EDTA was adjusted to the size of the culture vessel (6-well = 300 µl; 10 cm dish = 1 ml; T- 75 = 1 ml; T-175 = 3 ml) and the reaction stopped with medium by adding 3x the volume of trypsin-EDTA. The cells were cultured at 37 °C, 5 % CO_2 and 20 % O_2 in a CO_2-incubator.

2.4.2.1. Cryopreservation and thawing

For cryopreservation, HEK-293 EBNA cells were washed twice with PBS and detached by trypsin-EDTA (**table 2.5**). The cell suspension was centrifuged by 300 x g for 5 min, the supernatant decanted, the pellet resuspended in cold cryo-media and filled in cryo-tubes. First, the cells were placed in the CoolCell® at -80 °C overnight and transferred to a liquid nitrogen tank for long term storage.

To initiate cell culture from cryopreservation, the frozen cells were quickly thawed and mixed with pre-warmed DMEM/F12 containing 10 % FBS. After centrifugation at 300 x g for 5 min the cell pellet was resuspended in fresh DMEM/F12 containing 10 % FBS. Then, the cells were transferred to the required vessels and cultured at 37 °C, 5 % CO_2 and 20 % O_2 in a CO_2-incubator.

Cryo-media	50 %	DMEM/F12
	40 %	FBS
	10 %	DMSO

2.4.2.2. Transfection and selection

Cloning of full-length rat *COMP* and *THBS4* into the pCEP-Pu V162 expression vector was already done before starting this project.

The cells were transfected using the non-liposomal FuGENE® 6 transfection reagent. 300 000 HEK-293 EBNA cells were seeded in each well of a 6-well plate and cultured in 2 ml DMEM/F12 containing 10 % FBS per well. When a confluence of 75-85 % was reached, the medium was changed and the transfection mix prepared. 193 µl DMEM/F12 medium (without FBS) and 1 µg in 1 µl COMP or TSP-4 V162 vector were mixed and 6 µl FuGENE® 6 transfection reagent added, without touching the edges of

the tube. The vector-FuGENE® transfection mix was mixed by inverting the tube several times and incubated for 15 min at RT. The transfection mix was dropwise added to the cells and the plate swivelled before culturing overnight. On the following day, the medium was changed (DMEM/F12 containing 10 % FBS) and the viability of the cells monitored by light microscopy. 24 h later, 0.5 µg puromycin was added to the cells to select positively transfected cells over a period of 10 to 14 days.

2.4.2.3. Collection of the cell culture supernatant

The cells were expanded from one well of a 6-well plate (2 ml medium) to one T-75 flask (10 ml medium) and finally to a triple-layer flask (100 ml medium). When a confluence of 90-95 % was reached, the medium was replaced by a DMEM/F12 medium containing only 1 % FBS to avoid an interfering of too many serum proteins at the purification step. The cell culture supernatant was then collected from the triple-layer flasks and renewed daily for a period of 5 days. To remove cell debris, the supernatant was centrifuged for 20 min at 18 000 x g at 4 °C and filtered through a FaltenFilter (5-13 µm). Before storage at 4 °C, 2 mM of the proteinase inhibitors PMSF and NEM were added. The supernatant was directly used for the purification of recombinant COMP and TSP-4 after the last collection time point at day 5 (**2.10. Protein purification with affinity chromatography**).

2.4.3. Culture of HUVECs

Human umbilical vein endothelial cells (HUVECs) (Lonza) were used to analyse the effect of COMP and TSP-4 on angiogenesis and vascularisation.

Cryopreserved HUVECs were thawed, mixed with pre-warmed endothelial cell growth media-2 (EGM-2), centrifuged at 300 x g for 5 min at RT and cultured in EGM-2 medium at 37 °C, 5 % CO_2 and 20 % O_2. The EGM-2 medium was refreshed every third day and the downstream experiments (migration, proliferation and tube formation assays) started when cells reached a confluency of 85-95 %. Before starting the downstream experiments, cells were washed twice with PBS, centrifuged at 300 x g for 5 min and resuspended in endothelial cell basal media-2 (EBM-2) supplemented with 0.1 % BSA. The cells were detached with trypsin-EDTA (**table 2.5**) and counted with a Neubauer chamber (**2.5. Cell counting**). The volume of trypsin-EDTA was adjusted to the

size of the culture vessel (T-75 = 1 ml; T-175 = 3 ml) and the reaction stopped with medium by adding 3x the volume of trypsin-EDTA.

2.5. Cell counting

The number of cells was counted by using the Neubauer improved cell counting chamber. The Neubauer chamber consists of 4 larger squares, each divided into 16 smaller squares. A cover glass was put on top of the central area of the Neubauer chamber and filled with 10 µl of the cell-dye solution. Therefore, 10 µl of the cell suspension was carefully mixed with 10 µl trypan blue. The Neubauer chamber was placed on the light microscope stage and the cells counted. The counted living cells appear white, while the excluded dead or damaged cells are stained blue. All 4 larger squares were counted and the cell concentration calculated with the following formula.

$$\text{Cell concentration (cells/ml)} = \frac{\text{nr. of cells x 10 000}}{\text{nr. of squares}} \text{ x dilution factor}$$

2.6. Cell cytotoxicity assay

The LDH cytotoxicity detection kit was used to measure the lactate dehydrogenase (LDH) activity in the cell culture supernatant. LDH is only released from damaged cells.

Cell culture supernatants of TGF-β1, COMP and TSP-4 stimulated cells were collected after 24 h. Pure culture medium served as a background control and the supernatant of unstimulated cells as a negative control. As a positive control, cells were severely damaged by incubating them with DMEM/F12 containing 1 % Triton X-100 for 10 min. To prepare the reaction mix, solution A (catalyst) was diluted 1:46 with solution B (dye solution). 50 µl of cell culture supernatant or medium were mixed with 50 µl reaction mix in a 96-well plate. After 30 min incubation at RT in the dark, the absorbance was measured at 450 nm.

2.7. Histology

2.7.1. Preparation of paraffin embedded tissue sections

Osteochondral cylinders were punched out with specific harvesting instruments from the femoral condyles of 7 OA patients (age: min. = 50 years; max. = 85 years; gender: 2 male and 5 female). The generated osteochondral cylinders were fixed in 4 % paraformaldehyde in PBS (pH 7.4) overnight at 4 °C and decalcified in 10 % EDTA (pH 7.4) for 7 to 14 days before preparing them for paraffin embedding by an automated embedding machine (**table 2.11**).

Table 2.11: Protocol for tissue preparation with an automated embedding device

Reagents	Incubation time and temperature
70 % EtOH	4x 1 h RT
96 % EtOH	2x 1 h RT
100 % EtOH	1x 1 h RT
100 % EtOH	1x 2 h RT
Xylene	2x 1 h RT
Xylene	1x 2 h RT
Paraffin	2x 1 h 60 °C
Paraffin	1x 80 min 60 °C

The processed tissue was embedded in paraffin and transferred to a cold plate for paraffin solidification. Paraffin blocks were pre-cooled, before preparing 5 µm tissue sections with the microtome. Tissue sections floating in a water bath (42 °C) were collected using object slides, dried overnight at 37 °C and stored at RT until usage.

2.7.2. Deparaffinization and rehydration of tissue sections

Before staining, the tissue sections were deparaffinized and rehydrated according to the protocol in **table 2.12.**

Table 2.12: Working steps to deparaffinize and rehydrate paraffin sections

Reagents	Incubation time
Xylene	2x 5 min
Isopropanol	2x 5 min
96 % EtOH	3 min
90 % EtOH	3 min
70 % EtOH	3 min
dH_2O	5 min
PBS	5 min

2.7.3. Histological staining of cartilage tissue sections

Before histological staining, tissue sections were deparaffinized and rehydrated as described in **2.7.2. Deparaffinization and rehydration of tissue sections**. Proteoglycans were stained with Safranin-O and non-collagenous structures, like bones with Fast-green. First, the nuclei were stained for 5 min in Weigert's Iron haematoxylin and the slides washed 4x in dH_2O, before treating with 1 % acetic alcohol for 2 sec. After another 3 rinses in dH_2O, slides were incubated in 0.02 % Fast-green for 1 min, 1 % acetic acid for 30 sec, and 1 % Safranin-O for 30 min. After a brief rinse in 95 % EtOH, tissues were dehydrated (3× 95 % EtOH, 2× 100 % EtOH, and 3× xylene), embedded in Entellan and coverslipped. The slides were air-dried and analysed by light microscopy.

2.7.4. Immunohistological staining of cartilage tissue sections

The immunohistological detection of COMP, TSP-4 and Matn-3 was performed with AEC (3-amino-9-ethylcarbazole), a substrate of the horseradish peroxidase (HRP), generating a red reaction product, visualising the localisation of the proteins.

Before immunohistological staining, tissue sections were deparaffinized and rehydrated as described in **2.7.2. Deparaffinization and rehydration of tissue sections**. An antigen retrieval step and a peroxidase block were performed before antibody staining. The volumes of the reagents were adjusted to the area to cover the whole section. Tissue sections used for TSP-4 staining were treated with 250 U hyaluronidase in PBS (pH 5) for 15 min at 37 °C. Staining for COMP and Matn-3 required an antigen retrieval with 20 µg/ml proteinase K in proteinase K buffer (10 mM NaCl, 50 mM Tris base, 10 mM EDTA in ddH_2O, pH 7.4) for 15 min at 37 °C.

The endogenous peroxidase activity was blocked with 0.3 % H_2O_2 in dH_2O for 10 min at RT. Unspecific binding sites were blocked with 2.5 % normal horse serum (included in the ImmPRESS™ kit) for 20 min at RT. Primary antibodies (**table 2.6**) were diluted in 1 % BSA and added to the tissue, for incubation overnight at 4 °C. After incubation with the primary antibody, the tissues were washed 3x with PBS-T following the incubation with the ImmPRESS™ (peroxidase) polymer anti-rabbit IgG reagent for 30 min at RT. For detection, the AEC-2-component kit was used according to the manufacturer's instructions. 20 µl AEC concentrate was mixed with 1 ml AEC substrate and immediately used. The colour development was stopped with dH_2O, the tissues embedded in Kaiser's

glycerol gelatine and coverslipped. The slides were air-dried and analysed by light microscopy.

As a negative control, tissues were stained without the addition of the primary antibody to exclude unspecific binding of the secondary antibody (data not shown).

2.7.5. Immunofluorescence staining of primary chondrocytes

Cultured chondrocytes in chamber slides were fixed with 300 µl Shandon™ zinc formal-fixx™ (diluted 1:5 with dH_2O) for 20 min at RT, washed 3x with 500 µl PBS and permeabilized with 350 µl 0.3 % Triton X-100 in PBS for 10 min at RT. Unspecific binding sites were blocked with 350 µl blocking buffer for 1 h at RT. Primary antibodies were diluted in 1 % BSA in PBS to the recommended concentration (**table 2.6**) and 300 µl transferred to the cells. The primary antibody incubation was performed overnight at 4 °C. After 3x 5 min washing with PBS-T, 300 µl of the secondary antibodies, diluted in 1 % BSA in PBS (**table 2.8**) were added for 1.5 h at RT in the dark. The cells were washed twice 5 min with PBS-T and once 5 min with PBS before removing the plastic chambers of the chamber slides and mounting with the DAPI fluoroshield mounting medium. The slides were air-dried in the dark and analysed by fluorescence microscopy. DAPI was visualised at a wavelength of 461 nm, AlexaFluor 488 at 516nm and AlexaFluor 594 at 617 nm.

Blocking buffer	1 %	BSA
	1 %	Goat serum
		in PBS

2.8. Light and fluorescence microscopy

Cultured cells were observed with the Olympus CKX41 light microscope and the cellSens Entry software. Images of Safranin-O and crystal violet staining of chondrocytes were also taken with the Olympus microscope. All other, light and fluorescence images of stained tissue sections and cells were taken with the Nikon Eclipse Ti and the NIS Elements BR 4.40.00 software.

2.9. Protein extraction

2.9.1. Sequential and total protein extraction from articular cartilage

Articular cartilage of human knee femoral condyles was scraped off from areas with specific OA severity grades (G1, G2, and G3/4). Only patients, showing all three severity grades were included (n: 10 in each group; age: min. 47 years; max. 87 years; gender: 5 male and 5 female). The cartilage from areas with different severity grades was collected separately, washed with PBS and cut into pieces (1–2 mm^3). Cartilage pieces were transferred into tubes, weighed and processed immediately. Proteins were sequentially extracted, first with a mild and then with a harsh buffer (see below) overnight at 4 °C on a rotator at 40 rpm. 10x the volume (ml per gram) of chilled buffer were added. The proteinase inhibitors PMSF and NEM were added freshly to all buffers at a concentration of 2 mM. After 24 h incubation with the mild buffer, the extracts were clarified by centrifugation at 17 000 x g, 5 min at 4 °C and the supernatants stored at −20 °C. The remaining cartilage pieces in the pellet were reextracted in an identical manner with the harsh buffer. Also, the total amount of proteins was extracted by adding only the harsh buffer overnight [54].

Mild buffer	0.15 M	NaCl
	50 mM	Tris base
		pH 7.4, in ddH_2O
Harsh buffer	4 M	Guanidine hydrochloride
	50 mM	Tris base
	10 mM	EDTA
		pH 7.4, in ddH_2O

Proteins extracted with the mild and/or the harsh buffer (sequential and total) were precipitated with 10x the volume of 96 % EtOH for 24 h at −20 °C. The protein precipitate was concentrated by centrifugation at 17 000 x g, 10 min at 4 °C and the pellet washed with a mixture of 9-parts 96 % EtOH and 1-part TBS for 2 h at 4 °C with gentle agitation. After centrifugation at 17 000 x g, 10 min at 4 °C the supernatant was completely removed and the pellets air-dried, before resuspension in 60 µl 1× Laemmli buffer (in ddH_2O). Protein aliquots were cooked for 5 min at 95 °C before storing at −20 °C or loading onto a gel (**2.12. SDS-polyacrylamide gel electrophoresis (PAGE)**).

Laemmli buffer (4x)	250 mM	Tris-HCl, pH 6.8
	40 %	Glycerol
	0.04 %	Bromophenol blue
	8 %	SDS
		in ddH_2O

2.9.2. Total protein extraction from primary chondrocytes

Primary chondrocytes, cultured in 6-well plates were washed 3x with PBS. 50 µl 2x Laemmli buffer was added and the protein lysate collected with a cell scraper. The protein suspension was cooked for 5 min at 95 °C before storing at −20 °C or loading onto a gel (**2.12. SDS-polyacrylamide gel electrophoresis (PAGE)**).

Laemmli buffer (2x)	1000 µl	Laemmli buffer (4x)
(working stock)	800 µl	PhosphoSafe™
	200 µl	β-mercaptoethanol

2.10. Protein purification with affinity chromatography

Recombinant proteins were purified with the Strep-Tactin® XT superflow high capacity gravity-flow columns. Strep-tagged proteins bind the Strep-Tactin® pockets in the column matrix. To remove the bound proteins from the matrix, biotin, the natural ligand of streptavidin is loaded to displace the strep-tagged protein.

After equilibration with 2 column bed volumes (CV) buffer W, the column was loaded with the collected cell culture supernatant (**2.4.2.3. Collection of the cell culture supernatant**) by using the WET FRED device, which enables the autonomous transfer of the supernatant to the column by hydrostatic pressure, overnight. The next day, the column was washed, with 5x 1 CV buffer W and the proteins eluted by BXT buffer. In total, 9 protein fractions were eluted with either 600 µl (fraction 1) or 500 µl (fraction 2-9) BXT buffer. The protein concentration was measured (**2.11. Protein quantification**) and the protein quality analysed by SDS-PAGE, staining the whole proteins (**2.13. Protein staining**) and specific recombinant proteins (**2.14. Immunoblot analysis**). After protein elution, the column was regenerated by washing with 15 CV 10 mM NaOH and stored at 4 °C until reuse.

Buffer W	100 mM	Tris-HCl, pH 8.0
	150 mM	NaCl
	1 mM	EDTA
		in ddH_2O
Buffer BXT	100 mM	Tris-HCl, pH 8.0
	150 mM	NaCl
	1 mM	EDTA
	50 mM	Biotin
		in ddH_2O

2.11. Protein quantification

The Qubit protein assay kit contains a fluorescent dye, specifically binding proteins. Only the protein bound fluorophore emits a signal detected by the Qubit fluorometer.

First, the Qubit working solution was prepared by mixing the Qubit reagent 1:200 with the Qubit buffer. 10 µl of each standard was diluted with 180 µl Qubit working solution. Depending on the expected protein amount, 1-20 µl of the protein solution was mixed with Qubit working solution to a final volume of 200 µl. Before measurement, the mixtures were vortexed and incubated for 15 min at RT in the dark. The Qubit fluorometer calculated the final protein amount and displayed it in µg/ml.

2.12. SDS-polyacrylamide gel electrophoresis (PAGE)

Protein extracts and serum samples mixed with Laemmli buffer were separated in an SDS-PAGE (214) using a Mini-PROTEAN® Tetra-cell system at 200 V. According to the protein size, gels with different polyacrylamide concentrations were used. Non-reduced protein extracts from OA cartilage and non-reduced serum samples of OA patients and healthy controls were separated by SDS-PAGE using 5 % or 8 % polyacrylamide gels. Reduced pig chondrocyte lysates were loaded onto 10 % polyacrylamide gels. First, the separating gel with individual polyacrylamide concentrations was filled between the glass slides and the polymerisation induced by the addition of TEMED and APS. To even the gel surface the gel solution was directly overlayed by isopropanol. The isopropanol was completely removed, before adding the stacking gel (4 %). The combs were applied without creating any bubbles. After polymerisation, the combs were removed and the

protein samples loaded. To estimate the protein size either the precision plus protein™ dual color standard or the prestained protein ladder was loaded.

Separating gel

	5 %	8 %	10 %
Acrylamide (40 %)	1.5 ml	2.4 ml	3 ml
Separating gel buffer	3 ml	3 ml	3 ml
H_2O	7.5 ml	6.6 ml	6 ml
APS (10 %)	120 µl	120 µl	120 µl
TEMED	20 µl	20 µl	20 µl

Stacking gel

	4%
Acrylamide (40 %)	300 µl
Stacking gel buffer	750 µl
H_2O	1.95 ml
APS (10 %)	30 µl
TEMED	10 µl

Separating gel buffer	1.5 M	Tris base
	0.4 %	SDS
		pH 8.8, in ddH_2O
Stacking gel buffer	0.5 M	Tris base
	0.4 %	SDS
		pH 6.8, in ddH_2O
Gel running buffer (10x)	250 nM	Tris base
	2 M	Glycine
	1 %	SDS
		in ddH_2O

2.13. Protein staining

PageBlue™ or Roti®Blue staining solutions were used to stain all proteins separated by SDS-PAGE.

PageBlue™ protein staining solution was applied after the gels were washed 3x 10 min with ddH_2O overnight at RT with gentle agitation. To remove any background the staining solution was decanted and the gels washed with ddH_2O.

Roti®Blue staining solution was added to the gel after a brief wash in ddH_2O and incubated overnight at RT with gentle agitation. The next day, the staining solution was decanted and the gels washed in 25 % MeOH until the background staining diminished.

Roti®Blue staining solution	120 ml	H_2O
	40 ml	MeOH
	40 ml	Roti®Blue

2.14. Immunoblot analysis

2.14.1. Transfer

The tank method was performed, by using the mini Trans-blot® electrophoretic transfer cell to transfer the proteins onto a 0.45 µm PVDF membrane. Before blotting the PVDF membrane was activated with 99 % methanol for 10 sec, kept in ddH_2O for 2 min and equilibrated in transfer buffer for at least 5 min. Fibre pads and filter paper were soaked in transfer buffer before building the blot complex on the blotting cassette. Therefore, fibre pad, filter paper, gel, PVDF membrane, filter paper and fibre pad are stacked in that order from the bottom to the top. All bubbles were removed with a roller and the closed cassette placed into the blotting chamber, containing transfer buffer and an ice block to prevent overheating. The blotting was performed at 200 mA for 1 h at 4 °C.

Towbin buffer (10x)	250 nM	Tris base
	2 M	Glycine
	0.1 %	SDS
		in ddH_2O

Transfer buffer (1x)	100 ml	Towbin buffer (10x)
	50 ml	MeOH
	850 ml	ddH_2O

2.14.2. Antibody detection

After electrophoresis, proteins bound to the PVDF membrane were ready for antibody detection. To prevent an unspecific antibody binding, the membrane was blocked with either 10 % skim milk (in TBS-T) for the detection of ECM proteins or 5 % BSA (in TBS-T) for the detection of (phosphorylated) Smads, Erk and GAPDH for 1 h at RT with gentle agitation. Then, the membrane was incubated with specific primary antibodies (**table 2.6**) diluted in blocking buffer overnight at 4 °C. The next day, the membrane was washed 5x 5 min with TBS-T buffer and incubated with the corresponding secondary antibody (**table 2.8**), diluted in blocking buffer for 1 h at RT, before 5x 5 min washing with TBS-T buffer.

The Strep-Tactin®-HRP conjugate (**table 2.7**) was used to detect the Strep-Tag II. Therefore, the membrane was blocked in PBS blocking buffer for 1 h at RT with gentle agitation. Directly after blocking the membrane was washed 3x 5 min with PBS-T. The Strep-Tactin®-HRP conjugate was first pre-diluted 1:100 in PBS (containing 0.2 % BSA and 0.1 % Tween-20) and then from this pre-dilution 10 µl diluted in 10 ml PBS-T. The membrane was incubated with the antibody for 1 h at RT with gentle agitation. Then the membrane was washed twice 1 min with PBS-T and twice 1 min with PBS.

PBS blocking buffer	3 %	BSA
	0.05 %	Tween-20
		in PBS

The protein bands were visualised by incubating the membrane 5 min with 10 ml ECL working solution and an analysis with the Chemi DocTM XRS+ molecular imager and the ImageLab™ software. The band intensities were quantified with ImageJ.

ECL solution	0.1 M	Tris-HCl, pH 8.5
	225 mM	p-Coumaric acid
	1.25 mM	Luminol
		in ddH_2O
ECL working solution	10 ml	ECL solution
	30 µl	H_2O_2 (3 %)

To detect different proteins on the same membrane, the primary and/or secondary antibody was/were removed by stripping buffers. After stripping off the antibodies, the membrane was blocked and incubated with primary antibodies, according to the protocol above. The membranes were stripped with a mild or harsh stripping buffer, depending on the strength of the antibody binding, the species of the following new antibody and the size of the target protein. Every membrane stripping, especially under harsh conditions causes a loss of protein, thus predominantly the mild stripping buffer was used. Anti-pSmad2 and anti-GAPDH were stripped off with the harsh stripping buffer while all others were removed under mild conditions.

For harsh stripping, the membrane was transferred into pre-warmed stripping buffer in a closed vessel. After an incubation of 45 min at 50 °C with gentle agitation the stripping buffer was removed and the membrane rinsed under tap water for 2 min. To completely remove β-mercaptoethanol, the membrane was additionally washed twice 5 min with TBS-T.

For a mild stripping, the membrane was washed twice 15 min with mild stripping buffer at RT with gentle agitation. Then, the membrane was washed twice 10 min with PBS and twice 5 min with TBS-T.

Mild stripping buffer	15 g	Glycine
	1 g	SDS
	10 ml	Tween-20
		pH 2.2, in 1l ddH_2O
Harsh stripping buffer	20 ml	SDS (10 %)
	12.5 ml	Tris-HCl (0.5 M, pH 6.8)
	0.8 ml	β-mercaptoethanol
	67.5 ml	ddH_2O

2.14.3. Dot Blot

Proteins were directly spotted onto a membrane and not separated by size like in SDS-PAGE. To avoid pre-wetting of the membrane, a nitrocellulose membrane instead of PVDF was used for this experiment. This method was used to control the protein expression levels of transfected HEK-293 EBNA cells.

1-2 µl cell culture supernatant or purified protein were directly spotted onto a 0.45 µm nitrocellulose membrane. After drying the membrane, the protocol for antibody detection (**2.14.2. Antibody detection**) was followed.

2.15. RNA isolation

RNA was isolated from chondrocytes with the NucleoSpin®RNA/protein purification kit according to the manufacturer's manual. In brief, cells in culture were lysed with a mix of the enclosed lysis buffer with β-mercaptoethanol. Then, the cell lysate was collected with a cell scraper and transferred into a tube. Cells, already pelleted were directly lysed in the lysis buffer mix. After vortexing, the cell lysates were loaded onto the NucleoSpin® filter column for filtration and the RNA bound to the membrane in the NucleoSpin® RNA/protein column. After a desalting step, the contained DNA was digested by rDNase. The membrane was washed and dried before pure RNA was eluted in RNase-free H_2O. Eluted RNA was directly used for concentration measurement (**2.16. RNA quantification**) and either stored at -80 °C or used for cDNA synthesis (**2.17. cDNA synthesis**).

2.16. RNA quantification

The NanoDrop OneC is a spectrophotometer, used to determine the concentration and purity of RNA. The absorption maximum of DNA and RNA is at 260 nm, while proteins exhibit an absorbance of 280 nm.

Therefore, 1 µl RNA was loaded onto the sensor pedestal and the concentration described as µg/µl. RNase-free H_2O was used as a blank. Between different samples, the sensor was cleaned with RNase-free H_2O.

2.17. cDNA synthesis

RNA was converted into cDNA with reverse transcriptase by using the qScript cDNA supermix according to the manufacturer's manual. The reaction mix (**table 2.13**) was prepared in PCR tubes and the cDNA synthesised in the qTOWER3G thermal cycler by using the protocol in **table 2.14**. The synthesised cDNA was stored at -20 °C or directly used as a template for (q)PCR (**2.18. (quantitative) Polymerase chain reaction (PCR or qPCR)**).

Table 2.13: Composition of the cDNA mix

Standard cDNA mix	
8 µl	qScript reaction mix
2 µl	qScript RT
20 µl	RNA
10 µl	Nuclease-free H_2O
40 µl	Total

Table 2.14: Protocol used for cDNA synthesis

Cycles	**Temp**	**Time**
1x	22 °C	5 min
1x	42 °C	30 min
1x	85 °C	5 min
1x	4 °C	∞

2.18. (quantitative) Polymerase chain reaction (PCR or qPCR)

(q)PCR was used to amplify and quantify amounts of DNA sequences in a thermal cycler by various heating and cooling steps. All primer sequences are shown in **table 2.9**. All reactions were performed in doublets by using the qTOWER3G thermal cycler.

To amplify cDNA via PCR, the Taq PCR master mix kit was used. Standard PCR mix and PCR protocol are shown in **table 2.15** and **2.16**. The PCR products were either stored at -20°C or directly separated by size (**2.19. Agarose gel electrophoresis**).

Table 2.15: Composition of the PCR mix

Standard PCR mix	
10 µl	Taq PCR master mix
2 µl	Fw primer (10 nM/µl)
2 µl	Rev primer (10 nM/µl)
10 ng	cDNA
variable	ddH_2O
20 µl	Total

Table 2.16: Protocol used for PCR

Cycles	**Temp**	**Time**	**Steps**
1x	94 °C	1 sec	Initial denaturation
36x	94 °C	30 sec	Denaturation
	64 °C	30 sec	Primer annealing
	72 °C	60 sec	Elongation
1x	4 °C	∞	Cooling

The PerfeCTa SYBR® green supermix was used to quantify specific genes by qPCR. Standard qPCR mix and qPCR protocol are shown in **table 2.17** and **2.18**.

Table 2.17: Composition of the qPCR mix

Standard qPCR mix	
10 µl	SYBR green supermix
2 µl	Fw primer (10 nM/µl)
2 µl	Rev primer (10 nM/µl)
7 ng	cDNA
variable	ddH_2O
20 µl	Total

Table 2.18: Protocol used for qPCR

Cycles	**Temp**	**Time**	**Steps**
1x	95 °C	2.5 min	Initial denaturation
40x	95 °C	15 sec	Denaturation
	60 °C	30 sec	Primer annealing
Melt curve			

2.19. Agarose gel electrophoresis

PCR amplicons were analysed by using a 1.8 % agarose gel. Therefore, agarose was transferred to 100-150 ml TBE buffer (1x) and boiled up in the microwave until agarose was completely dissolved and the solution clear. The solution was cooled down to ~60 °C under rinsing water. GelRed nucleic acid gel stain was added to a final concentration of 1x and mixed by swivelling. The liquid agarose was filled into the gel tray and combs added. During the gel polymerization, the PCR amplicons were prepared for loading. Thereby, half the volume of orange G loading dye was added to the amplicons. To estimate the size of the PCR products 3 µl of the GeneRuler™ 1 kb DNA ladder working solution was loaded. The electrophoresis was performed with 120 V for 1.5 h in 1x TBE buffer in the Sub-Cell GT cell horizontal electrophoresis system.

Orange G loading dye	0.075 %	Orange G
	30 %	Glycerol
GeneRuler™ 1 kb DNA ladder (working solution)	1 µl	DNA ladder
	1 µl	TriTrack DNA loading dye
	4 µl	ddH_2O

The gels were analysed with the Chemi DocTM XRS+ molecular imager and the ImageLab™ software and the band intensities quantified with ImageJ. The band intensities of all genes were normalised to the band intensity of *GAPDH*. The band size of every PCR amplicon was counterchecked with the expected band size to validate specificity.

2.20. Migration assay

A migration assay was performed to test the ability of COMP and TSP-4 to attract chondrocytes or HUVECs. Therefore, the transwell system with ThinCert™ cell culture inserts containing a polyethylene terephthalate (PET) membrane with a pore size of 8 µm, was used (**Fig.2.2.A**). This membrane separates the upper compartment of the insert and the lower compartment of the culture plate, forming a migration chamber. The cells placed in the upper compartment of the insert can migrate into the membrane by adding attracting substances to the lower compartment. The migrated cells can then be visualised by staining their nuclei with DAPI.

In a pilot study, the migration of chondrocytes to the negative and positive control was tested for 6 h, 8 h and 10 h. A migration time of 10 h was considered as the most stable and conclusive incubation time and all following experiments performed under this condition. Within the pilot study, the number of chondrocytes migrated into the membrane and through the membrane to the lower compartment was analysed. To count the cells in the lower compartment, the cells were allowed to attach for 2 h before fixation. The majority of chondrocytes was detected within the membrane and only a few in the lower compartment. The amounts of the chondrocytes detected in the lower compartment were comparable between conditions, therefore, only chondrocytes in and on the bottom of the membrane were counted in the following experiments.

400 µl medium (chondrocyte = DMEM/F12 and HUVEC = EBM-2) containing 0.1 % BSA with either 10 µg/ml COMP or 10 µg/ml TSP-4 were added to the lower compartment of a 24-well plate. As a positive control, chondrocytes were attracted with 10 ng/ml platelet-derived growth factor-BB (PDGF-BB) (215) and HUVECs with EGM-2 medium. As a negative control, the plenty medium was added in the lower compartment. Chondrocytes were directly used after isolation from knee cartilage and HUVECs cultured until confluency was reached. Both cell types were washed twice with PBS before used in migration assays. 50 000 cells in 200 µl medium were transferred to the upper compartment of the inserts. After 10 h incubation at 37 °C, 5 % CO_2 and 20 % O_2, the cells within and on the bottom of the membrane were fixed with 400 µl Shandon™ zinc formal-fixx™ for 20 min at RT. Therefore, Shandon™ zinc formal-fixx™ working solution (1:5 diluted in dH_2O) was prepared in another 24-well plate and the inserts transferred into the solution. After fixation, the inserts were transferred to a plate filled with ddH_2O and the liquid in the inserts replaced with ddH_2O. The 24-well plate with the inserts was sealed with parafilm and stored at 4°C overnight. The following day, the non-migrated cells on top of the membrane were removed by flashing the insert with ddH_2O and swabbing it with a cotton bud. The inserts were then transferred to a new 24-well plate filled with 400 µl DAPI solution (DAPI stock = 40 µg/ml; diluted 1:100 in PBS). No liquid was added in the upper compartment during this 5 min incubation step at RT in the dark. The inserts were quickly placed in tap water and transferred to a new 24-well plate filled with 400 µl ddH_2O. 200 µl ddH_2O was added to the upper compartment. The migrated cells were then imaged with a

fluorescent microscope at a wavelength of 461 nm. 5 pictures from different areas of the membrane were taken (**Fig.2.2.B**) and the number of cells counted with ImageJ. Based on the negative control, the fold change of COMP, TSP-4 and the positive control were calculated. All technical replicates were performed at least in doublets.

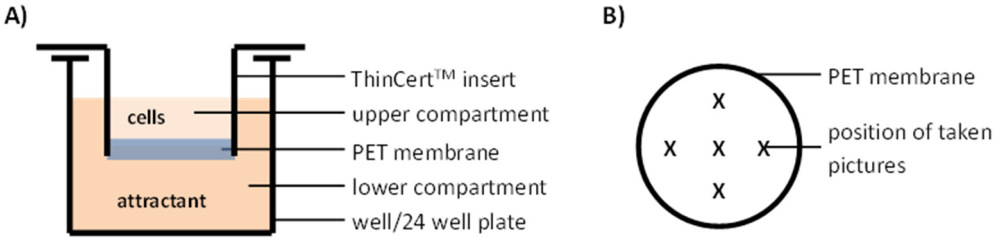

Figure 2.2: Schematic image of a migration assay
A) Schematic drawing of the migration chamber and **B)** the position of the membrane, where pictures were taken.

2.21. Attachment assay

An attachment assay was performed to investigate the attachment of chondrocytes to COMP and TSP-4 in a monolayer system. In that manner, wells of a 96-well plate were coated with 10 µg/ml COMP and TSP-4 in PBS. As a negative control, 100 mg/ml BSA and as a positive control, 10 µg/ml fibronectin, were used. 100 µl of recombinant protein, in the indicated concentration, were added to each well and incubated overnight at 4°C. The following day, the wells were washed twice 5 min with PBS and once 5 min with DMEM/F12 containing 0.1 % BSA. After blocking with 100 µl 1 % BSA for 3 h at RT, chondrocytes were added at a concentration of 50 000 cells in 100 µl DMEM/F12 containing 0.1 % BSA. Chondrocytes were incubated for 1 h at 37 °C and 5 % CO_2 in a CO_2-incubator. Following the incubation, the supernatant was carefully removed and the wells briefly washed twice with PBS. Chondrocytes were fixed with 100 µl Shandon™ zinc formal-fixx™ (1:5 dilution in ddH_2O) for 20 min at RT. Cells were washed 3x 5 min with PBS and stained with 100 µl 0.1 % crystal violet (dissolved in ddH_2O) for 30 min at RT. The cells were washed 3x 5 min with ddH_2O and imaged with a light microscope. The number of cells was counted and the fold change to the negative control calculated. All technical replicates were performed in triplicates.

2.22. Proliferation assay

To test the effect of COMP and TSP-4 on HUVEC proliferation the EdU cell proliferation kit was used. EdU (5-ethynyl-2'deoxyuridine) an analogue to the nucleoside thymidine was added to the cell culture medium and incorporated in the newly synthesised DNA of proliferating cells and fluorescently labelled in an additional step. The fluorescence labelled EdU is then detectable with a fluorescence microscope. A parallel DAPI staining of all cells allows the calculation of proliferating cells.

7 500 cells in 300 µl EGM-2 medium were seeded in each well of a 48-well plate cultivated overnight at 37 °C and 5 % CO_2. The next day, the EGM-2 medium was replaced by EBM-2 medium (always containing 0.1 % BSA) and the cells cultivated for 8 h at 37 °C and 5 % CO_2. After the starving period, HUVECs were incubated with EBM-2 medium, containing 2 µl/ml EdU (10 µM in DMSO) and 10 µg/ml COMP or TSP-4 for 24 h. EBM-2 medium was used as a negative and EGM-2 medium as a positive control. The next day, the cells were directly fixed with 4 % formalin for 15 min at RT and permeabilized with 0.5 % Triton X-100 in PBS for 20 min at RT. During the permeabilization time, the click reaction cocktail was prepared. For a successful experiment, the ingredients have to be added chronologically and the reaction cocktail used within 15 min.

EdU stock (10 mM)	5 mg	EdU
	2 ml	DMSO
Buffer additive (10x)	200 g	Buffer additive
	2 ml	ddH_2O
Reaction cocktail	379 µl	ddH_2O
	50 µl	Reaction buffer (10x)
	20 µl	Catalyst solution
	1 µl	Dye azide (10 mM)
	50 µl	Buffer additive (10x)
	500 µl	Total

After removing the permeabilization solution, the cells were quickly washed with 3 % BSA in PBS and incubated with 100 µl reaction cocktail for 30 min at RT in the dark. The cells were washed twice with 3 % BSA in PBS and DAPI stained (1:10 000 in PBS) for 5 min at RT in the dark. The cells were washed with PBS and analysed in a fluorescence

microscope. The proliferating, EdU positive cells could be observed at a wavelength of 516 nm and the DAPI stained cells at 461 nm. 5 pictures were taken and the number of cells counted with ImageJ. The percentage of proliferating cells was calculated, based on the total cell count. All technical replicates were performed in triplicates.

2.23. Tube formation assay

A tube formation assay was performed to study the effects of COMP and TSP-4 on angiogenesis. The Geltrex™ basement membrane matrix was used to provide a 3D environment, better reflecting the *in vivo* conditions. This allows the cells to disrupt the surrounding matrix and form 3D tubular structures (**Fig.2.3**).

Therefore, the Geltrex™ matrix was thawed overnight at 4°C and 50 µl of the soluble matrix pipetted in each well of a pre-cooled 96-well plate with pre-cooled pipette tips. All bubbles were removed and the plate swivelled for homogenous distribution. Following, the soluble Geltrex™ was polymerized for 30 min at 37 °C.

HUVECs were resuspended in EBM-2 medium containing 0.1 % BSA and 10 µg/ml COMP or TSP-4. EBM-2 medium containing 0.1 % BSA was used as a negative control and EGM-2 medium as a positive control. 15 000 cells in 100 µl medium were added onto the Geltrex™ matrix of each well and cultured at 37 °C and 5 % CO_2 for 24 h. After 6 h and 24 h, the tube network was analysed by light microscopy and the tube length as well as the number of junctions evaluated after 24 h. All technical replicates were performed in triplicates.

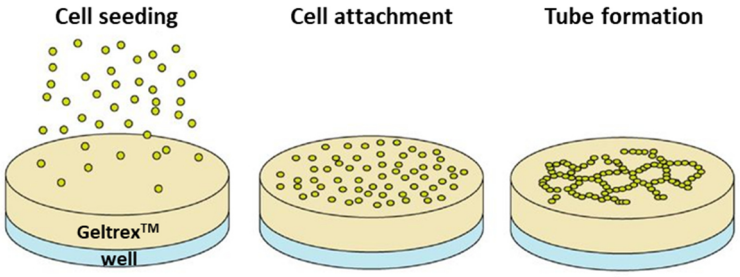

Figure 2.3: Tube formation assay
HUVECs are seeded onto the Geltrex™ matrix, attach and form a tubular network within 24 h. (modified from © ibidi GmbH)

2.24. Surface plasmon resonance spectroscopy

The interaction between proteins was measured with the Biacore 2000. This machine enables real-time monitoring of protein interaction by using the surface plasmon resonance (SRP) technology. The ligand, is covalently immobilised on the sensor surface of a CM5 sensor chip, while the analyte, is in suspension and induced to the surface to pass over the ligand in a continuous flow. The binding and dissociation of the analytes are detected and recorded in response units (RU) (**Fig.2.4**).

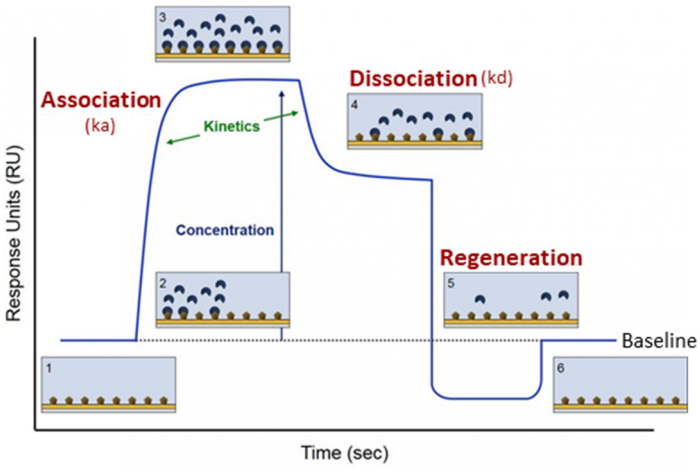

Figure 2.4: Illustration of a sensorgram, showing the procedure of surface plasmon resonance spectroscopy
A sensorgram, showing the response unites (RUs) against the time (sec). At the beginning of the report, a baseline signal (**1**) of the unmodified sensor chip is visible. After inducing the analyte, a ligand-analyte binding occurs (**2**), observable in an increase of the RUs. After a completed analyte injection (**3**), the analytes start to dissociate from the surface (**4**), resulting in a decrease in the RUs. The injection of the regeneration buffer (**5**) results in the removal of all remaining analytes bound to the surface and restores the baseline level (**6**). Modified from https://shared-resources.dhvi.duke.edu/dhvi-core-facilities/dhvi-bia-core.

To couple the ligand, TGF-β1 to the sensor surface the Biacore system was equilibrated with running buffer at a flow rate of 5 µl/min. After activating the CM5 chip with 0.05 M NHS/0.2 M EDC (Biacore AB), 50 µl TGF-β1 (1500 RU) were injected with a flow rate of 5 µl/min. All free binding sites were blocked with 50 µl 1 M ethanolamine (pH 8.5; Biacore AB) and the chip washed twice with 5 µl running buffer (Biacore AB).

All experiments were performed at 25 °C and with a CM5 sensor chip coupled with 1500 U TGF-β1. As a reference, a flow cell without an immobilised ligand was used. A 1:2 dilution series from a concentration of 160 nm to 0 nm of the analytes, COMP and TSP-4 were prepared in running buffer. A volume of 120 µl of each concentration per cycle was required. The system was equilibrated at a flow rate of 30 µl/min with running

buffer and the experiment started when a stable baseline was reached. The injection of the analyte was started and data were collected for kinetic analysis. One analyte concentration per cycle was injected, starting with the lowest concentration. The chip was regenerated after each cycle with 2 M NaCl.

The BIAevaluation software 3.0 was used to create a sensorgram, showing the response against the time. By doing a multi-cycle kinetic, several analyte concentrations were induced in separate cycles, resulting in multiple curves in the sensorgram. By fitting the curves to the mathematical 1:1 model, the association rate (ka), dissociation rate (kd) and the dissociation constant (K_d) was evaluated.

2.25. Statistical analysis

Statistical analysis was performed by using the SigmaPlot software. Differences between groups were evaluated with the appropriate statistical test and post-hoc analyses, as mentioned in the figures. Correlations between groups were analysed with the Spearman rank test (r). A p-value ≤ 0.05 was considered as a significant difference ($p \leq 0.05$*; $p \leq 0.01$**; $p \leq 0.001$***).

3. Results

3.1. Collection and scoring of human articular cartilage

Knee condyles from 21 patients undergoing endoprosthetic knee replacement surgery, at the Orthopaedic University Hospital Friedrichsheim (Frankfurt/Main, Germany), were obtained. The morphological appearance of the articular cartilage was visually graded, based on the scoring system of the Osteoarthritis Research Society International (OARSI) (**Fig.3.1**). The cartilage surface of knee condyles was inspected and intact cartilage areas with a smooth surface and no fissures were scored as grade 1 (G1). Cartilage areas, showing superficial discontinuities and fissures were scored as grade 2 (G2), and areas with deep fissures or exposure of the subchondral bone, as grade 3 and grade 4, respectively (G3 or G4). The amount of cartilage received from areas of G3 and especially G4 was limited. Therefore, grade 3 and grade 4 samples were combined and referred to as G3/4. Healthy cartilage, from non-OA patients were generally classified as grade 0 (G0).

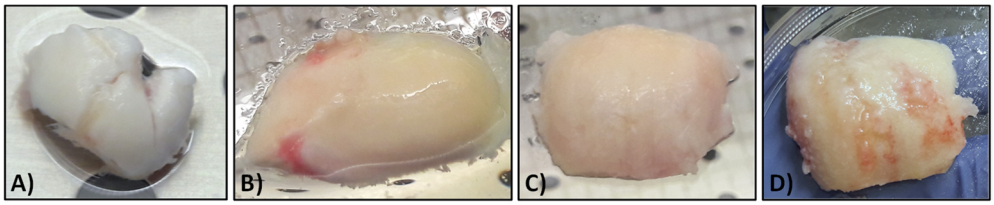

Figure 3.1: Femoral knee condyles of human OA patients
Pictures of femoral knee condyles received from OA patients undergoing endoprosthetic knee replacement surgery. Condyles were visually scored, based on the scoring system of the Osteoarthritis Research Society International (OARSI). Thereby, healthy cartilage (G0) (**A**) and three severity grades (G1, G2 and G3/4) were distinguished: (**B**) G1: Intact cartilage with a smooth surface and no fissures; (**C**) G2: Cartilage with superficial discontinuities and fissures and (**D**) G3-4: deep fissures or exposed subchondral bone, respectively.

3.2. TSP-4 is hardly detectable in healthy but widely expressed in OA cartilage

A characteristic of OA is extracellular matrix degradation but also the new synthesis of distinct ECM proteins. The presence and distribution of proteoglycans were investigated by Safranin-O staining of cartilage sections. Proteoglycans were ubiquitously and homogeneously stained in healthy cartilage but started to be degraded, in OA cartilage, continuously from G1 to G3/4 (**Fig.3.2.B–E**). The continuous degradation of proteoglycans in OA cartilage confirmed the visual scoring of OA severity grades by its articular surface condition. In stage G3/4, the superficial and the upper transitional zones were already degraded, and cell cluster formation observed (**Fig.3.2.I''**). TSP-4 was hardly detectable in healthy cartilage and only observable as faint staining in the superficial zone (blue boxes). In general, OA tissues, independently of severity grade, were more intensely stained than healthy cartilage. The most intense TSP-4 staining was seen in the transitional zone (yellow boxes) of OA cartilage, in areas where proteoglycans were still detectable but already started to be degraded. The TSP-4-positive area expands and the borders become blurry with increasing severity grade. Besides, the ubiquitous distribution of TSP-4 in the ECM, especially in the transitional zone, intracellular staining could be detected. In deep cartilage layers (black boxes), the interterritorial staining was weaker compared to the transitional zone and a stronger pericellular as well as intracellular staining was detected. The overall staining intensity seems to increase with severity (**Fig.3.2.F–I**). Minor changes in the protein distribution depending on OA severity could be detected (**Fig.3.2.F'–I'''**). In the deep zone, the signal intensity in the interterritorial matrix was increased in G3/4 compared to G1 and G2 cartilage (**Fig.3.2.F'''–I''**). COMP was ubiquitously and homogenously distributed in healthy cartilage but continuously degraded in all OA tissues (**Fig.3.2.J-M**). In the most damaged G3/4 area, a re-expression of COMP could be detected, especially in the upper cartilage layers (**Fig.3.2.M**). Matn-3 was weekly stained in all zones of healthy cartilage, mainly in close proximity to chondrocytes and intracellularly but the staining intensity increased with severity grade, especially in the territorial and interterritorial matrix (**Fig.3.2.N-Q**). ECM remodelling in OA results in COMP degradation and re-expression in upper areas as well as in increased protein levels of Matn-3 and especially TSP-4, in zones it is usually not expressed (**Fig.3.2.R**).

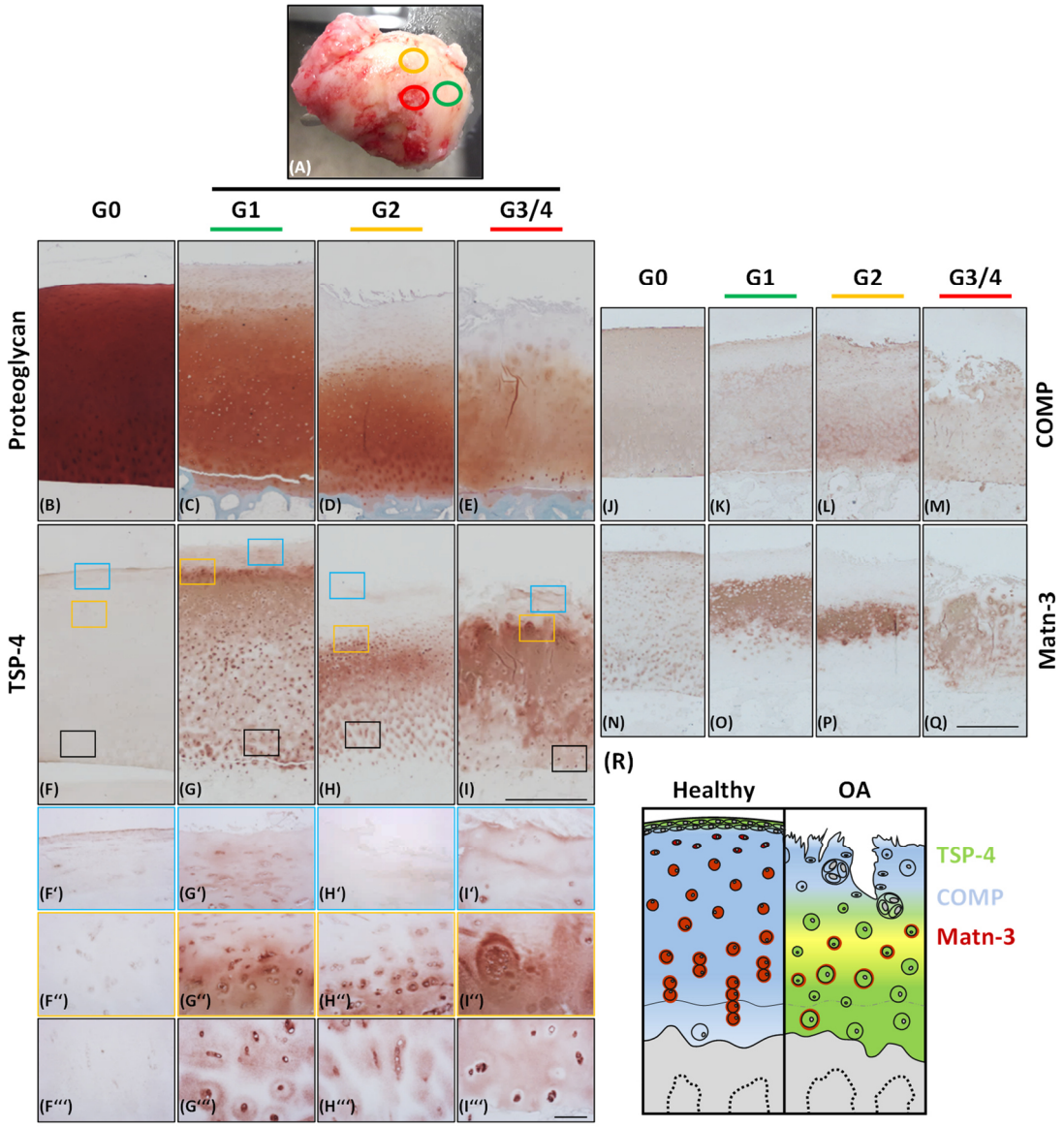

Figure 3.2. Proteoglycan and ECM protein localisation in healthy and OA articular cartilage
A) Osteochondral cylinders were generated from femoral condyles and the severity grade was determined by visual inspection (green = grade 1 [G1], orange = grade 2 [G2], red = grade 3/4 [G3/4]). Proteoglycans were stained with Safranin-O/Fast-green in healthy [G0] (**B**), G1 (**C**), G2 (**D**), and G3/4 (**E**) OA cartilage, taken from the knee condyle shown above (**A**). Proteoglycan degradation is paralleling with progressing OA severity. TSP-4 levels increase from G0 (**F**) to G1 (**G**), G2 (**H**), and G3/4 (**I**) OA cartilage. 40× magnification of the marked areas (blue = superficial zone, orange = transitional zone, black = deep zone) drawn in picture **F-I**, representing the differential distribution of TSP-4 in surface areas (**F'–I'**), the transitional zone, where the most intensive staining occurred (**F''–I''**), and deep areas (**F'''–I'''**) of OA cartilage. COMP levels decrease from G0 (**J**) to G1 (**K**), G2 (**L**) and G3/4, although at that point, also a re-expression, is observed in the superficial layers (**M**). Matrilin-3 (Matn-3) levels increase from G0 (**N**), G1 (**O**), G2 (**P**) and G3/4 (**Q**). **R**) Schematic representation of the distribution of TSP-4, COMP and Matn-3 in healthy and OA cartilage. Representative pictures from different donors are shown. (HC: n = 3; OA: n = 7) scale bar (**B–Q**): 1 mm; (**F'–I'''**): 100 µm. Modified from (205)

3.3. Pentameric TSP-4 amount increases with OA severity grade

Increased TSP-4 and Matn-3 protein levels could be observed in OA cartilage by immunohistological staining. For quantitative evaluation of oligomeric TSP-4, COMP and Matn-3 in OA progression, immunoblots were performed. Pentameric TSP-4 has a theoretical molecular mass of ~700 kDa, COMP of 500 kDa and tetrameric Matn-3 of 250 kDa. Total proteins were extracted from the same knee condyle, from areas, showing different OA severity grades of several OA patients (**Fig.3.3.A**). The detection of TSP-4 showed a certain variability in protein amounts between individual patients but was commonly increasing from G1 to G3/4 (**Fig.3.3.B**). For a better comparison of the protein amounts between patients, the fold change of G2 and G3/4 to G1 was calculated. The analyses revealed an increased level of TSP-4 from G1 to G3/4 ($p = 0.01$**) and from G2 to G3/4 ($p = 0.037$*) but not from G1 to G2 ($p = 0.869$) (**Fig.3.3.C**). The increase of TSP-4 protein level also correlated positively with OA severity grade ($p = 0.001$***; $r = 0.567$) (**Fig.3.3.D**). COMP and Matn-3 protein levels were comparable between OA severity grades, although a slight but not significant increase with severity was observable for both proteins (**Fig.3.3.B, F, G, I, J**). No differences in the protein levels of TSP-4, COMP and Matn-3 at any severity grade could be observed between male and female patients (**Fig.3.3.E, H, K**).

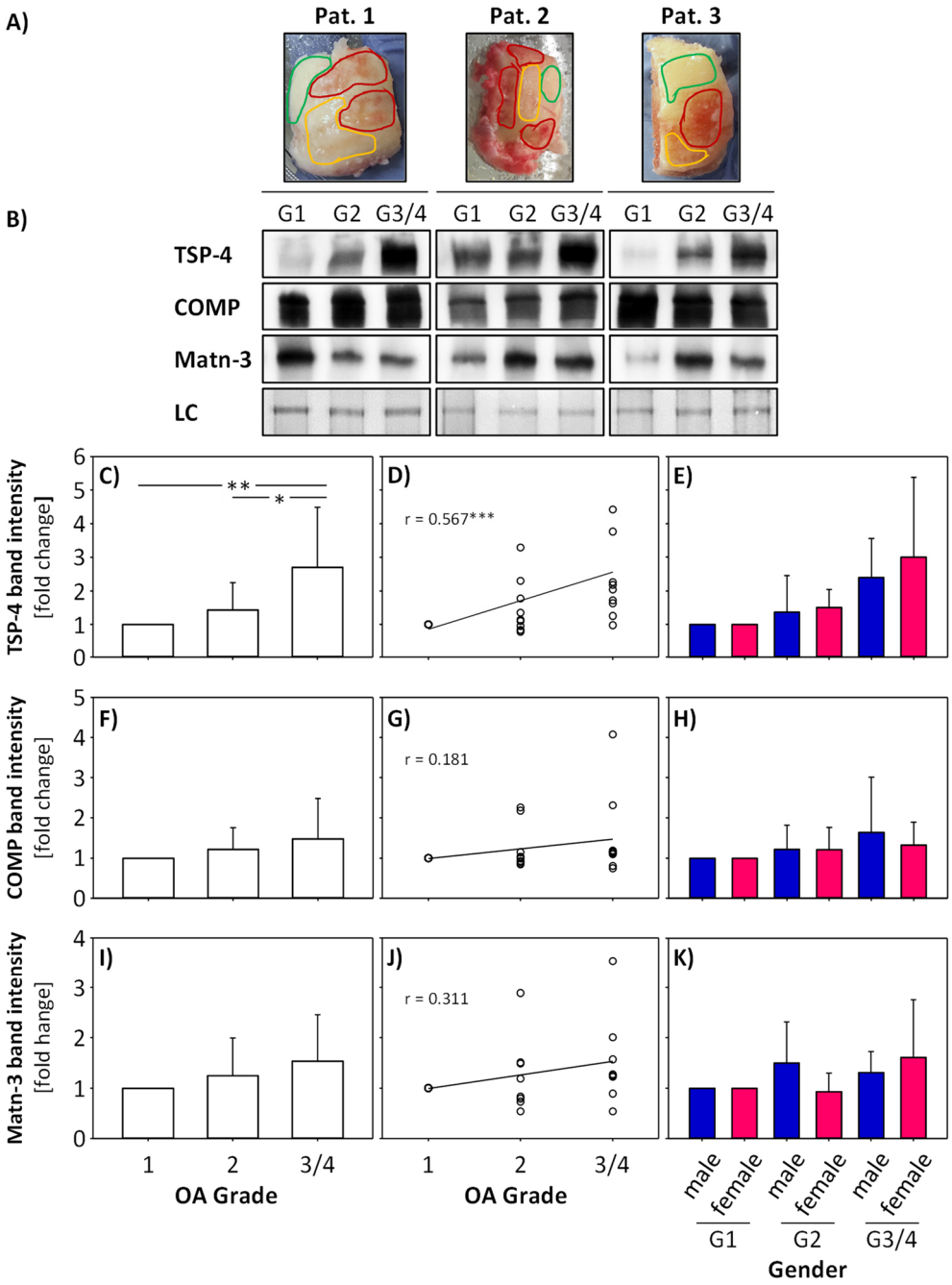

Figure 3.3: Detection of ECM proteins in extracts from OA knee articular cartilage
A) Representative knee condyles from three OA patients with highlighted areas of different severity grades from which proteins were isolated (green = grade 1 [G1], orange = grade 2 [G2], red = grade 3/4 [G3/4]). **B**) Protein extracts from each OA severity grade were analysed by immunoblot to detect TSP-4, COMP and Matn-3. PageBlue™ was used as a control to demonstrate equal loading. Statistical analyses of TSP-4 (**C**), COMP (**F**) and Matn-3 (**I**) between OA severity grades. Correlation of TSP-4 (**D**), COMP (**G**) and Matn-3 (**J**) with OA severity (black line). Levels of TSP-4 (**E**), COMP (**H**) and Matn-3 (**K**) in females and male OA patients at different severity grades. Representative immunoblots are shown (COMP, TSP4: n = 10 and Matn-3: n = 8). Values are represented as means + SD and significance ($p < 0.05$*; $p \leq 0.01$**; $p < 0.001$***) analysed by Friedman test with Tukey post-hoc analysis or Mann–Whitney U test as well as the correlation with the Spearman rank test. Matn-3 = matrilin-3; Pat. = patient; OA = osteoarthritis; LC = loading control. Modified from (205)

3.4. *THBS4* and *COMP* gene expression is not increasing during OA

TSP-4 levels were massively increased in OA cartilage and correlated positively with the OA severity grade. To investigate if this increase is due to increased transcriptional activity, RNA was isolated from OA cartilage areas, showing different severity grades (G1- G3/4) and used for PCR. No significant differences in Matn-3 protein levels could be detected. Therefore, only TSP-4 and COMP, as a close family member, were further investigated. Sequences of *THBS4* (TSP-4 gene), *COMP* and the housekeeping gene *GAPDH* (glyceraldehyde-3-phosphate-dehydrogenase) were analysed. Genes were amplified and separated according to their size by agarose gel electrophoresis (**Fig.3.4.A**). The levels of transcripts were comparable between all OA severity grades for both genes, *THBS4* (**Fig.3.4.B**) and *COMP* (**Fig.3.4.C**). *THBS4* band intensity was decreased at G2 or G3/4 compared to G1 in patient 4 and patient 6, respectively. However, this decrease was not significant and none of the patients showed an increased gene expression in late-stage OA (**Fig.3.4.A**).

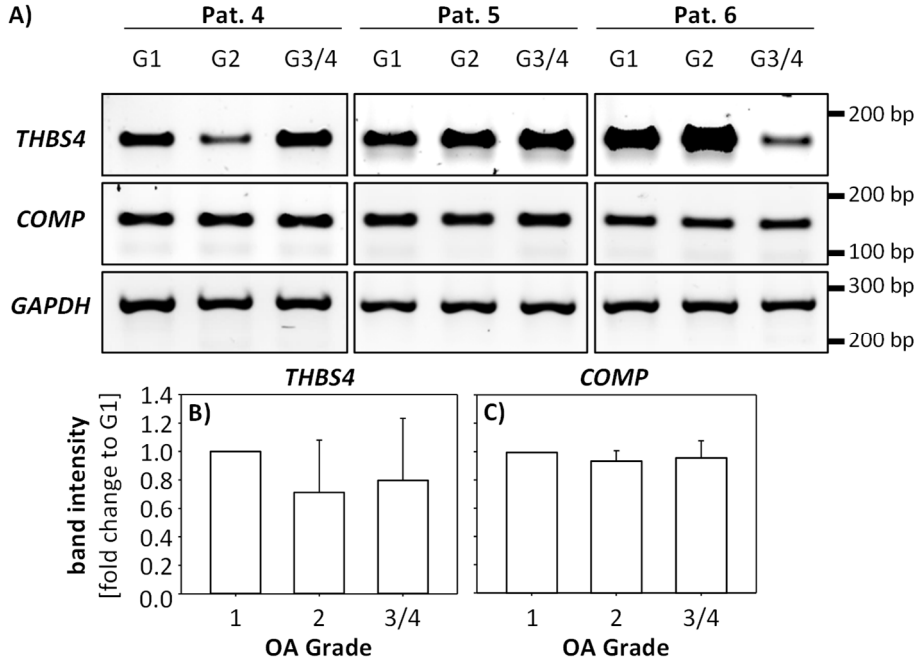

Figure 3.4: TSP-4 and COMP gene levels are comparable between OA severity grades
Gene expression levels of *THBS4* and *COMP* were investigated by PCR and agarose gel electrophoresis. **A**) Representative gels showing the RNA levels of *THBS4*, *COMP* and *GAPDH* of three OA patients. *THBS4* and *COMP* amplicons were normalised to the housekeeper *GAPDH*. **B**) Statistical analysis of the band intensities from different OA severity grades. Values are presented as means + SD and significance ($p < 0.05$*; $p < 0.01$**; $p < 0.001$***) analysed by Friedman test with Tukey post-hoc analysis. OA severity grades: grade 1 (G1), grade 2 (G2), and grade 3/4 (G3/4). (n = 6); Pat. = patient; OA = osteoarthritis. Modified from (205)

3.5. TSP-4 and COMP anchorage in cartilage differ between OA severity grade

TSP-4 protein level increases with OA severity grade but no differences at the RNA level could be detected. To investigate the cause of increased TSP-4 content in OA the protein anchorage in cartilage, showing different grades of damage, was analysed. For that, proteins were sequentially extracted from OA cartilage, first with a mild buffer to extract soluble and weakly anchored proteins followed by a harsh buffer to extract all remaining and tightly anchored proteins in the same piece of tissue. Also, total proteins were extracted immediately with the harsh buffer as described above for the second extraction step. (**Fig.3.5.A, B**)

The comparison of the different extractions resulted in faint signals for weakly anchored proteins, while tightly anchored protein gave a strong signal for TSP-4 (**Fig.3.5.C**). This result showed in general a tight anchorage of TSP-4 and COMP (not shown) in the matrix. To allow an interpretation of the faint signals and correlation with the severity grade, six times the amount of proteins extracted under mild conditions were loaded.

No significant differences between severity grades of weakly anchored TSP-4 could be detected, although, a conspicuously intense band, visible at G1 and/or G2 compared to G3/4 (**Fig.3.5.D**). The profile of harsh extracted TSP-4 was almost identical to that of single-step total extracted protein. In contrast to the weakly anchored TSP-4, only a weak signal could be detected at G1 compared to G2 and G3/4 of the tightly anchored protein. Also, weakly anchored COMP tended to be more in intact compared to degraded cartilage, but the profiles of weakly and tightly anchored COMP (**Fig.3.5.E**) were in general similar throughout severity grades. No differences, in protein anchorage could be seen between males and females, at any stage of OA (data not shown).

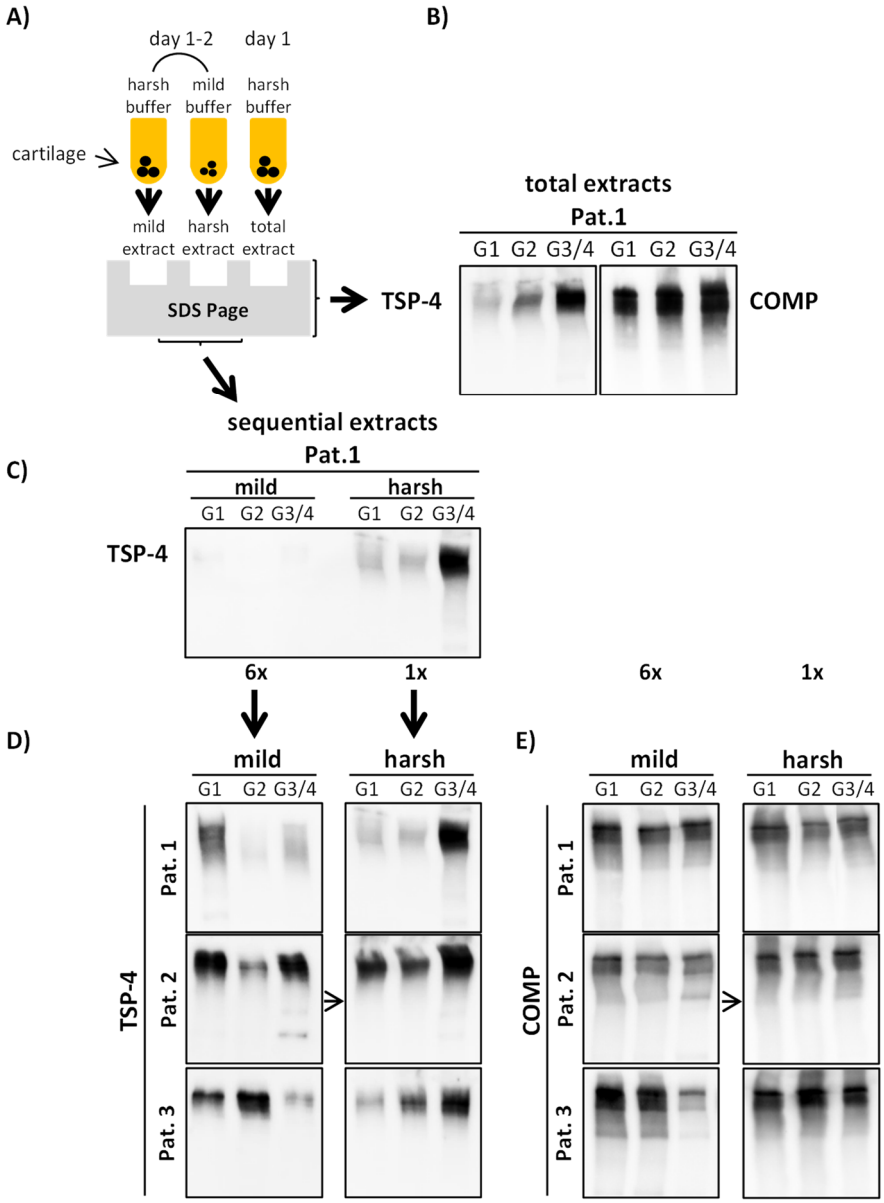

Figure 3.5: Sequential protein extraction of TSP-4 and COMP from OA knee articular cartilage
A) Schematic representation of the workflow to sequentially extract proteins. First, proteins were extracted overnight with a mild buffer and supernatants were collected on the following day. Remaining cartilage pieces were resuspended in a harsh buffer to extract also the tightly anchored proteins. Total proteins were directly collected after adding the harsh buffer to the cartilage pieces and extraction for 24 h. The amounts of the total (**B**), weakly-, and tightly-anchored TSP-4 (**D**) and COMP (**E**) in OA patients were analysed via immunoblot. Separation of equal amounts of proteins extracted under mild and harsh conditions shows a faint signal of weakly anchored proteins, while tightly anchored proteins gave strong signals (**C**). Therefore, six-fold amounts of proteins, extracted under mild conditions were loaded to detect differences in anchorage between severity grades. Representative immunoblots were shown (n = 10). OA severity grades: grade 1 (G1), grade 2 (G2), and grade 3/4 (G3/4). Pat. = patient. Modified from (205)

3.6. TSP-4 levels are increased in sera of OA patients

Following the finding of increased TSP-4 levels in OA cartilage, the presence of TSP-4 in serum samples was investigated to test its potential as a diagnostic marker. Pentameric and fragmented TSP-4 levels were analysed in sera of healthy controls (HCs) and OA patients via immunoblot assays (**Fig.3.6.A**). No significant differences in the amount of total ($p = 0.151$) or pentameric TSP-4 ($p = 0.375$) could be found between HCs and OA patients (**Fig.3.6.B, C**) even though there might be a tendency of more uncleaved pentameric protein in sera of HCs compared to OA patients. Interestingly, several fragments of TSP-4 could be found in sera of both, HCs and OA patients. By analysing the abundance of specific TSP-4 fragments, it was found that fragment 1 ($p = 0.03$) and fragment 2 ($p = 0.023$) were significantly increased in OA patients compared to HCs (**Fig.3.6.D, E**). Amounts of fragment 3 ($p = 0.844$) and fragment 4 ($p = 0.139$) were comparable between HCs and OA patients (diagrams not shown). In summary, total and pentameric TSP-4 levels were comparable, but the amount of specific TSP-4 fragments was significantly different in healthy and OA sera

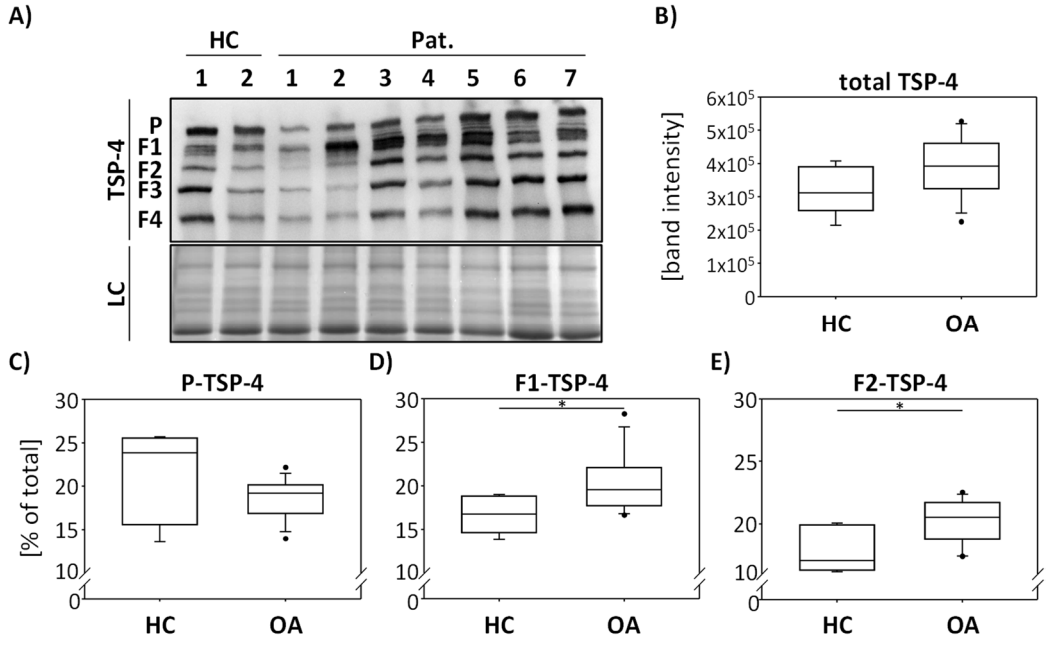

Figure 3.6: Detection of TSP-4 in sera of healthy donors and OA patients
Sera from healthy controls (HC) and OA patients (Pat.) were collected and TSP-4 levels analysed. **A**) Immunoblots show the pentameric TSP-4 and derived fragments (F1–4). PageBlue™ staining was used as a loading control (LC). Statistical evaluation of the total (**B**), pentameric (P) TSP-4 (**C**) and the derived fragment 1 (**D**) and fragment 2 (**E**) in OA patients. A representative immunoblot is shown (n = 18). Data are represented, as box blots and significance ($p < 0.05$*) analysed by the Mann–Whitney U test. Dots in **B-E** represent outliers. OA = osteoarthritis. Modified from (205)

In the first part of this project, the expression and distribution of TSP-4 in healthy and OA cartilage was shown for the first time. While its protein levels positively correlated with the OA severity grade, the levels of COMP were comparable.

The results indicate that both proteins are part of the ECM remodelling in OA. However, the involvement of COMP and TSP-4 in OA associated processes is not known so far. Therefore, in the following experiments the effect of COMP and TSP-4 on chondrocyte cluster formation, differentiation and ECM synthesis will be investigated.

3.7. Production of recombinant COMP and TSP-4

To investigate the effects of COMP and TSP-4 on chondrocytes, recombinant proteins have to be produced and purified in sufficient amounts and quality, first.

The recombinant proteins were purified from the supernatant via their Strep-Tag II, using an affinity chromatography column. The integrity and the amount of recombinant proteins were investigated by immunoblot analyses, detecting both the protein-linked Strep-Tag (**Fig.3.7.A, D**) and the proteins, COMP and TSP-4 directly (**Fig.3.7.B, E**). Potential contamination with other proteins was checked by comparison with PageBlue^{TM} stained gels (**Fig.3.7.C, F**). The immunoblot and gel analyses of recombinant COMP showed in addition to the pentameric protein (~500 kDa) also some fragmentation products (**Fig.3.7.A-C**), which resembled the COMP fragments detected in OA cartilage (**Fig.3.5.B, E**). The immunoblot and gel analyses of recombinant TSP-4 showed predominantly the pentameric protein (~700 kDa) with few fragmentation products (**Fig.3.7.D-F**), again resembling those that have been detected in OA cartilage (**Fig.3.5.B, D**). All produced recombinant proteins fulfilled the quality criteria to mimic their natural occurring counterparts and were used for downstream experiments.

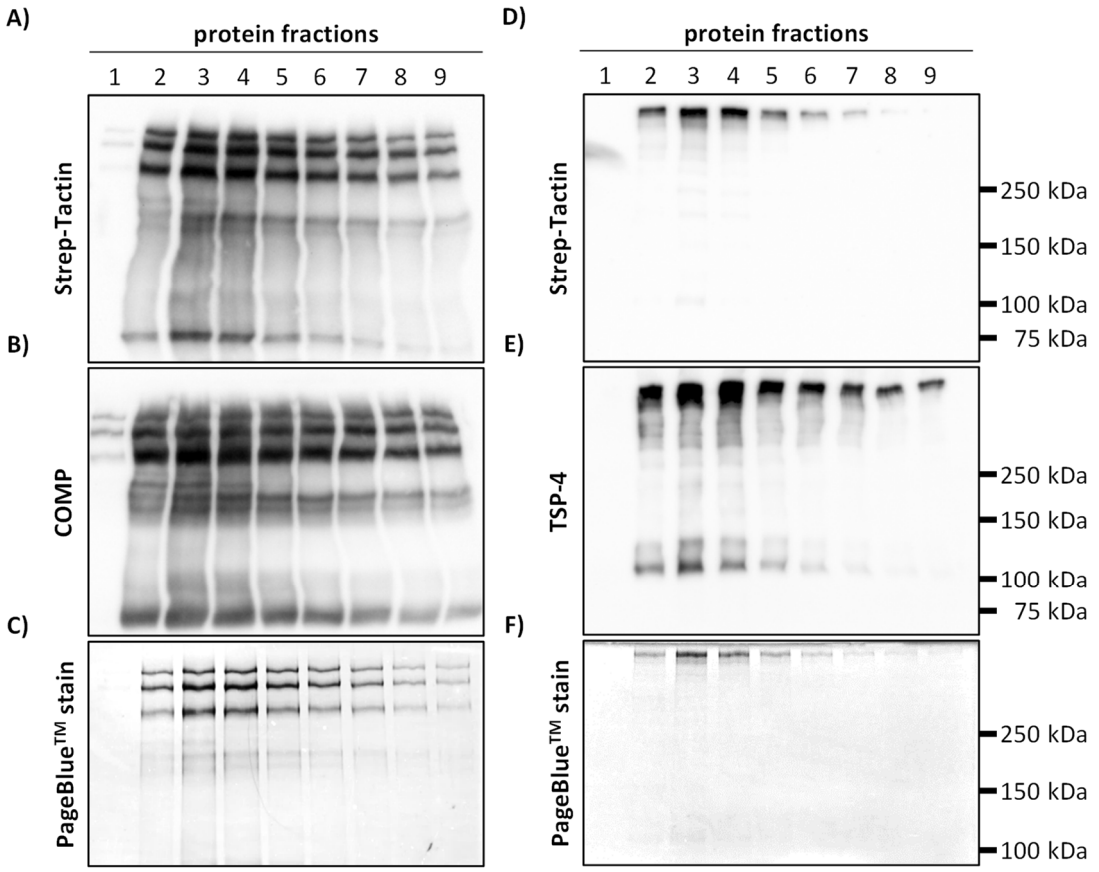

Figure 3.7: Characterisation of recombinant COMP and TSP-4
Recombinant COMP and TSP-4 were produced in a eukaryotic system and purified by affinity chromatography. The quality of the produced proteins was analysed in nine elution fractions by immunoblot, detecting the recombinant protein by using a specific Strep Tag II **(A, D**) or protein-specific (**B, E**) antibodies. The purity of COMP and TSP-4 was analysed via PageBlue™ gel of total proteins (**C, F**).

3.8. COMP, TSP-4 and TGF-β1 do not affect chondrocyte viability

Before *in vitro* assays are performed the potential cytotoxic effects of COMP, TSP-4 and TGF-β1 were excluded via lactate dehydrogenase (LDH) assay. None of the tested compounds, alone or in combination, had a cytotoxic effect on primary pig chondrocytes within 24 h. (**Fig.3.8**)

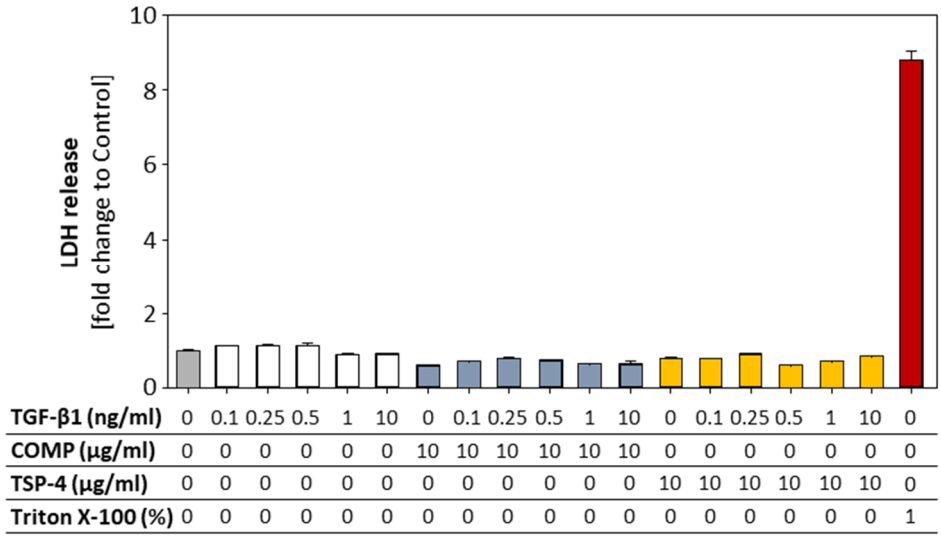

Figure 3.8: COMP, TSP-4 and TGF-β1 have no cytotoxic effect on primary chondrocytes
Primary pig chondrocytes were stimulated, with 10 µg/ml COMP (blue), 10 µg/ml TSP-4 (orange) and different concentrations of TGF-β1 (white) for 24 h. Cytotoxicity was assessed with the lactate dehydrogenase (LDH) assay, measuring the amount of released LDH. None of the tested conditions showed any signs of cytotoxicity. Unstimulated cells were used as control (grey) and 1 % Triton X-100 was added for 10 min to permeabilize cells, which served as death control (red).

3.9. COMP but not TSP-4 promotes chondrocyte migration

Interactions between chondrocytes and ECM components can influence cell mobility and anchorage. To determine the potential of COMP and TSP-4 as chondrocyte attractants, the migration capacity of young pig chondrocytes, along a gradient was investigated via transwell assays. As attractants, COMP (10 µg/ml) and TSP-4 (10 µg/ml) were added to the lower compartment and chondrocytes in the upper compartment were allowed to migrate for 10 h (**Fig.3.9.A**). PDGF-BB (10 ng/ml) was used as a positive and standard medium as a negative control. COMP ($p = 0.014$) and PDGF-BB ($p = 0.012$) could attract chondrocytes compared to the control group (**Fig.3.9.B**). The number of cells migrating towards TSP-4 was significantly lower as towards PDGF-BB ($p = 0.049$)

and similar to the control. (**Fig.3.19.B**). This assay demonstrated that COMP but not TSP-4 has the potential to attract chondrocytes (**Fig.3.9.C**).

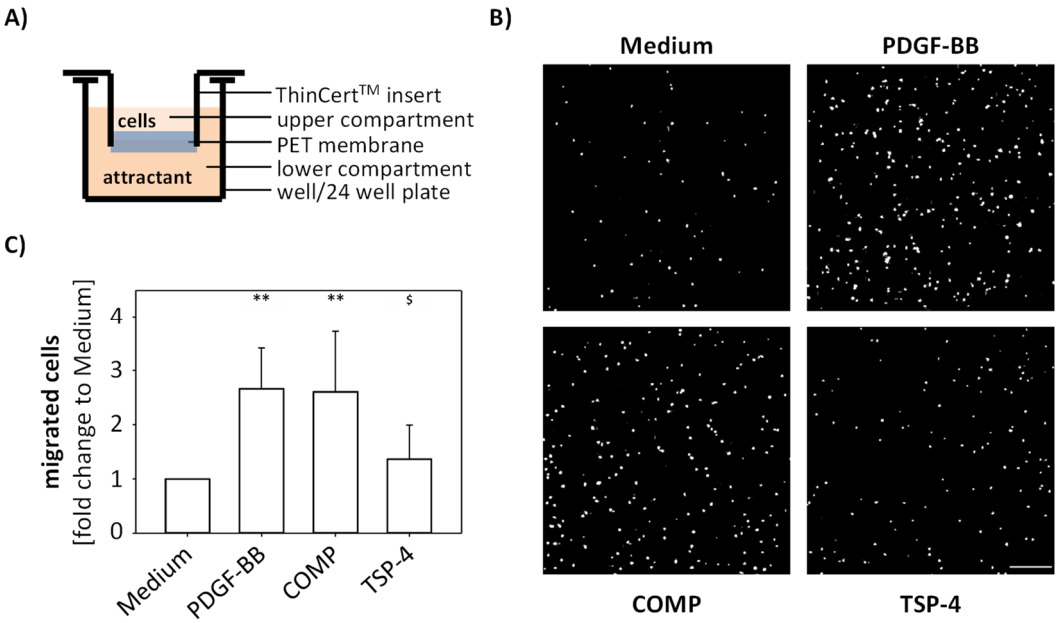

Figure 3.9: Migration capacity of chondrocytes to COMP and TSP-4
A) Schematic illustration of the transwell system. Pig chondrocytes were attracted with COMP (10 µg/ml) or TSP-4 (10 µg/ml) for 10 h. **B**) Representative images of migrated chondrocytes stained with DAPI. **C**) Migrated cells were counted and statistically evaluated. COMP but not TSP-4 could attract chondrocytes. Each bar shows the mean + SD and significance (to medium: $p < 0.05$*, $p < 0.01$** and to PDGF-BB: $p < 0.05^{\$}$) was analysed with the Friedman test and Tuckey post-hoc test. The standard medium was used as a negative and PDGF-BB (10 ng/ml) as a positive control. (n = 4); scale bar = 100 µm.

The majority of OA patients are older than 60 years and to make a statement if COMP could also attract aged and osteoarthritic chondrocytes, we isolated chondrocytes from cartilage areas with visible OA lesions of an old mini-pig. The response of chondrocytes to PDGF-BB decreases with age (215) and served, in this assay as a negative marker of chondrocyte migration and age. Indeed, the response of aged chondrocytes to PDGF-BB diminished, but COMP was still able to attract chondrocytes and TSP-4 had no effect (**Fig.3.10.A, B**). These data show that COMP can attract chondrocytes, independently of age and disease, while TSP-4 does not contribute to cell migration.

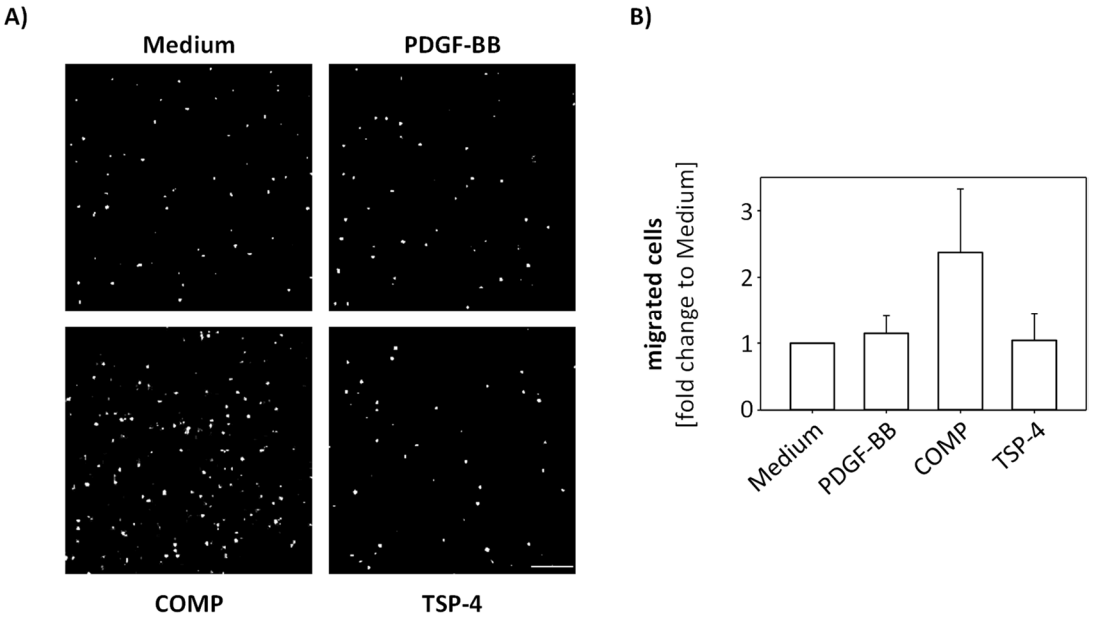

Figure 3.10: Migration capacity of old chondrocytes to COMP and TSP-4
A) Schematic illustration of the transwell system. Pig chondrocytes were attracted with COMP (10 µg/ml) or TSP-4 (10 µg/ml) for 10 h. **B**) Representative images of migrated chondrocytes stained with DAPI. The standard medium and PDGF-BB (10 ng/ml) were used as negative controls. (n = 1, in doublets); scale bar = 100 µm.

3.10. COMP mediates chondrocyte attachment while TSP-4 does not

To investigate if COMP can also facilitate the attachment and anchorage of the attracted chondrocytes, wells of a 96-well plate were coated with 10 µg/ml COMP. TSP-4 could not attract chondrocytes, but it might be involved in the anchorage of surrounding chondrocytes, therefore, wells were also coated with 10 µg/ml TSP-4. 10 µg/ml fibronectin was used, as a positive control and 100 mg/ml BSA as a negative control. Chondrocytes were incubated in the coated wells for 1 h, the attached cells stained with crystal violet and analysed by light microscopy (**Fig.3.11.A, B**). Chondrocytes attached to fibronectin ($p = 0.003$) and COMP ($p = 0.012$) but not to TSP-4 ($p = 0.18$). Also, an increased attachment for COMP compared to TSP-4 ($p = 0.007$) was observed.

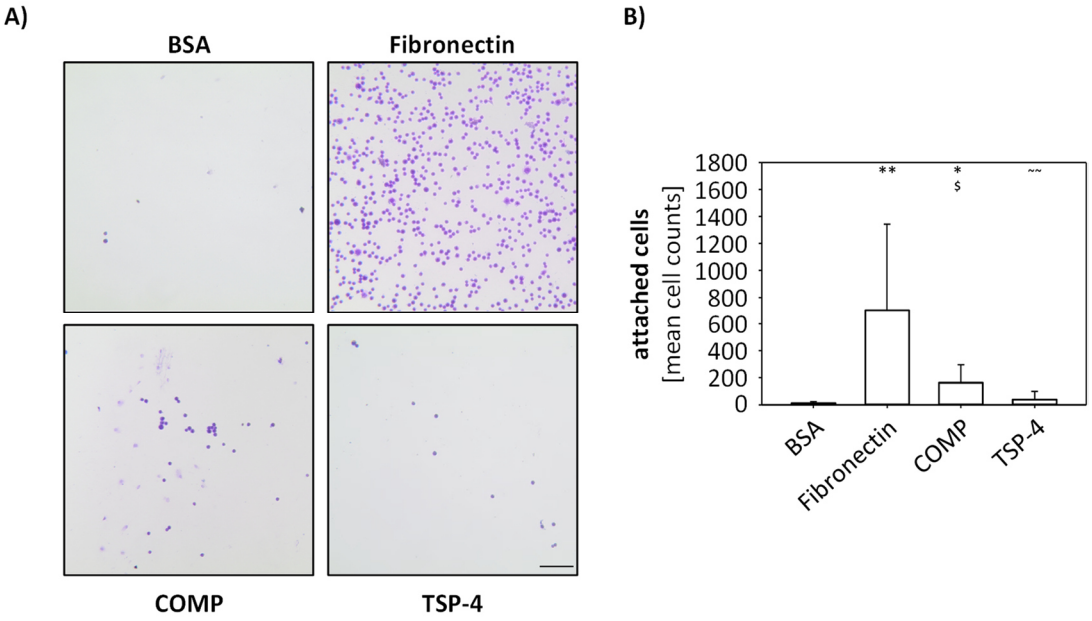

Figure 3.11: Effect of COMP and TSP-4 on chondrocyte attachment
The attachment capacity of primary pig chondrocytes was investigated by incubating chondrocytes for 1 h in COMP (10 µg/ml) and TSP-4 (10 µg/ml) coated wells. **A**) Representative images of crystal violet stained cells attached to the well surface. **B**) Chondrocytes attached to fibronectin and COMP but not to BSA or TSP-4. Each bar shows the mean + SD and significance (to BSA $p < 0.05$*, $p < 0.01$**, to fibronectin $p < 0.05^{\$}$ and COMP $p < 0.01^{\sim\sim}$) was analysed with the Friedman test and the Student-Newman-Keuls Method post-hoc test. Fibronectin (10 µg/ml) was used as a positive and BSA (100 mg/ml) as a negative control. (n = 5); scale bar = 100 µm.

3.11. COMP and TSP-4 induce expression of OA-relevant genes

After showing that COMP can attract chondrocytes and contribute to their anchorage, I was curious if COMP but also TSP-4 can induce the synthesis of ECM or OA associated genes. To investigate, a direct effect of COMP and TSP-4 on the expression of OA-relevant genes, primary pig chondrocytes were stimulated with 10 µg/ml COMP or TSP-4 and the gene expression levels analysed after 6 h and 24 h. Cells were stimulated with 0.5 ng/ml TGF-β1 as a general activator of gene expression. Chondrocytes were also stimulated with a combination of COMP or TSP-4 with TGF-β1 to investigate possible modulatory effects on transcriptional processes. After 6 h (**Fig.3.12**), TGF-β1 stimulation resulted already in a weak upregulation of *COL1A1* ($p = 0.013$), *COL2A1* ($p < 0.001$), *COL12A1* ($p < 0.001$), *ACAN* ($p < 0.001$), *COMP* ($p < 0.001$), *THBS4* ($p = 0.002$), *MATN3* ($p < 0.001$) and *VEGF* ($p = 0.005$) compared to the unstimulated control. COMP as well as TSP-4 stimulation could also increase the expression level of *COL2A1* (COMP: $p = 0.003$; TSP-4: $p = 0.009$) and *COMP* (COMP: $p = 0.003$; TSP-4:

p < 0.001). TSP-4 stimulation resulted further in the increase of *COL12A1* (p = 0.013) and *ACAN* (p = 0.02). The analysis of the effect of COMP and TSP-4 on TGF-β1 induced gene expression revealed that additional TSP-4 could further increase the expression levels of *COL12A1* (p = 0.018) and *VEGF* (p = 0.012). COMP did not affect TGF-β1 induced gene expression, and none of both proteins caused a reduction in the gene expression levels.

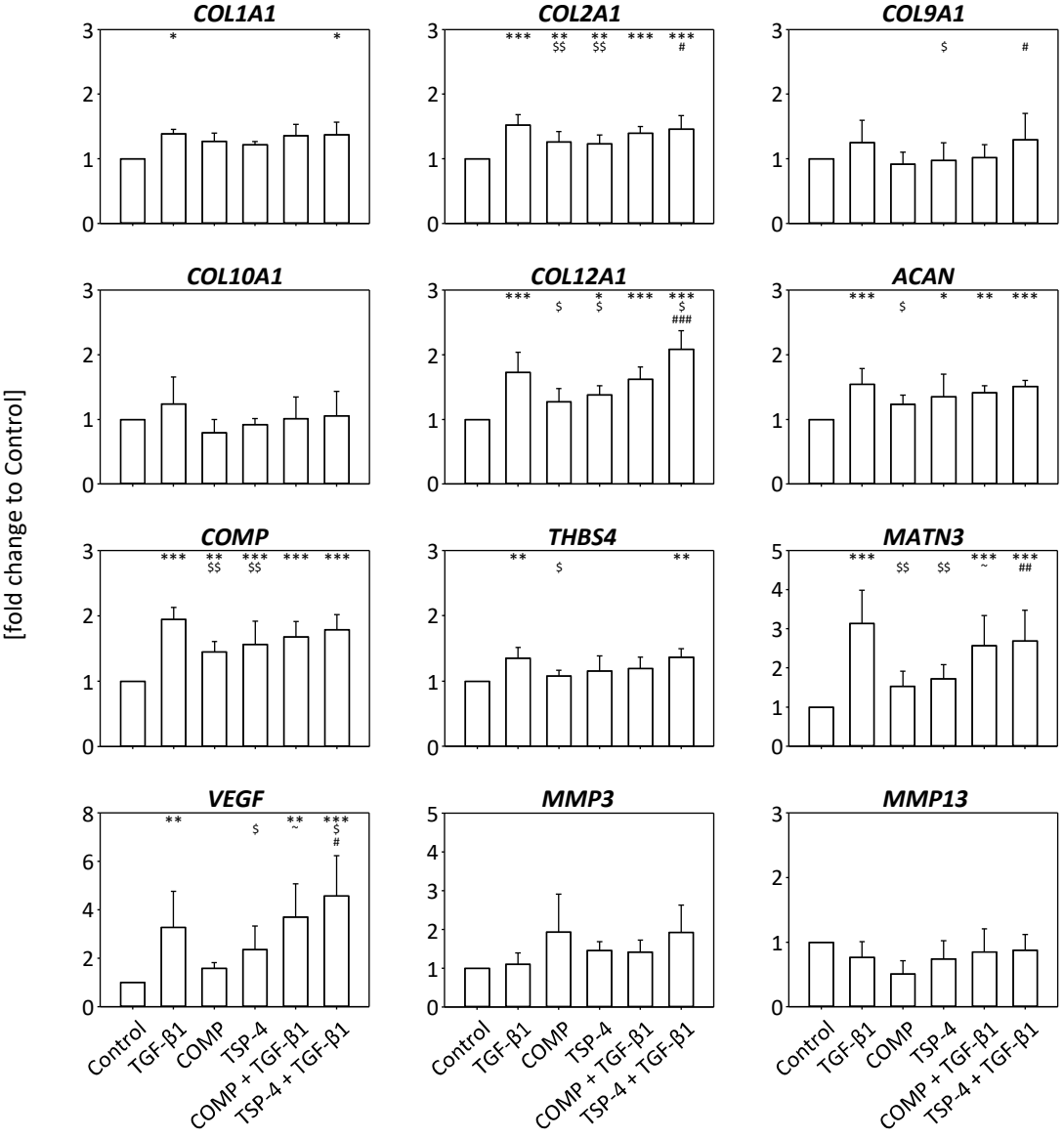

Figure 3.12. COMP and TSP-4 induced gene expression after 6 h
Gene expression was analysed by qPCR after chondrocyte stimulation with COMP (10 µg/ml), TSP-4 (10 µg/ml), TGF-β1 (0.5 ng/ml) for 6 h. Relative gene expression (fold change to control) is represented as mean + SD and significance (p ≤ 0.05*, p ≤ 0.01** and p ≤ 0.001***) analysed with the Friedman test and either the Tuckey or Dunnett's post-hoc test. Relative gene expression was normalised to *GAPDH*. Asterisks* indicate significance to unstimulated control, the dollar$ to TGF-β1, the wave~ to COMP and the rhombus# to TSP-4. (n = 4)

qPCR analyses after 24 h (**Fig.3.13**), showed that TGF-β1 increased the gene expression of *COL1A1* ($p = 0.022$), *COL2A1* ($p = 0.007$), *COL9A1* ($p < 0.001$), *COL10A1* ($p = 0.002$), *COL12A1* ($p < 0.001$), *ACAN* ($p = 0.022$), *THBS4* ($p = 0.022$), *MATN3* ($p < 0.001$) and *MMP3* ($p < 0.001$) compared to the unstimulated control. COMP and TSP-4 alone did not affect gene expression levels but COMP stimulation resulted in an increased expression of COL9A1 ($p = 0.051$) compared to TSP-4. Both proteins in combination with TGF-β1 could increase *VEGF* (COMP: $p = 0.006$; TSP-4: $p = 0.04$) and *MMP13* (COMP: $p = 0.016$; TSP-4: $p = 0.04$) gene expression compared to the unstimulated control after 24 h. TSP-4, in combination with TGF-β1, could further increase the gene expression of *COMP* ($p = 0.025$). Also, after 24 h no downregulation of any gene could be observed by additional stimulation with COMP or TSP-4.

The comparison of the mean 2^-ΔΔCT values of genes significantly upregulated by COMP or TSP-4, such as *COMP*, *ACAN*, *COL2A1* and *COL12A1* after 6 h and 24 h revealed comparable values, showing that no further upregulation could be observed with 18 h. Although, stimulation with COMP reduced the expression of *MATN3* between 6 h and 24 h ($p = 0.005$). TGF-β1 treatment further increased the expression of *COL9A1* ($p = 0.050$), *COL12A1* ($p = 0.007$), *MMP3* ($p = 0.045$) and *MMP13* ($p = 0.050$) between 6 h and 24 h. Also, *COL12A1* expression was further increased by the combination of TGF-β1 with COMP ($p = 0.011$) or TSP-4 ($p = 0.024$) from 6 h to 24 h. While the additional treatment with TSP-4 lead to an increase of *MMP13* ($p = 0.017$) expression, the addition of COMP showed a tendency to increase *COL10A1* ($p = 0.052$) from the 6 h to 24 h time point.

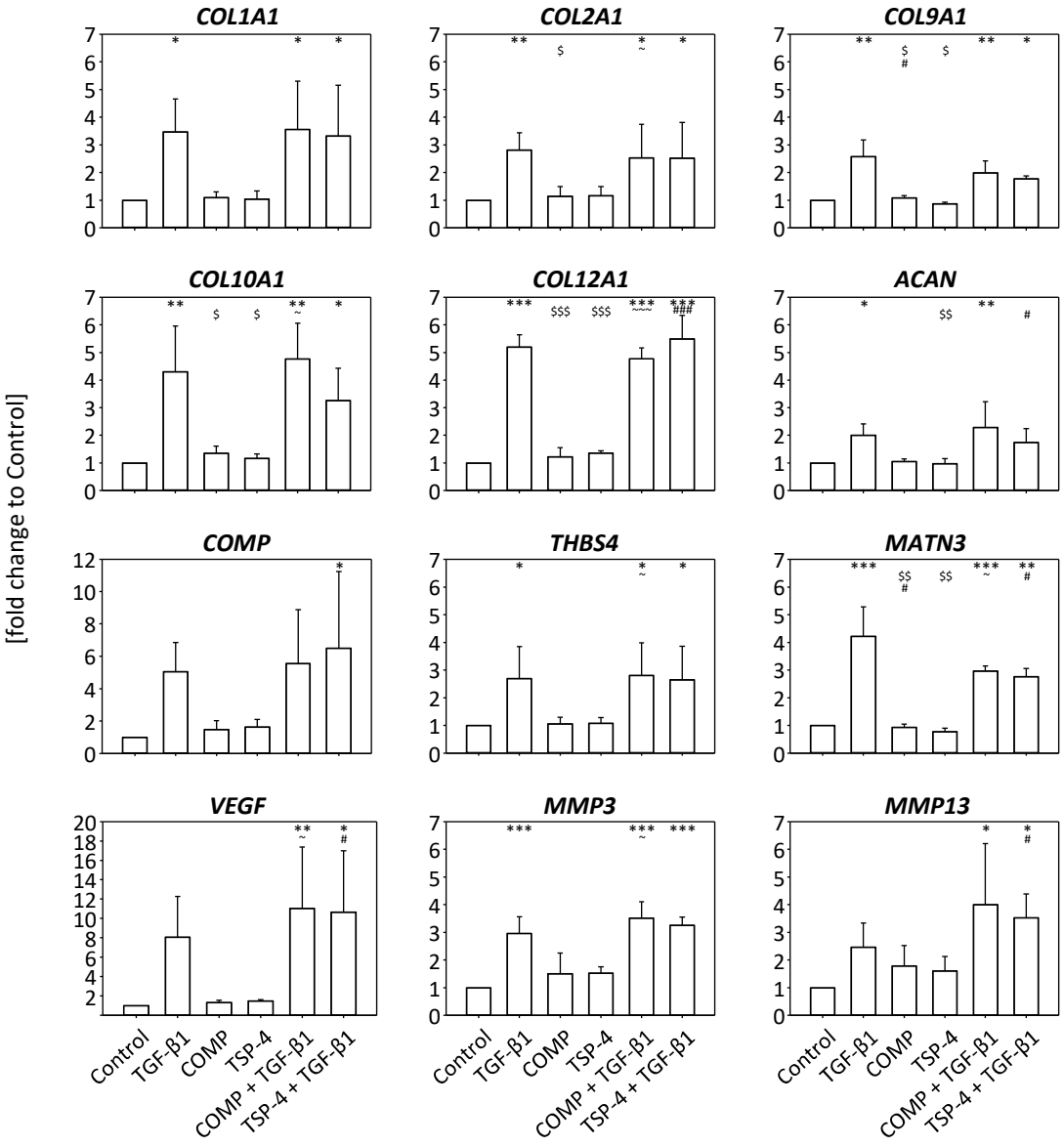

Figure 3.13. COMP and TSP-4 induced gene expression after 24 h
Gene expression was analysed by qPCR after chondrocyte stimulation with COMP (10 µg/ml), TSP-4 (10 µg/ml) and TGF-β1 (0.5 ng/ml) for 24 h. Relative gene expression (fold change to the control) is represented as mean + SD and significance ($p \leq 0.05$*, $p \leq 0.01$** and $p \leq 0.001$***) analysed with the Friedman test and either the Tuckey or Dunnett's post-hoc test. Relative gene expression was normalised to *GAPDH*. Asterisks* indicate significance to unstimulated control, the dollar$ to TGF-β1, the wave~ to COMP and the rhombus# to TSP-4. (n = 3)

3.12. COMP and TSP-4 contribute to the regulation of collagen matrix formation

The influence of COMP and TSP-4 on gene expression was weak after 24 h, but observable. A direct correlation of gene and protein level is not always applicable; therefore, the effect of COMP and TSP-4 on collagen synthesis and matrix integration was investigated. Chondrocytes were stimulated with COMP (10 µg/ml), TSP-4 (10 µg/ml), TGF-β1 (0.5 ng/ml) or in combination of TGF-β1 with COMP or TSP-4 for 7 days. TGF-β1 was used as a regulator of collagen synthesis and to observe potential modulating or synergistic effects of COMP and TSP-4. As a negative control, chondrocytes were cultured in standard medium. Collagen matrix formation was investigated by immunofluorescence staining (**Fig.3.14.A**). COMP and TSP-4 contributed to the matrix formation of collagen II, IX and XII while no effect on collagen I and a slight decrease of collagen X could be observed. TGF-β1 enhanced the matrix formation of collagen I, II and XII while reducing collagen IX levels and not affecting collagen X. Investigating the effect of COMP and TSP-4 on TGF-β1 induced matrix formation showed a decrease of collagen I, X and XII levels as well as an increase of collagen II. TGF-β1 associated collagen IX reduction could not be reversed by COMP or TSP-4. Data are represented as bar graphs in **Supp.1**.

Collagens that are not integrated into the cell-associated matrix remain soluble and can be detected in the cell culture supernatant. Therefore, the amounts of different collagen types were analysed by immunoblot assays (**Fig.3.14.B**). Soluble collagen IX could only be detected in supernatants of cells treated with COMP, either alone or in combination with TGF-β1. This result showed that COMP contributes to the synthesis of collagen IX, even though its deposition into the matrix seems not intensively increased. Increased amounts of soluble collagen I and XII could be observed only in TGF-β1 stimulated cells: This upregulation parallels the increase of protein in the matrix. Interestingly, the amount in the same proteins in the supernatant could be reduced by the addition of COMP or TSP-4. The signals for collagen X and collagen II in the supernatant were either very weak or even absent indicating that these proteins are quantitatively incorporated into the cell-associated matrix.

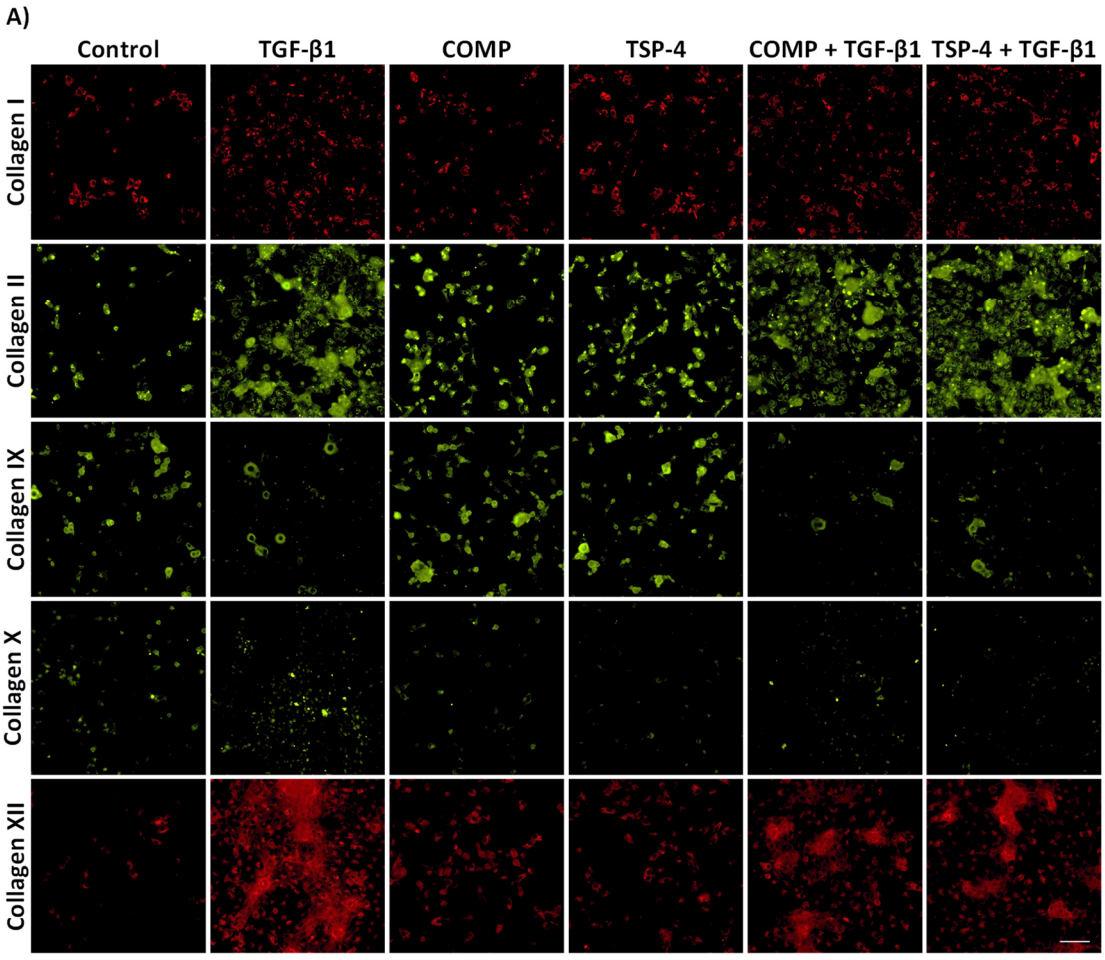

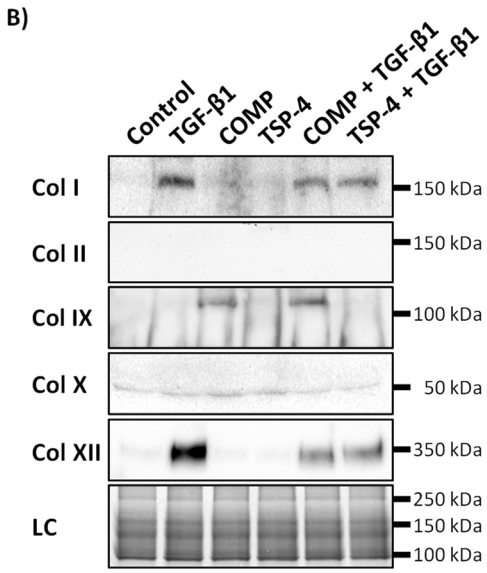

C)

	TGF-β1	COMP	TSP-4	COMP + TGF-β1	TSP-4 + TGF-β1
Col I	↑↑	-	-	↑	↑
Col II	↑↑	↑	↑	↑↑↑	↑↑↑
Col IX	↓↓	↑	↑	↓	↓↓
Col X	-	↓	↓	↓	↓
Col XII	↑↑↑	↑	↑	↑↑	↑↑

Figure 3.14: COMP and TSP-4 induced collagen matrix formation and secretion
Chondrocytes were stimulated with COMP (10 µg/ml), TSP-4 (10 µg/ml) alone or in combination with TGF-β1 (0.5 ng/ml) for 7 days **A**) Immunofluorescence staining of collagen (Col) I, II, IX, X and XII at day 10. **B**) Immunoblot assays of chondrocyte supernatants at day 10. Roti®Blue staining of proteins was used as a loading control (LC). **C)** Table, connecting data of soluble and matrix integrated collagens. The arrows mark the increase (↑) or decrease (↓) compared to the control. No changes are indicated, by a minus (-). Three arrows indicate a strong, two arrows, a

moderate and one arrow a mild regulation compared to the control. (n = at least 2 per group); unstimulated cells were used as a control; scale bar = 100 µm

To connect the findings of ECM and soluble collagens (**Fig.3.14.C**), COMP and TSP-4 stimulation increased the level of collagen II, IX and XII as well as decreased collagen X. TGF-β1 increased the expression of collagen I, II and XII while reducing collagen IX. These effects, on collagen I and XII were weakened by the addition of COMP and TSP-4 while the increase of collagen II was further enhanced.

3.13. COMP and TSP-4 do not affect proliferation but suppress chondrocyte dedifferentiation

Reactivated chondrocytes in OA proliferate and dedifferentiate to collagen I producing cells. COMP and TSP-4 affect collagen II matrix deposition and suppress TGF-β1 induced collagen I expression. To test if COMP and TSP-4 can directly or indirectly modulate these processes, chondrocytes were stimulated with COMP (10 µg/ml) or TSP-4 (10 µg/ml) alone and in combination with TGF- β1 (0.5 ng/ml) for 7 days. The number of cells as well as the ratio of collagen I and collagen II positive cells were evaluated at day 10. TGF-β1 served as an inducer of chondrocyte proliferation. COMP ($p = 0.99$) and TSP-4 ($p = 0.86$) alone had no effect on cell proliferation and cell number after 10 days were comparable to untreated control (**Fig.3.15.A, B**). TGF-β1 ($p = 0.003$) alone and in combination with COMP ($p = 0.002$) or TSP-4 ($p < 0.001$) resulted in an increased cell number. The dual treatments with TGF-β1 also increased the cell numbers compared to the equivalent single treatments with COMP ($p = 0.013$) and TSP-4 ($p = 0.023$). These data show that COMP and TSP-4 do not affect cell proliferation, neither directly nor by modulating the TGF-β1 induced proliferation.

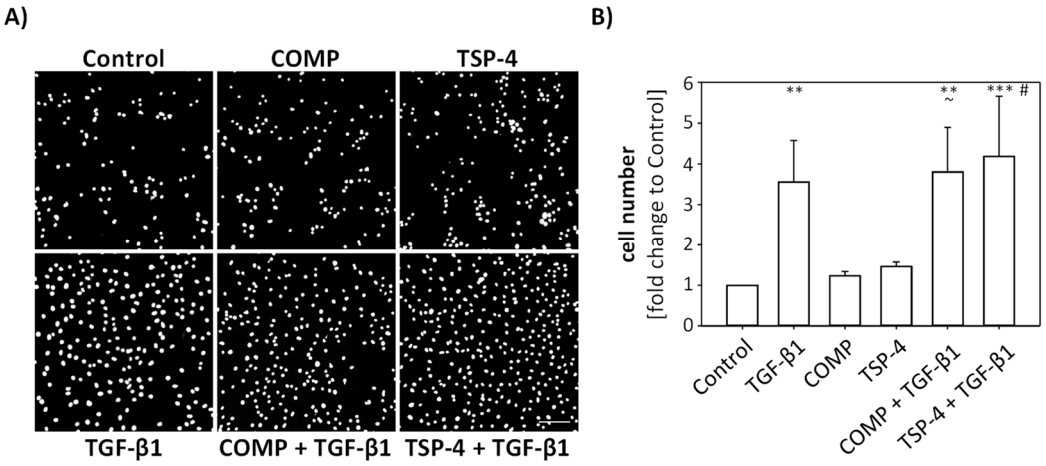

Figure 3.15: Chondrocyte proliferation capacity
Chondrocytes were stimulated with COMP (10 µg/ml) or TSP-4 (10 µg/ml) for 7 days. **A**) Nuclei were DAPI stained at day 10. **B**) The fold changes of the counted nuclei are represented and each bar shows the mean + SD. The significant differences between the control and all other conditions were calculated with the One Way ANOVA and the Dunnett's post-hoc test. Differences between COMP, TGF-β1 and COMP + TGF-β1 as well as TSP-4, TGF-β1 and TSP-4 + TGF-β1 were calculated with the One Way ANOVA and the Tuckey post-hoc test. Differences to the control are indicated by an asterisk *, to COMP by waves ~ and to TSP-4 by rhombus #, as well as significance indicated by $p \leq 0.05$*#~; $p \leq 0.01$**; $p \leq 0.001$***. (n = 3); scale bar = 100 µm.

The percentage of cells expressing collagen I and collagen II, respectively, was investigated by immunofluorescence double staining (**Fig.3.16.A**). Collagen I and collagen II expressing cells were counted and the percentage of collagen expressing cells calculated (**Fig.3.16.B**). The percentage of collagen I and collagen II expressing cells was comparable between the control ($p = 0.21$) and TGF-β1 ($p = 0.22$) treated cultures. All other treatments, stimulation with COMP ($p = 0.003$), TSP-4 ($p = 0.03$) or in combination with TGF-β1 (COMP: $p = 0.05$; TSP-4: $p = 0.02$) resulted in a shift towards collagen II producing cells. Furthermore, collagen I producing cells were less in cultures treated with COMP ($p = 0.025$) and the co-stimulations of TGF-β1 with COMP ($p = 0.007$) and TSP-4 ($p = 0.004$). The stimulation with TSP-4 ($p = 0.056$) showed a trend of a reduced number of collagen I positive cells. The opposite was observed for collagen II producing cells which numbers increased in cultures treated with COMP ($p = 0.033$), TSP-4 ($p = 0.042$) and in combination of TGF-β1 with COMP ($p = 0.034$) and TSP-4 ($p = 0.010$).

These results show a COMP and TSP-4 associated suppression of chondrocyte dedifferentiation in monolayer culture.

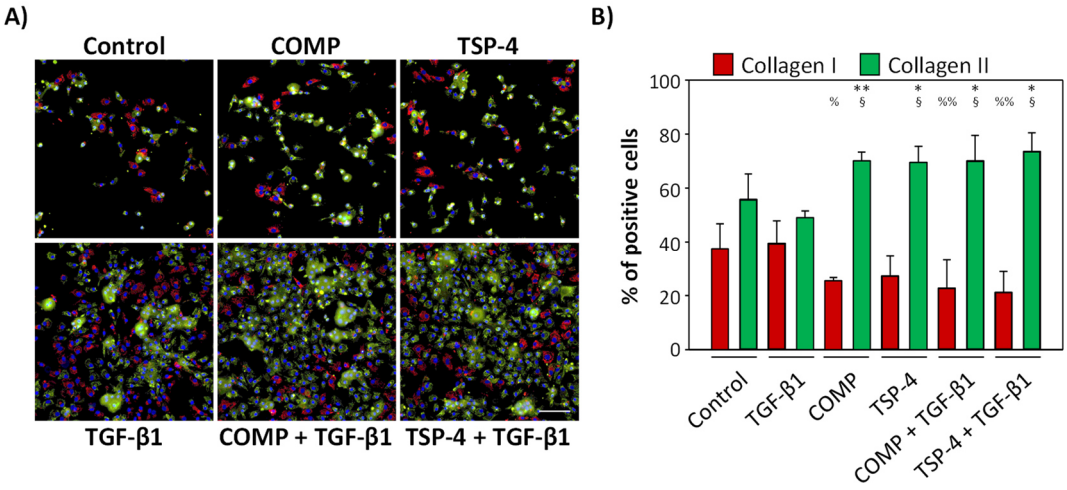

Figure 3.16: Chondrocyte differentiation capacity
Chondrocytes were stimulated with COMP (10 µg/ml) or TSP-4 (10 µg/ml) for 7 days. **A**) Immunofluorescence staining of collagen I (red), collagen II (green) and nuclei (blue) at day 10. **B**) Percentages of chondrocytes expressing collagen I and II are represented and each bar shows the mean + SD. The significant difference between collagen I and collagen II positive cells was calculated with the paired t-test. Significance was indicated as $p \leq 0.05$*; $p \leq 0.01$**. Differences of collagen I and collagen II positive cells to the control were calculated with the Friedman test and the Dunnett's post-hoc test. Significance is indicated as $p \leq 0.05^{\%\text{ or }\S}$; $p \leq 0.01^{\%\% \text{ or } \S\S}$, respectively. TGF-β1 (0.5 ng/ml) served as an inducer of proliferation and collagen synthesis and unstimulated cell as a control. (n = 3); scale bar = 100 µm.

3.14. COMP and TSP-4 modulate proteoglycan deposition as well as matrix protein secretion and integration

Collagen expression could be regulated by COMP and TSP-4, in the following experiments, their capacities to modulate the synthesis of proteoglycan and adaptor-proteins will be investigated. Chondrocytes were stimulated with 10 µg/ml COMP and TSP-4, 0.5 ng/ml TGF-β1 alone and in the combination for 7 days. As a control, chondrocytes were cultured in standard medium. Proteoglycans were stained with Safranin-O as well as COMP, TSP-4 and Matn-3 detected by immunofluorescence staining (**Fig.3.17.A**). TGF-β1 stimulation enhanced COMP expression and proteoglycan deposition but severely reduced Matn-3 and did not affect TSP-4 levels. COMP and TSP-4 stimulation alone resulted in increased proteoglycan deposition but did not affect COMP and Matn-3 levels. However, COMP stimulation could increase the matrix associated TSP-4 level, alone and in combination with TGF-β1. The additional treatment with COMP could further promote its own matrix formation, while the addition of TSP-4 caused a reduction in COMP levels. TSP-4 and Matn-3 matrix formation was not affected by the

dual treatments. Matn-3 level was lowest in cultures treated with TGF-β1, as observed for collagen IX. Immunofluorescence double staining revealed a strong co-localisation of Matn-3 and collagen IX (**Supp.2**). Data are represented as bar graphs in **Supp.1**.

Adaptor proteins, not integrated into the matrix can be detected in the cell culture supernatant by immunoblot assays (**Fig.3.17.B**). The analyses revealed no differences in the amount of soluble COMP or Matn-3. Soluble TSP-4, was only detected in supernatants of cultures stimulated with TSP-4, although the amount was reduced when treated in combination with TGF-β1. Even if the matrix associated TSP-4 seems reduced by TSP-4 stimulation, there is still a synthesis ongoing, but the integration capacity in the matrix is impaired. To summarise the results received about soluble and matrix integrated proteins (**Fig.3.17.C**), the stimulation with either COMP or TSP-4 increased the level of proteoglycans. COMP also enhanced the amount of TSP-4 in the matrix, while TSP-4 stimulation itself inhibited its own matrix integration. TGF-β1 increased the levels of COMP and proteoglycans while reducing Matn-3. The upregulation of proteoglycans was further increased by the addition of COMP and TSP-4. Only, the addition of TSP-4 could reduce the TGF-β1 induced matrix formation of COMP.

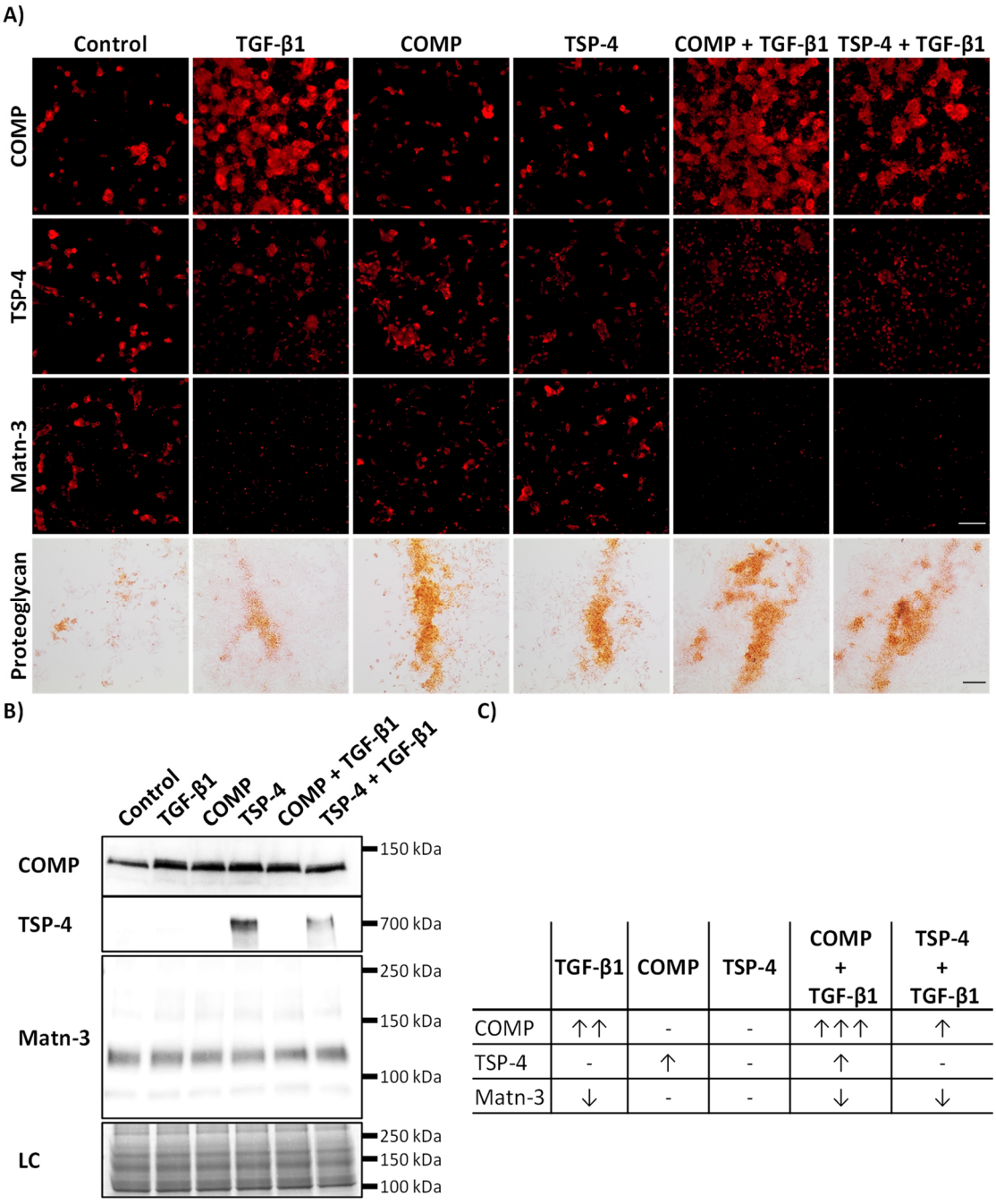

	TGF-β1	COMP	TSP-4	COMP + TGF-β1	TSP-4 + TGF-β1
COMP	↑↑	-	-	↑↑↑	↑
TSP-4	-	↑	-	↑	-
Matn-3	↓	-	-	↓	↓

Figure 3.17: Matrix formation and secretion of proteoglycan and adaptor-proteins in monolayer culture

Chondrocytes were stimulated with COMP (10 µg/ml), TSP-4 (10 µg/ml) or TGF-β1 (0.5 ng/ml) or in combination with TGF-β1 for 7 days. **A**) Immunofluorescence staining of COMP, TSP-4 and Matn-3, as well as Safranin-O staining of proteoglycans at day 10. **B**) Immunoblot assays of chondrocyte supernatants at day 10. Roti®Blue staining of proteins was used as a loading control (LC). **C**) Table, connecting the results of soluble and matrix integrated proteins. The arrows mark the increase (↑) or decrease (↓) compared to the control. No changes are indicated, by a minus (-). Three arrows indicate a strong, two arrows, a moderate and one arrow a mild regulation compared to the control. (n = at least 2 per group); unstimulated cells were used as a control; scale bar immunofluorescence staining = 100 µm and Safranin-O staining = 200 µm

3.15. COMP and TSP-4 induce Erk1/2 signal pathway while Smad signalling is not affected

In order to identify the signalling pathway that links COMP and TSP-4 stimulation to a cellular response, Erk and Smad pathways were analysed. To this end, chondrocytes were stimulated with 10 µg/ml COMP or TSP-4 for 30 min and phosphorylated Erk1/2, Smad2/3 and Smad1/5/9 detected by immunoblot analyses. Both COMP and TSP-4 induced the phosphorylation of Erk1/2 (**Fig.3.18.A**) but not of Smad2 or Smad1/5/9 (**Fig.3.18.B**).

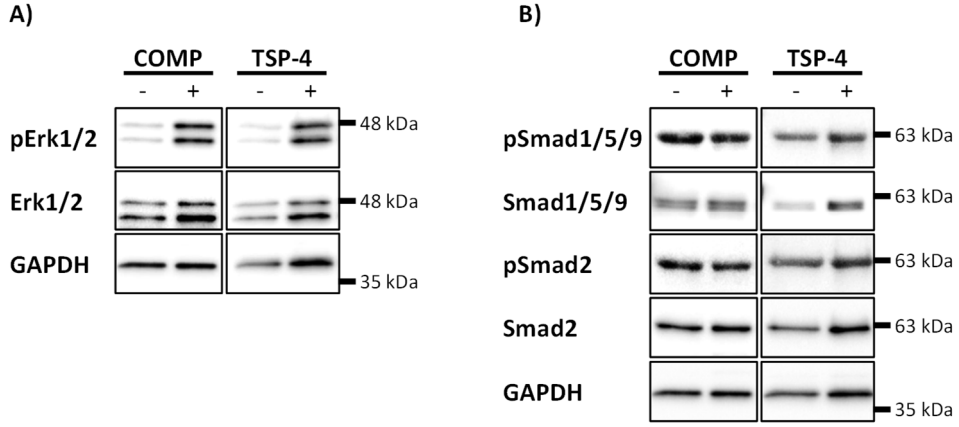

Figure 3.18: Smad and Erk phosphorylation in chondrocytes
Chondrocytes were stimulated with 10 µg/ml COMP or TSP-4. Cell extracts were harvested and Smad as well as Erk proteins detected by immunoblot. **A**) Representative immunoblots showing the detection of pErk1/2, Erk1/2 and GAPDH. **B**) Representative immunoblots showing the detection of pSmad1/5/9, Smad1/5/9, pSmad2, Smad2 and GAPDH. (n = 4).

3.16. COMP and TSP-4 modulate TGF-β1 induced Erk1/2 signalling

The effect of TGF-β1 on the collagen matrix formation was modulated by the simultaneous addition of COMP and TSP-4, respectively. Therefore, their capacity to modulate TGF-β1 induced Erk signalling was investigated. The phosphorylation of Erk1/2 was investigated after 30 min of stimulation with 10 µg/ml COMP or TSP-4 and different concentrations of TGF-β1 (0.1; 0.25; 0.5; 1 and 10 ng/ml). Erk1/2 was maximally phosphorylated after treatment with 0.25 ng/ml TGF-β1 (**Fig.3.19.A**). The additional stimulation with TSP-4 shifted this phosphorylation maximum to a TGF-β1 concentration of 0.5 ng/ml (**Fig.3.19.C**). The most intense Erk1/2 phosphorylation with simultaneous COMP treatment was found at 0.1 ng/ml TGF-β1 and continuously decreased with increasing TGF-β1 concentrations (**Fig.3.19.B**). The phosphorylation maximum at

0.1 ng/ml TGF-β1 was weaker than that of COMP alone. These results show that TSP-4 attenuates the TGF-β1 induced Erk1/2 signalling in contrast to COMP, which capacity to induce Erk1/2 phosphorylation itself is suppressed by TGF-β1.

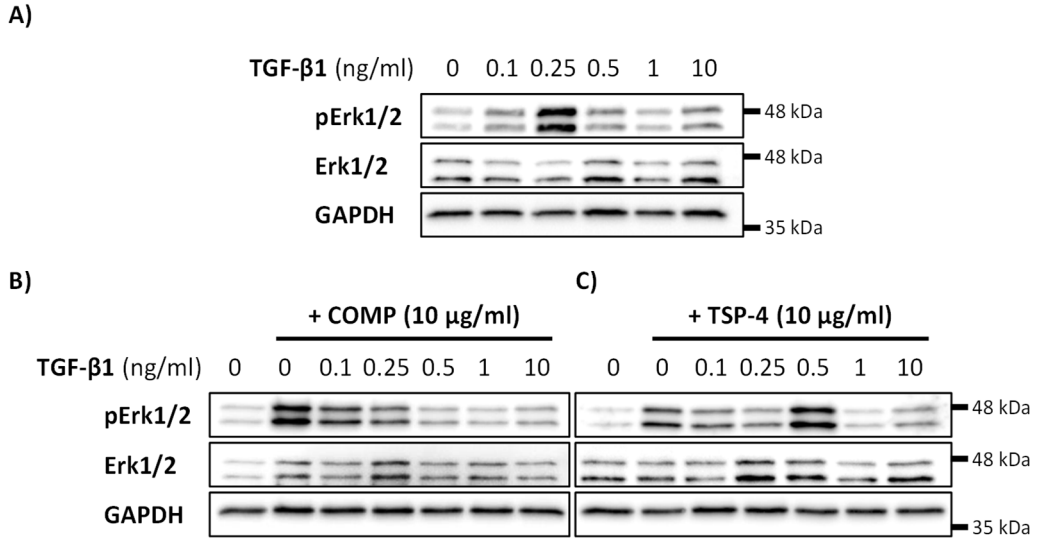

Figure 3.19: Modulation of TGF-β1 induced Erk1/2 signalling in chondrocytes
Chondrocytes were stimulated with indicated concentrations of TGF-β1 alone or in combination with COMP (10 µg/ml) or TSP-4 (10 µg/ml) before Erk1/2 proteins were detected by immunoblot. **A**) Representative immunoblots show the concentration-dependent TGF-β1 induced phosphorylation of Erk1/2 (pErk1/2). Total Erk1/2 levels remain largely unchanged and GAPDH was used as a loading control. Representative immunoblots show the influence of COMP (**B**) and TSP-4 (**C**) on the concentration-dependent TGF-β1 induction of Erk1/2 phosphorylation. (n = 4)

3.17. TSP-4 but not COMP can modulate TGF-β1 induced Smad signalling

COMP and TSP-4 could directly induce Erk1/2 signalling and simultaneously modulate the phosphorylation capacity of TGF-β1. However, even though both proteins were unable to induce Smad signalling on their own they might have the potential to modulate TGF-β1 induced Smad signalling, as observed for Erk1/2. Therefore, chondrocytes were stimulated with 10 µg/ml COMP and TSP-4 alone or in combination with different concentrations of TGF-β1 (0.1; 0.25; 0.5; 1 and 10 ng/ml). The maximum of Smad1/5/9 as well as Smad2 phosphorylation was observed at a concentration of 1 ng/ml TGF-β1 (**Fig.3.20.A**). The addition of COMP and TSP-4 did not affect Smad1/5/9 phosphorylation (**Fig.3.20.B, C**). The simultaneous stimulation with TSP-4 enhanced the TGF-β1 induced Smad2/3 signalling by shifting the phosphorylation maximum of Smad2 from 1 ng/ml to 0.25 ng/ml TGF-β1 (**Fig.3.20.C**). In contrast, COMP showed no

modulatory capacity (**Fig.3.20.B**). These results show that COMP does not affect Smad signalling, while TSP-4 can modulate the bioactivity of TGF-β1 to induce Smad2 phosphorylation.

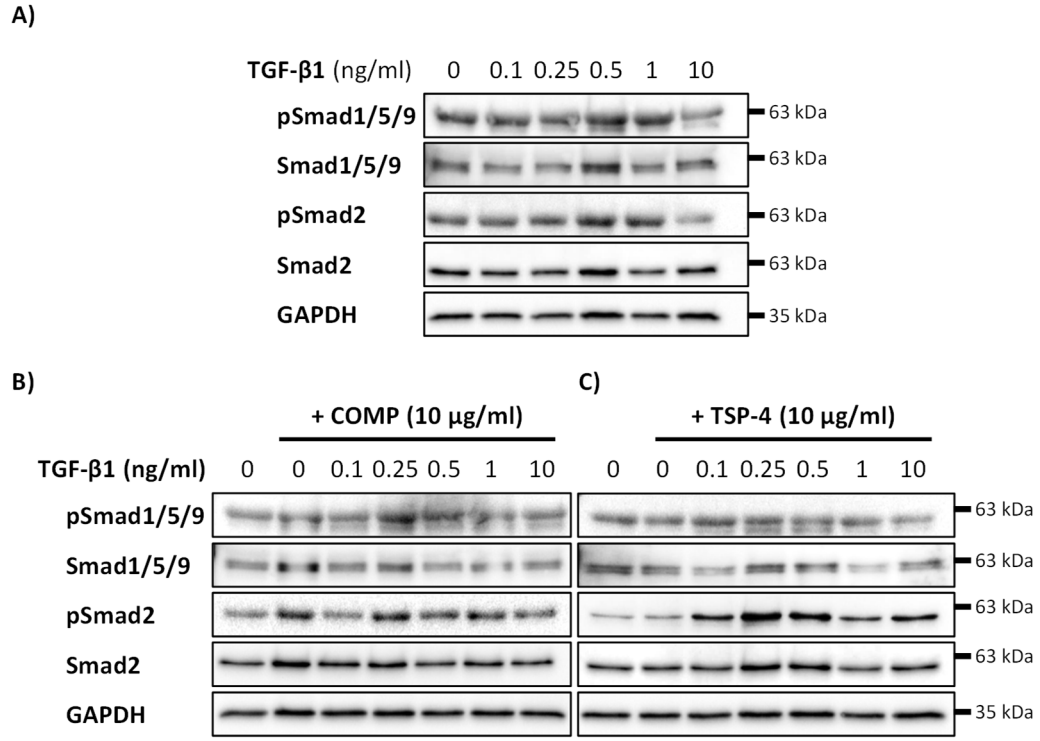

Figure 3.20: Modulation of TGF-β1 induced Smad signalling in chondrocytes
Chondrocytes were stimulated with different concentrations of TGF-β1 (0.5 ng/ml) alone or in combination with COMP (10 µg/ml) or TSP-4 (10 µg/ml) before Smad proteins were detected by immunoblot. **A**) Representative immunoblots show the concentration-dependent TGF-β1 induced phosphorylation of Smad1/5/9 (pSmad1/5/9) and Smad2 (pSmad2) as well as total Smad1/5/9, Smad2 and GAPDH. Representative immunoblots show the influence of COMP (**B**) and TSP-4 (**C**) on the concentration-dependent TGF-β1 induction of Smad1/5/9 and Smad2 phosphorylation. (n = 4)

3.18. COMP and TSP-4 binding capacity to TGF-β1

COMP and TSP-4 had similar capacities to contribute to the ECM formation and could further modulate TGF-β1 induced Erk1/2 signalling. COMP is known to interact with TGF-β1, thereby modulating the bioactivity of TGF-β1 (87). However, if TSP-4 also directly interacts with TGF-β1 is not known. Therefore, the interaction of both proteins with TGF-β1 was characterised in surface plasmon resonance measurements using the Biacore system. The protein-protein interaction profiles show that both COMP (**Fig.3.21.A**) and TSP-4 (**Fig.3.21.B**) interact with TGF-β1. According to the calculated K_d value, the binding of TGF-β1 to TSP-4 seems stronger than to COMP. However, the value lies in a rather similar range and due to the low dissociation rate of COMP, a direct comparison is difficult (**Fig.3.21.C**). The kinetic data were calculated based on a 1:1 model using the Biacore software and include chi^2, association rate (ka), dissociation rate (kd) and the dissociation constant (K_d).

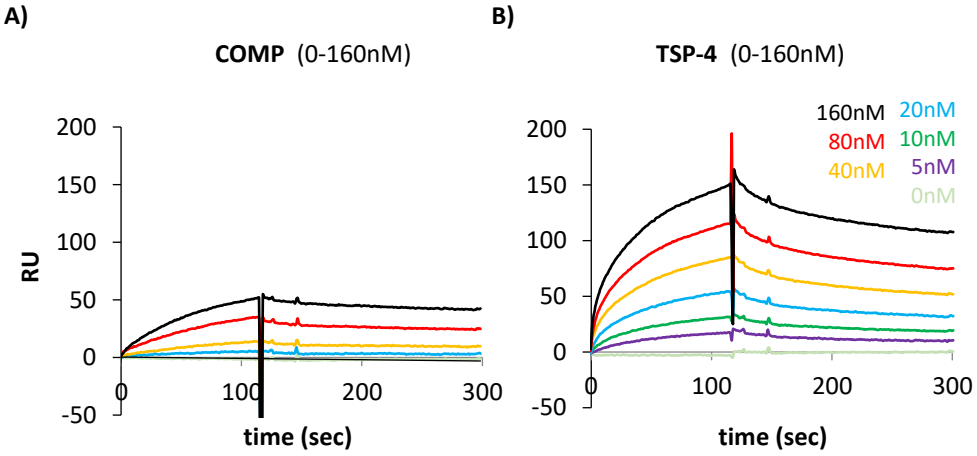

C)

Ligand	Analyte	Model	chi^2	ka (1/Ms)	kd (1/s)	K_d (nM)
TGF-β1	COMP	1:1	4.6	1.71^{-4}	3.92^{-4}	22.9
TGF-β1	TSP-4	1:1	10.3	1.41^{-5}	8.89^{-4}	6.30

Figure 3.21: Surface plasmon resonance measurements to analyse the interaction of COMP and TSP-4 with TGF-β1
Protein-protein interaction profiles showing the binding of COMP and TSP-4 to TGF-β1. Surface plasmon resonance sensorgrams generated with the Biacore system are shown for COMP (**A**) and TSP-4 (**B**). Resonance signals expressed as response units (RU), indicate the degree of binding between COMP and TSP-4 with TGF-β1. COMP and TSP-4 were used in concentrations from 160 nM to 5 nM and injected to the immobilised TGF-β1 on a CM5 chip. **C**) Table, showing the data received from the Biacore assays. The association rate (ka), the dissociation rate (kd), the dissociation constant (K_d) and the chi^2 are represented. The kinetic 1:1 model (Langmuir model) was used to calculate these parameters.

4. Discussion

The ECM of articular cartilage is a highly complex network composed of several elements, hierarchically organised and specifically distributed, accordingly to their functional characteristics. This architecture provides the biomechanical properties of articular cartilage, enabling a painless and frictionless motion. (5)

In OA, the articular cartilage is the target of degradation, which is paralleled by a loss of function, leading to immobility and pain (142). During disease progression, the ECM is continuously degraded (79, 142, 155, 164, 165), resulting in a reduced density of the ECM network and increased accessibility of ECM components to chondrocytes. The interaction of ECM components with chondrocytes causes a reactivation and affects the chondrocyte phenotype (15, 17). As a severe consequence, the cartilage homeostasis is disturbed by dysregulated anabolic and catabolic processes, involving especially the Erk and Smad signalling pathways (142, 150, 169, 216). Besides, the increased ECM degradation also a re-expression of ECM proteins, such as collagen II, Matn-3 and COMP (79, 154, 156, 157) occurs. The new synthesis of ECM proteins might be an attempt of the articular cartilage to induce repair mechanism to counteract the ECM degradation and slow down the disease progression. So far, the spectrum of regulated proteins in OA is poorly understood as well as the contribution of these proteins in OA typical processes.

4.1. TSP-4 is present in healthy cartilage and severely upregulated in OA

TSP-4 is expressed in various tissues (106, 107, 109) and rapidly upregulated in disease (111-123) but barely investigated in articular cartilage. In this project, it was shown for the first time, that TSP-4 is weakly expressed in healthy articular cartilage and severely increased in OA. The localisation of TSP-4 in healthy cartilage is restricted to the superficial zone, suggesting a contribution to its specific biomechanical properties. The superficial zone is the stiffest zone with the highest tensile strength (6, 217) to protect the subjacent cartilage layers from the shear forces during articulation (5). TSP-4 as an adaptor-protein might contribute to these properties by strengthening the network stability and modulate fibril assembly as it was shown in other tissues (109) or for its family member COMP (85). The response of TSP-4 to substrate stiffness and mechanical

alterations (218, 219) could be an attempt to strengthen ECM components as a response to tissue injury and the reason of a continuous expression in the superficial layer, which is the first area of damage during trauma or mechanical overload. Also, in OA development and progression, the superficial zone is the first point of damage. A change in the composition of this and underlying zones, as a damage response to provide different biomechanical properties seems likely. In that manner, a severe upregulation of TSP-4, already before visual degradation of the cartilage surface, was observed. An intense ECM remodelling during OA progression occurred, proteoglycans were continuously degraded from early to severe OA, starting at the superficial zone and Matn-3 localisation was restricted to the transitional zone and expanded to deeper zones in late-stage OA. COMP was initially degraded but re-expressed in later OA stages, especially in the upper cartilage zones. TSP-4 is abundantly expressed, specifically in the transitional and deep zones of OA cartilage, suggesting a change of the biomechanical properties of these zones to strengthen the cartilage resilience.

In contrast to COMP and Matn-3, TSP-4 amounts accumulate with increasing OA severity grade. No differences between males and females could be detected, indicating a damage-associated rather than a gender-specific upregulation. The increased TSP-4 synthesis could not be confirmed on the gene level, suggesting an extended half-life or decelerated protein turnover. Also, a change of the OA associated ECM composition might lead to an altered protein anchorage, meaning the loss and exposure of additional binding sites, due to protein degradation and synthesis. Investigations of the ECM in genetically modified mouse lines demonstrated similar phenomena, showing the lack of one specific protein altering the anchorage of other ECM components (31, 220, 221). To investigate this possibility in more detail, the anchorage of TSP-4 and COMP were analysed by extracting proteins under mild and harsh conditions. Protein levels unaffected by anchorage would result in a similar extraction profile under mild and harsh conditions as well as in the same protein ratio. However, the highest amount of TSP-4, extracted under harsh conditions was observed in G3/4 while this did not occur under mild conditions. To a great extent, TSP-4 is tightly anchored in the ECM but seems to be weaker in an intact G1 compared to an altered and damaged G3/4 matrix, suggesting an anchorage depending on the OA severity grade. Comparable, but less obvious results were obtained for COMP, indicating that similar structures cause similar

functions. TSP-4 is predominantly released and degraded in an early OA stage, while integration and accumulation, in the ECM, were promoted in later OA stages. This differences in protein anchorage might be due to additional binding sites on ECM components but cannot predict the behaviour of these interactions. To investigate the gene expression of *THBS4* and *COMP* in more detail, another method would be preferable, like *in situ* hybridisation, allowing direct detection of the RNA synthesis on the tissue sections enabling a comparison with the protein localisation.

The distribution of TSP-4 in OA cartilage occurs predominantly in the transitional and the deep zone as well as in all regions around the chondrocytes. Its high expression, specifically in the area, where proteoglycans started to be degraded suggests a contribution to stabilise the degrading ECM. So far, it is not known if TSP-4 can directly interact with aggrecan or other proteoglycans, as it was shown for other thrombospondin family members (51, 222) but it is quite likely that the structurally similar TSP-4 shares this function and supports the integrity of proteoglycans in the ECM. Additionally, the finding that TSP-4 anchorage is tighter in a severely degraded compared to a relatively intact ECM indicates a stabilising function. The re-expression of other ECM proteins in OA was primarily interpreted as an attempt to inhibit and decelerate further matrix degradation (223-225). In that manner, TSP-4 might also protect the articular cartilage by compensating the loss of matrix proteins and strengthening the ECM network by cross-linking several components, such as collagen II, III, V or fibronectin (103).

Its close family member COMP is ubiquitously expressed in healthy cartilage but is a target of degradation and re-expression in OA. Due to the re-expression, COMP levels in OA cartilage are similar at all severity grades, showing that chondrocytes are exposed to COMP theoretically at any time point, including health and OA. Although, in OA, COMP is not only presented to chondrocytes in its matrix-associated form but also as a soluble protein, newly synthesised. Contrary, TSP-4 is mainly accessible to chondrocytes since earliest OA, suggesting an additional functional role to that of COMP. The differential distribution of COMP and TSP-4 in health and OA, suggests the participation of COMP in ECM maintenance while TSP-4 promotes ECM protection already at the onset of damage. Besides, the stabilising roles of these proteins, a direct effect on

chondrocytes was not reported, so far. Therefore, the functional roles of COMP and TSP-4 in OA relevant processes were investigated and compared.

4.2. Functional roles of COMP and TSP-4 in articular cartilage

The distribution and expression of COMP and TSP-4 were investigated in human OA articular cartilage samples isolated from the femoral knee condyles. Due to the limitation in human cartilage samples, the heterogeneity of patients and potential OA-associated changes, even in healthy-looking areas of OA cartilage, it was decided to perform all further *in vitro* experiments in healthy non-OA chondrocytes. However, healthy articular cartilage from human knee joints are rare and could not be acquired in sufficient amounts. Other cartilage types, e.g. costal cartilage, would be a suboptimal alternative due to its characteristics as non-weight bearing cartilage including its different matrix composition and biomechanical properties (226). From all animal models, pigs show the highest similarities to humans, regarding their anatomy, physiology and genetics (227). Similar to humans, pigs develop a degenerative joint disease later in their life, comparable to human OA (228). Therefore, healthy pig articular cartilage from the knee joint was assessed as the best chondrocyte source to receive conclusive data about the role of COMP and TSP-4 in articular cartilage in health and OA onset.

4.2.1. The effect of TSP-4 and COMP on chondrocyte migration, attachment and proliferation

TSP-4 in OA and COMP, especially in health are distributed in all regions of the cartilage, including the pericellular matrix, which is relevant for chondrocyte integration and interaction (229). One of the hallmarks of OA is chondrocyte cluster formation, a process not very well understood (230). The clustering of chondrocytes either occurs as a result of proliferation (231, 232) or migration (233) of surrounding cells. Histological staining showed the formation of cell clusters predominantly in the close proximity to fissures in the upper part of the cartilage, where COMP and TSP-4 were expressed. A repopulation of damaged cartilage areas with chondrocytes would promote the ECM repair by the synthesis of new ECM proteins. In the performed experiments, neither

COMP nor TSP-4 could contribute to chondrocyte proliferation, but COMP was demonstrated to attract chondrocytes and accomplish their anchorage.

A conservative dogma reveals that chondrocytes are immobilised in articular cartilage and unable to move, due to the dense extracellular matrix surrounding the cells. However, especially in OA the ECM is characterised by a loosened structure and an altered composition, allowing an increased migratory capacity of chondrocytes. Other *in vitro* studies, revealed that cells from the surrounding tissue migrated to the site of induced cartilage damage to repopulate the area, contributing to repair (234, 235). Additionally, a specific cell population isolated from late-stage OA cartilage was able to migrate into and through the matrix of intact OA cartilage (236). The importance of these findings is to break the dogma and strengthen the idea of migrating cells in articular cartilage. COMP re-expression in OA occurs predominantly in the upper zones of cartilage, where the ECM degradation is most pronounced and proteoglycans are already completely lost. It is attractive to speculate that the re-expression of COMP could form a gradient that can attract cells from neighbouring areas and mediate their attachment (86, 110) via binding to surface integrin receptors, like α5β1 and αvβ3 (86), both expressed on healthy and osteoarthritic chondrocytes (237). Integrins are surface receptors and mediate, besides cell attachment and migration several other processes, including cell proliferation, survival, cell signalling, cartilage homeostasis and ECM organisation (238). The α5β1 integrin was also reported to be involved in cell migration for other cells (239, 240) and might mediate the COMP associated cell migration and attachment, but further studies are needed to confirm this theory. Integrins are dysregulated in OA, among others by activation of ECM degradation products, leading to inflammation and ECM degradation (241, 242), suggesting that differential ligands may induce different downstream signalling pathways. Also, the integrin receptor profile is changing, including the new synthesis of α4 integrin, which is involved in cell motility, important for cluster formation occurring in late-stage OA (243, 244). However, TSP-4 had no impact on the migratory capacity of aged OA chondrocytes, while COMP was still able to attract them. Based on these findings, we showed that COMP but not TSP-4 mediates chondrocyte migration, independently of age and disease as well as their attachment. These data suggest that COMP and TSP-4 are prone to different chondrocyte receptors, fulfilling distinct tasks maybe as a consequence of their specific

distribution in the ECM. TSP-4 is insignificant for chondrocyte migration, but a rapid upregulation in injury is associated with the regulation of matrix protein synthesis and ECM remodelling (108, 112, 245), both processes highly relevant in OA. Also, induction of ECM protein synthesis seems highly likely and beneficial for COMP after mediating chondrocyte migration and attachment.

4.2.2. The effect of COMP and TSP-4 on ECM synthesis and formation

COMP was shown to directly induce gene expression in hepatocellular carcinoma cells, relevant for disease progression (246) and modulated those, induced by TGF-β1 in mink lung epithelial cells (87). TGF-β1 is a so-called general inducer of transcription in chondrocytes, due to the expression of several ECM proteins, like aggrecan, collagen II (90) or COMP (91) and was used as a reference in this study. Watanabe et. al (133) demonstrated induction of *acan* expression 6 h after stimulation with TGF-β1, which continuously increased until the final time point at 24 h. Therefore, gene levels were analysed after 6 h to detect a rapid response and after 24 h to receive a more detailed expression profile.

After 6 h, COMP and TSP-4 induced the upregulation of *COL2A1* and *COMP* expression. Additionally, TSP-4 could induce the expression of *ACAN* as well as *COL12A1* indicating a role of COMP and TSP-4 in repair and especially of TSP-4, in tissue remodelling. Besides, the COMP associated reduction in *MATN3* expression after 24 h, no significant differences in the expression patterns could be observed by the treatment with COMP or TSP-4. The mean 2^-ΔΔCT values of these genes are comparable between time points, except *ACAN* expression, which seemed to return to the basal levels after 24 h. In general, the expression levels induced by COMP and TSP-4 did not further increase from 6 h to the 24 h time point. Investigations on periosteal chondrocytes, treated with 200 µg/ml COMP (20 times the amount from our experiments) for 7 and 21 days revealed a decrease of *COL10A1* expression at both time points, although no differential regulation of *COL2A1*, *ACAN* or *COL1A1* (247). Based on this study, no dramatic increase in gene expression would be expected by COMP or TSP-4 at later time points. Although, the faint increase in *COL9A1* expression by COMP compared to TSP-4 at the 24 h time point, might have become more obvious. Both proteins induced genes,

relevant for ECM maintenance and repair already at an early time point but are in general weak inducers of transcription.

Gene expression data provided an overview of COMP and TSP-4 regulated genes but are of minor significance, due to the variety of processes affecting the final amount of protein. mRNAs might be the target of degradation, leading to a lower transcription rate but still resulting in the production of a proper amount of proteins caused by an effective translation. Also, the other way round, a high gene expression rate can result in a low amount of protein, due to post-translational modification and following degradation processes. Therefore, the effect of COMP and TSP-4 on protein synthesis and ECM formation was investigated.

COMP and TSP-4 increased the synthesis and matrix integration of collagen II, collagen IX, collagen XII and proteoglycan while inhibiting those of collagen X. The increased expression of the main ECM components, collagen II and proteoglycan on gene and protein level as well as their potential to enhance TGF-β1 induced collagen II and proteoglycan synthesis demonstrate the involvement of both proteins in cartilage repair by restoring tensile strength and elasticity (5). Collagen II is the predominant collagen fibril in articular cartilage (22) and its zonal specific biomechanical as well as structural properties are achieved by its interaction with different ECM components, resulting in a heterogeneity of collagen II fibrils (23, 24, 35). Therefore, also the effect of COMP and TSP-4 on the expression of minor collagens, like collagen IX and XII are of great interest.

Collagen XII, TSP-4 and COMP are all localised in the superficial zone in healthy cartilage, which possesses properties, such as stiffness to withstand the immense forces of articulation (6, 35). Therefore, it is not surprising that TSP-4 and COMP can induce collagen XII synthesis. Especially in OA, affecting all cartilage layers, increased collagen XII levels could support the stiffness and in that manner the integrity of the ECM. Due to the differential distribution of COMP in upper and TSP-4 in lower cartilage areas, collagen XII expression might contribute to the strengthening of all cartilage layers, but further experiments are necessary to confirm this interpretation. COMP and TSP-4 could induce the synthesis of collagen XII, but in combination with TGF-β1, this effect seems reversed, maybe due to a negative feedback loop. TGF-β1 stimulation resulted in high levels of immobilised and soluble collagen XII. These levels were much higher than that

seen in COMP and TSP-4 stimulated cells. Downregulation of collagen XII might be the consequence of the binding of TGF-β1 to COMP and TSP-4, blocking relevant binding sites, e.g. on growth factor receptors, as reported for COMP-BMP-2 (248). Also, a competition for intracellular proteins, essential in the signalling cascade within chondrocytes could be an explanation. Such a competition was shown for collagen II, which inhibits BMP signalling by negatively regulating intracellular Smad1 (130). Conspicuously, collagen XII amounts were low in conditions were collagen IX was enriched. Also, collagen IX-KO mice showed an increased amount of collagen XII distributed in areas where collagen XII is usually not expressed (220). Both, FACIT-collagens share sequence homologies and are associated with collagen organisation (249), indicating a compensatory role of collagen XII in the absence of collagen IX. While collagen IX is rather associated with thinner collagen fibrils, lacking decorin (22-24), collagen XII is a known interaction partner, suggesting the involvement in the organisation of collagen fibrils with larger diameter (36). This property would indicate an involvement in tissue preparation to withstand biomechanical forces.

COMP and TSP-4 stimulation had different effects on collagen IX expression, which was upregulated by both proteins. However, increased amounts of soluble collagen IX have only been detected in the supernatant of COMP stimulated cells, indicating an impaired matrix integration, by so far unknown mechanisms. On the gene level, a weak but significant upregulation of *COL9A1* was observed in COMP compared to TSP-4 stimulated cells. The upregulation on gene level could lead to an increased protein amount, not able to entirely integrate into the matrix, maybe due to missing binding sites. Important binding partners of collagen IX are COMP and Matn-3 (31, 220), which are either moderately present or absent in the cell-associated matrix and detected in the supernatant in all conditions. Matn-3 matrix integration was diminished in collagen IX-KO mice (31), suggesting that the integration capacities of both proteins may depend on each other. A co-localisation of collagen IX and Matn-3 were observed in most conditions, while TGF-β1 treatment reduced the amount of collagen IX and almost completely diminished Matn-3. Another possibility, stimulation with COMP might increase and promote the intracellular level of COMP, mediating collagen IX trafficking and secretion (250), resulting in protein complexes in the supernatant. COMP can directly bind to collagen IX with its C-terminal domain (82), suggesting a higher affinity

of collagen IX to COMP then to the few binding partners in the matrix. Collagen IX is entirely integrated into the cell-associated matrix when stimulated with TSP-4. The reason, therefore, might be the different binding properties of COMP and TSP-4 to collagen IX. While COMP is an important binding partner, TSP-4 cannot directly bind to collagen IX (220), excluding the possibility of a complex formation.

Furthermore, the stimulation with COMP and TSP-4 resulted in a partially reduced amount of collagen I and lead to a shift in direction collagen II positive cells. The percentage of collagen I and collagen II positive cells in control and TGF-β1 stimulated cells were comparable, indicating involvement of COMP and TSP-4 in suppressing chondrocyte dedifferentiation. Several studies reported that chondrocytes, cultured in monolayer become dedifferentiated, characterised by the loss of cartilage-specific markers, like collagen II, collagen IX and COMP as well an increase of collagen I (251, 252), just the opposite of the observations made after COMP and TSP-4 stimulation. Although, the loss of collagen IX, visible in TGF-β1 stimulated cultures, could not be reversed by an simultaneous treatment with COMP or TSP-4, supporting the observation that the loss of collagen IX is not reversible (251) and demonstrating an effect of TGF-β1 on the chondrocyte phenotype. Based on the present data, COMP as well as TSP-4 promote the repair of the ECM by inducing the synthesis of highly relevant ECM proteins and stabilising the chondrocyte phenotype by suppressing hypertrophy and dedifferentiation.

COMP was able to contribute to the synthesis of TSP-4 and further enhanced its own expression induced by TGF-β1, while TSP-4 seems to reduce the TGF-β1 induced COMP levels. The probability that COMP in combination with TGF-β1 could enhance its own expression, was already suggested by Haudenschild D. et al. (87) and might contribute to the integration of other, newly synthesised proteins, like collagen II or collagen XII and support in that manner the ECM stabilisation. TSP-4 seems to inhibit its own integration in the matrix, observable by high protein amounts in the supernatant. The mechanism or reason behind this observation is not known but suggested that less binding partners are available in the cell-associated matrix when cells were only stimulated with TSP-4. Additional treatment with TGF-β1 showed less soluble TSP-4, indicating that TGF-β1 induced ECM protein synthesis, providing necessary binding partners, like collagen II and collagen I (103), supporting TSP-4 matrix integration. Also,

a role as signalling molecule might be possible, for example via direct interaction with chondrocytes or growth factors, such as TGF-β1, contributing to tissue remodelling and regulation of collagen synthesis as shown here and described in other tissues (108). In this study, a direct interaction of TSP-4 with TGF-β1 was demonstrated and suggests that newly synthesised TSP-4 can bind to matrix integrated TGF-β1, observable by a lower amount of soluble TSP-4 in the supernatant of cultures treated with TGF-β1 together.

Immunofluorescence staining of chondrocyte cultures as well as immunohistological staining of OA cartilage showed an intracellular distribution of COMP and TSP-4, implying a transitional accumulation after their synthesis before secretion but also a possible intracellular function of these proteins. An intracellular involvement of TSP-4, in the ER stress response (253) was already reported. Here, TSP-4 acts as a chaperone in protein folding, trafficking and secretion (253, 254). TSP-1 is further involved in collagen I processing and assembly (255) as well as COMP, in the export and the following assembly into fibrils (85). The importance of COMP in collagen export, was demonstrated in studies, showing that the lack of COMP or a mutated version lead to a retention of ECM proteins, such as collagen I, collagen IX, collagen XII, decorin and Matn-3 in the ER (84, 100, 250). COMP and TSP-4 bind fibrillar collagens via the same GXKGHR motif (256), strengthen the theory that TSP-4 and COMP share their functions in protein trafficking. Although, they are distinguishable in their potential to bind collagen IX (82, 220), therefore, it might be possible that TSP-4 processes the trafficking of other proteins. The synthesis and ECM formation of collagen II, IX, XII and proteoglycan are promoted, thereby the intracellular function of TSP-4 might be involved in the secretion and assembly of collagen II and aggrecan, in addition to COMP, which is associated with the export of collagen IX and XII, contributing in ECM repair. However, further studies will be required to prove this hypothesis.

These data show that COMP and TSP-4, participating in processes promoting the formation, maintenance and repair of the ECM. Both proteins induced a weak but rapid upregulation of ECM relevant genes after 6 h and regulated the synthesis and ECM integration of collagens and proteoglycans, suggesting a potential to directly induce cell signalling pathways. Furthermore, a modulatory role of COMP and TSP-4 in TGF-β1 associated protein synthesis was observed. Although, if these effects correlate with the activation of Erk and Smad signalling was not investigated, so far.

4.2.3. COMP and TSP-4 modulate cell signalling pathways

In OA, a dysregulation of chondrocyte signalling causes a switch from anabolic to catabolic pathways, especially from anabolic Smad2/3 to the catabolic Smad1/5/9, by so far unknown reasons. Also, the anabolic Erk1/2 pathway shifts to a catabolic response, most likely due to a differential ligand-receptor binding. COMP and TSP-4 induced the expression of anabolic proteins, suggesting activation of Erk1/2 or Smad2/3 and inhibition of Smad1/5/9 due to the downregulation of catabolic proteins.

Indeed, COMP and TSP-4 could directly induce Erk1/2 phosphorylation in articular chondrocytes but failed to phosphorylate Smad2/3 or Smad1/5/9. Another ECM protein, collagen II was reported to suppress hypertrophy in articular chondrocytes by inducing the phosphorylation of Erk1/2 (130). The same publication showed the ability of collagen II to induce Smad2/3 phosphorylation, although this effect was not further investigated. Additionally, TGF-β1 can induce the expression of aggrecan and collagen II in chondrocytes via Erk1/2 and Smad2/3 signalling (90). Therefore, COMP and TSP-4 are suggested to mediate the upregulation of aggrecan, collagen II as well as the downregulation of collagen X via Erk1/2 signalling. COMP can induce Erk1/2 phosphorylation via CD36 receptor in primary hepatic stellate cells leading to the expression of collagen I (257). The CD36 receptor is present on healthy chondrocytes and even increases in OA (72), suggesting an association with chondrocyte-specific signalling to induce collagen II. No information about potential receptors for TSP-4 is available, but its association with Erk is once more controversial and tissue-dependent. TSP-4 can induce ERK1/2 phosphorylation as an acute stress response in failing hearts (218) but also drive forward neuronal differentiation by blocking Erk signalling (258). The stimulation of chondrocytes with COMP and TSP-4 might also result in the synthesis of ECM proteins, which can in turn mediate the synthesis of proteins primarily thought to be induced by COMP or TSP-4, like collagen II. Therefore, future experiments are necessary to confirm that COMP and TSP-4 induce the synthesis of collagen II and proteoglycans via Erk1/2 signalling. Inhibitors of the Erk signalling pathway will be used as well as specific receptor blockers, like for CD36 to identify the downstream produced proteins and the initiating receptors.

A study in zebrafish associated the Wnt-signalling pathway with collagen XII expression (259). Although, inhibition of Wnt signalling could not entirely abolish collagen XII (259), indicating an insufficient blocking of the inhibitor or the involvement of other signalling pathways. Interestingly, Wnt signalling is specifically detectable in the superficial zone of articular cartilage (260, 261), where also collagen XII is commonly expressed. In OA, Wnt signalling is dysregulated and mainly associated with ECM degrading processes, while its activity is necessary for ECM maintenance in health (262, 263). These data also suggest a ligand specific activation of downstream genes, like observed for Erk1/2 (90, 130, 169, 216). TGF-β1 signalling can synergise with those of Wnt to support the expression of Wnt associated genes (264), indicating an indirect effect of TGF-β1 in the regulation of Wnt-specific genes. Signalling via different pathways might explain the collagen XII upregulation by TGF-β1, COMP or TSP-4 single treatment as well as the downregulation by dual treatment. However, further experiments will be necessary to identify COMP and TSP-4 associated mechanisms, responsible for collagen XII upregulation.

Besides Smad2/3, TGF-β1, at a high concentration can also induce the phosphorylation of Smad1/5/9, resulting in the synthesis of collagen X (127). Stimulating chondrocytes with COMP and TSP-4 in combination with TGF-β1 attenuated the phosphorylation of Erk1/2, while only TSP-4 promoted the induction of Smad2/3 signalling. However, neither of the two proteins did affect Smad1/5/9 signalling, restricting the downregulation of collagen X to an Erk depending process. Modulatory effects of COMP were reported for TGF-β1 (87) and BMP-2 signalling (88, 248). In bone-marrow derived stem cell studies, COMP increased the BMP-2 induced phosphorylation of Smad1/5/9 (88). Although, in vascular smooth muscle cells the addition of COMP to BMP-2 resulted in a signal inhibition, by COMP blocking the BMP-2-receptor binding (248). In this study, also TSP-4 was shown to interact with TGF-β1, suggesting that the phosphorylation of Smad2/3 was promoted and Erk1/2 attenuated as a result of different receptor binding sites. COMP could not enhance the phosphorylation of Smad2/3 in contrast to TSP-4, suggesting once more that the receptor repertoire and protein binding motifs are partially distinguishable between these proteins. The activation of the Erk signalling pathway by COMP and TSP-4 might induce proteins, not investigated in this study but affecting the synthesis of additional

proteins, observable after 10 days in culture. Therefore, transcriptome analyses at different time points after stimulation could help to identify the whole spectrum of ECM proteins and growth factors involved in chondrocyte signalling. A COMP and TSP-4 mediated expression of TGF-β1 was not investigated in this project. TGF-β1 is synthesised as a latent complex and needs to be activated via cleavage of its propeptide (265). TSP-1 can bind via a specific sequence to the latent TGF-β1, leading to its activation (266). COMP and TSP-4 are lacking this TSP-1 domain and might not be able to activate the latent complex. If COMP and TSP-4 can directly or indirectly induce the synthesis of TGF-β1 as well as contribute to its activation by differential mechanisms will be investigated in future studies.

These data, demonstrate important and highly relevant roles for COMP and TSP-4 in cartilage homeostasis, maintenance and repair, which might be useful in the development of therapeutical applications.

4.2.4. Clinical application of COMP and TSP-4

The diagnosis of OA is usually based on radiographic images (176-178), although if cartilage damage is visible, the disease progressed already to a more severe stage. To diagnose OA at an earlier time point, allowing precautionary measures to stop disease progression, investigations to identify valuable biomarkers are performed. During OA progression, the activity of degrading enzymes varies, leading to the generation of specific degradation products, which are released from the ECM and diffuse to the synovial fluid and enter via the highly vascularised synovium (267) the blood circulation. The detection of such degradation products in the serum could be used as an invasive method to diagnose OA. Increased COMP levels were reported in OA (180, 189) and investigations on the clinical application of specific antibodies against COMP fragments (198, 199) are still ongoing. The presence of COMP in healthy cartilage still carries the risk of increased levels due to an OA unspecific degradation as a consequence of mechanical overload, for example excessive sports (268).

TSP-4, as a newly synthesised protein in OA with a weaker anchorage in an intact ECM, might be a valid biomarker to detect early OA. In the present study, the amount of pentameric as well as fragmented TSP-4 were detected in the sera of healthy controls (HCs) and OA patients via immunoblot. No differences, in the level of the total

(pentameric and fragmented) and pentameric TSP-4 could be detected between HCs and OA patients. Similar results were obtained earlier by another study (110), investigating TSP-4 levels in sera of HC and OA patients by enzyme-linked immunosorbent assay (ELISA). Although, they claimed that significance might have been reached by investigating a larger patient cohort. However, the ELISA technique does not allow a specification of the antibody binding. Therefore, it might be possible that also fragments were detected, resulting in an increased level of TSP-4. By distinguishing TSP-4 proteins in different structural conditions, the level of total TSP-4 seemed to increase in OA, while the amount of pentamers decreased. The presence of specific TSP-4 fragments was investigated in more detail, based on the valuable information received from other ECM proteins (199, 269). Thereby, two specific TSP-4 fragments (fragment 1 and 2) were increased in OA compared to HC sera, indicating that OA-related enzymes are responsible for this degradation pattern. Levels of fragment 3 and fragment 4 were not distinguishable between OA and HCs and consequently not directly associated with an OA related cleavage. To our knowledge, the mechanism, leading to TSP-4 cleavage and degradation is not known but assumed that MMP-9, MMP-13, ADAMTS-7, and ADAMTS-12 are potential candidates due to their upregulation in OA (127, 270, 271) and capacity to cleave COMP (272-274). Future studies are ongoing to identify enzymes cleaving TSP-4 as well as the effects of the cleavage products on chondrocytes. The functional and biochemical characterisation of the fragments will show if they are involved in the expression of inflammatory mediators and matrix-degrading enzymes, causing further cartilage damage as reported for other ECM proteins (168, 275). Furthermore, the investigation of sera from patients with suspicion of OA and different OA severity grades, classified by imaging techniques should provide more information about the potential of TSP-4 in the diagnosis of OA, especially at a stage before irreversible damage occurs.

Besides, the diagnostic application, COMP and TSP-4 might be useful in the treatment of OA. A promising alternative therapy to the total knee replacement is the ACI and MACI technique, resulting in the formation of cartilage tissue after transplanting chondrocytes into the side of damage (200). The limitation of these procedures is the *in vitro* expansion of chondrocytes, necessary for clinical applications but resulting in a dedifferentiated phenotype (203, 276). Dedifferentiation involves the downregulation

of the chondrocyte markers COMP, collagen IX and collagen II (251) as well as the upregulation of collagen I (277), resulting in the formation of cartilage with insufficient biomechanical properties (45). This phenotype can be reversed by transferring chondrocytes to 3D culture systems (251, 278, 279), but the downregulation of collagen IX as well as the upregulation of collagen I are permanent and cannot be reversed (251). Therefore, it is necessary to find culture systems to protect the chondrocyte phenotype and prevent any changes in the ECM expression. Growth factors, like the fibroblast growth factor 2 (280), variations in cell seeding concentrations (281, 282) or 3D culture conditions (251) are reported to prevent chondrocyte dedifferentiation. In this project, COMP and TSP-4 suppressed chondrocyte dedifferentiation in monolayer culture, independently of cell proliferation. Therefore, COMP and TSP-4 might be promising factors to maintain the chondrocyte phenotype during *in vitro* expansion. The advantage of monolayer cultures is easy handling and compared to 3D systems, the lower costs. The use of growth factors is delicate in clinical application, due to their widespread activities (283) and therefore, TSP-4 and COMP, which are both expressed in cartilage are preferable.

After *in vitro* expansion, chondrocytes are transplanted into the side of the defect, either directly or on scaffolds. The properties of porous scaffolds, like porosity, pore size (284, 285) and stiffness (286, 287) can be regulated by the incorporation of different components. Based on the data received in this project, incorporation of COMP and TSP-4 would be highly beneficial by improving cell anchorage, protecting chondrocytes phenotype and inducing the production of proteins, essential for ECM properties. The potential of COMP to attract chondrocytes can also improve the quality of cell-free scaffolds by supporting the scaffold population. The subsequent interaction of migrated cells with scaffold associated COMP and TSP-4 would further promote cartilage tissue formation. COMP and TSP-4 could improve the quality and survival of grafts by promoting the formation of cartilage tissue, resembling those of articular cartilage and its biomechanical properties. Therefore, this data might contribute to the wellbeing of OA patients and improve their life quality.

4.3. Conclusion

The data of this project demonstrate that chondrocytes in articular cartilage can activate mechanisms to protect and repair the ECM in injury and disease. COMP and TSP-4, distributed in different cartilage zones, contribute to the integrity and repair of the ECM by promoting chondrocyte migration, attachment and ECM protein synthesis as well as the stabilisation of the chondrocyte phenotype (**Fig.4.1**). Their involvement in direct and indirect cell signalling provides an overview of the complexity of the cartilage network and the ongoing processes in the ECM. Overall, OA leads to cartilage degradation, despite the protective effects of COMP and TSP-4. Maybe, the impact of inflammation and degradation overcomes the repair mechanisms by inducing catabolic as well as inhibiting anabolic pathways (169, 216). The cleavage products of ECM proteins might have a differential effect on chondrocytes by supporting ECM degradation. In that manner, COMP and TSP-4 fragments might also block relevant binding sites and may induce catabolic pathways on their own, substituting for intact COMP and TSP-4 in a negative way. However, the COMP and TSP-4 mediated repair processes might be responsible for the slow progression of OA, at least partially.

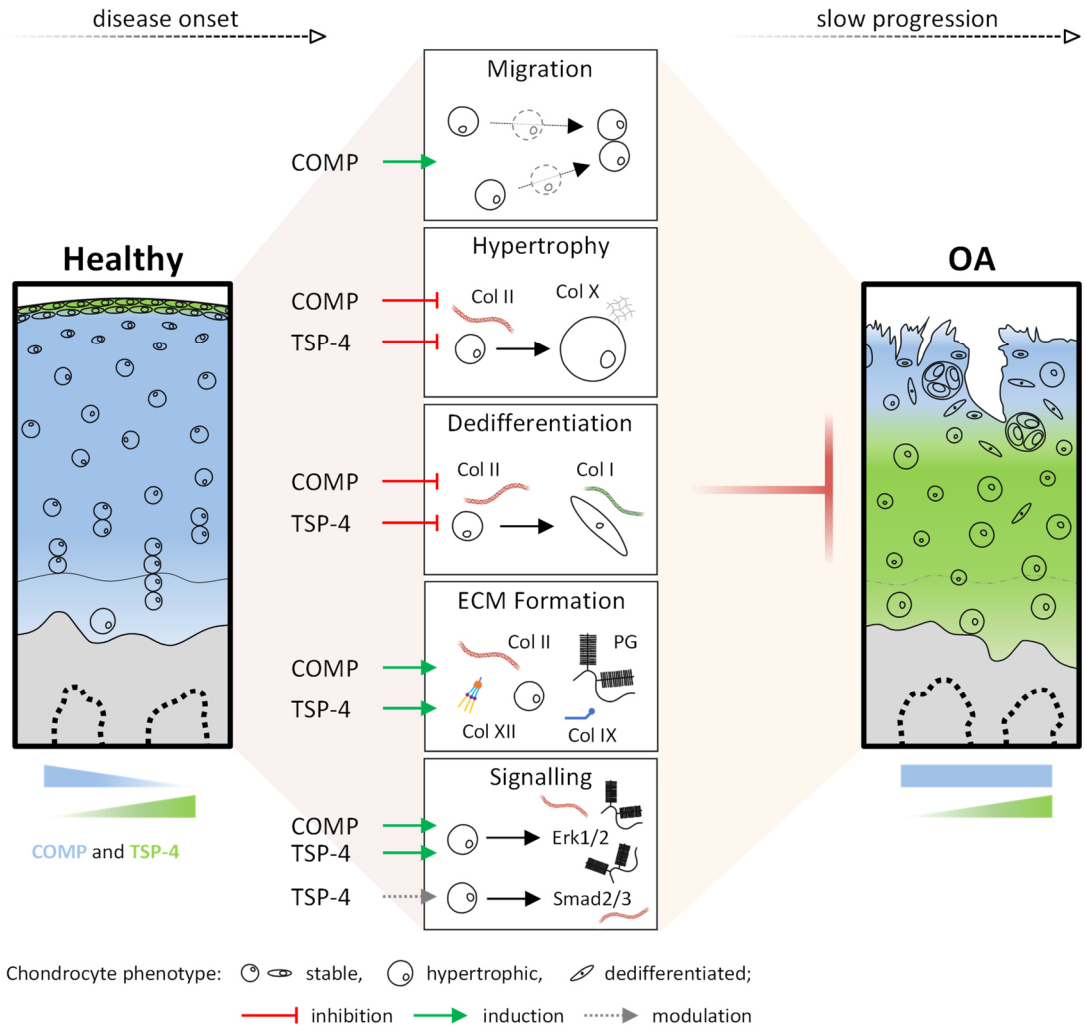

Figure 4.1: Schematic representation of the functional role and distribution of COMP and TSP-4 in articular cartilage

COMP and TSP-4 distribution, as well as protein levels in healthy and OA cartilage, are demonstrated in blue and green, respectively. Their impact on cartilage and OA relevant processes are indicated.

5. References

1. Athanasiou KA, Darling EM, Hu JC, DuRaine GD, Reddi AH. Articular cartilage: CRC Press; 2013.
2. Schünke M, Schulte E, Schumacher U, Voll M, Wesker K. Prometheus-LernAtlas der Anatomie: allgemeine Anatomie und Bewegungssystem: Georg Thieme Verlag; 2011.
3. Bhosale AM, Richardson JB. Articular cartilage: structure, injuries and review of management. British medical bulletin. 2008;87:77-95.
4. Staines KA, Pollard AS, McGonnell IM, Farquharson C, Pitsillides AA. Cartilage to bone transitions in health and disease. The Journal of endocrinology. 2013;219(1):R1-r12.
5. Sophia Fox AJ, Bedi A, Rodeo SA. The basic science of articular cartilage: structure, composition, and function. Sports health. 2009;1(6):461-8.
6. Kempson GE, Freeman MA, Swanson SA. Tensile properties of articular cartilage. Nature. 1968;220(5172):1127-8.
7. Zhang L, Hu J, Athanasiou KA. The role of tissue engineering in articular cartilage repair and regeneration. Crit Rev Biomed Eng. 2009;37(1-2):1-57.
8. Mansfield JC, Mandalia V, Toms A, Winlove CP, Brasselet S. Collagen reorganization in cartilage under strain probed by polarization sensitive second harmonic generation microscopy. J R Soc Interface. 2019;16(150):20180611.
9. Thielen NGM, van der Kraan PM, van Caam APM. TGFβ/BMP Signaling Pathway in Cartilage Homeostasis. Cells. 2019;8(9).
10. Pacifici M, Koyama E, Shibukawa Y, Wu C, Tamamura Y, Enomoto-Iwamoto M, et al. Cellular and molecular mechanisms of synovial joint and articular cartilage formation. Ann N Y Acad Sci. 2006;1068:74-86.
11. Goldring MB. Chondrogenesis, chondrocyte differentiation, and articular cartilage metabolism in health and osteoarthritis. Ther Adv Musculoskelet Dis. 2012;4(4):269-85.
12. Fortier LA, Barker JU, Strauss EJ, McCarrel TM, Cole BJ. The role of growth factors in cartilage repair. Clin Orthop Relat Res. 2011;469(10):2706-15.

13. Gao Y, Liu S, Huang J, Guo W, Chen J, Zhang L, et al. The ECM-cell interaction of cartilage extracellular matrix on chondrocytes. Biomed Res Int. 2014;2014:648459.
14. Hall AC. The Role of Chondrocyte Morphology and Volume in Controlling Phenotype-Implications for Osteoarthritis, Cartilage Repair, and Cartilage Engineering. Curr Rheumatol Rep. 2019;21(8):38.
15. Charlier E, Deroyer C, Ciregia F, Malaise O, Neuville S, Plener Z, et al. Chondrocyte dedifferentiation and osteoarthritis (OA). Biochem Pharmacol. 2019;165:49-65.
16. Schnabel M, Marlovits S, Eckhoff G, Fichtel I, Gotzen L, Vécsei V, et al. Dedifferentiation-associated changes in morphology and gene expression in primary human articular chondrocytes in cell culture. Osteoarthritis Cartilage. 2002;10(1):62-70.
17. van der Kraan PM, van den Berg WB. Chondrocyte hypertrophy and osteoarthritis: role in initiation and progression of cartilage degeneration? Osteoarthritis Cartilage. 2012;20(3):223-32.
18. Heinegård D, Saxne T. The role of the cartilage matrix in osteoarthritis. Nat Rev Rheumatol. 2011;7(1):50-6.
19. Ricard-Blum S. The collagen family. Cold Spring Harb Perspect Biol. 2011;3(1):a004978-a.
20. Luo Y, Sinkeviciute D, He Y, Karsdal M, Henrotin Y, Mobasheri A, et al. The minor collagens in articular cartilage. Protein Cell. 2017;8(8):560-72.
21. Eyre DR, Weis MA, Wu JJ. Articular cartilage collagen: an irreplaceable framework? Eur Cell Mater. 2006;12:57-63.
22. Eyre DR. Collagens and cartilage matrix homeostasis. Clin Orthop Relat Res. 2004(427 Suppl):S118-22.
23. Gottardi R, Hansen U, Raiteri R, Loparic M, Düggelin M, Mathys D, et al. Supramolecular Organization of Collagen Fibrils in Healthy and Osteoarthritic Human Knee and Hip Joint Cartilage. PLoS One. 2016;11(10):e0163552.
24. Hagg R, Bruckner P, Hedbom E. Cartilage fibrils of mammals are biochemically heterogeneous: differential distribution of decorin and collagen IX. J Cell Biol. 1998;142(1):285-94.

25. Fidler AL, Boudko SP, Rokas A, Hudson BG. The triple helix of collagens - an ancient protein structure that enabled animal multicellularity and tissue evolution. J Cell Sci. 2018;131(7):jcs203950.

26. Verzijl N, DeGroot J, Thorpe SR, Bank RA, Shaw JN, Lyons TJ, et al. Effect of collagen turnover on the accumulation of advanced glycation end products. J Biol Chem. 2000;275(50):39027-31.

27. Maroudas A, Palla G, Gilav E. Racemization of aspartic acid in human articular cartilage. Connect Tissue Res. 1992;28(3):161-9.

28. Fässler R, Schnegelsberg PN, Dausman J, Shinya T, Muragaki Y, McCarthy MT, et al. Mice lacking alpha 1 (IX) collagen develop noninflammatory degenerative joint disease. Proc Natl Acad Sci U S A. 1994;91(11):5070-4.

29. Hagg R, Hedbom E, Möllers U, Aszódi A, Fässler R, Bruckner P. Absence of the alpha1(IX) chain leads to a functional knock-out of the entire collagen IX protein in mice. J Biol Chem. 1997;272(33):20650-4.

30. Dreier R, Opolka A, Grifka J, Bruckner P, Grässel S. Collagen IX-deficiency seriously compromises growth cartilage development in mice. Matrix Biol. 2008;27(4):319-29.

31. Budde B, Blumbach K, Ylöstalo J, Zaucke F, Ehlen HW, Wagener R, et al. Altered integration of matrilin-3 into cartilage extracellular matrix in the absence of collagen IX. Mol Cell Biol. 2005;25(23):10465-78.

32. Blumbach K, Bastiaansen-Jenniskens YM, DeGroot J, Paulsson M, van Osch GJ, Zaucke F. Combined role of type IX collagen and cartilage oligomeric matrix protein in cartilage matrix assembly: cartilage oligomeric matrix protein counteracts type IX collagen-induced limitation of cartilage collagen fibril growth in mouse chondrocyte cultures. Arthritis Rheum. 2009;60(12):3676-85.

33. Brierley VH, Ayad S, Grant ME. Types II, VI and IX collagens in normal and osteoarthrotic human articular cartilage. Biochem Soc Trans. 1991;19(4):379S.

34. Yamagata M, Yamada KM, Yamada SS, Shinomura T, Tanaka H, Nishida Y, et al. The complete primary structure of type XII collagen shows a chimeric molecule with reiterated fibronectin type III motifs, von Willebrand factor A motifs, a domain homologous to a noncollagenous region of type IX collagen, and short collagenous domains with an Arg-Gly-Asp site. J Cell Biol. 1991;115(1):209-21.

35. Gregory KE, Keene DR, Tufa SF, Lunstrum GP, Morris NP. Developmental distribution of collagen type XII in cartilage: association with articular cartilage and the growth plate. J Bone Miner Res. 2001;16(11):2005-16.

36. Font B, Eichenberger D, Rosenberg LM, van der Rest M. Characterization of the interactions of type XII collagen with two small proteoglycans from fetal bovine tendon, decorin and fibromodulin. Matrix Biol. 1996;15(5):341-8.

37. Agarwal P, Zwolanek D, Keene DR, Schulz JN, Blumbach K, Heinegård D, et al. Collagen XII and XIV, new partners of cartilage oligomeric matrix protein in the skin extracellular matrix suprastructure. J Biol Chem. 2012;287(27):22549-59.

38. Koch M, Bohrmann B, Matthison M, Hagios C, Trueb B, Chiquet M. Large and small splice variants of collagen XII: differential expression and ligand binding. J Cell Biol. 1995;130(4):1005-14.

39. Taylor DW, Ahmed N, Parreno J, Lunstrum GP, Gross AE, Diamandis EP, et al. Collagen type XII and versican are present in the early stages of cartilage tissue formation by both redifferentating passaged and primary chondrocytes. Tissue Eng Part A. 2015;21(3-4):683-93.

40. Luckman SP, Rees E, Kwan AP. Partial characterization of cell-type X collagen interactions. Biochem J. 2003;372(Pt 2):485-93.

41. Aspden RM. Fibre reinforcing by collagen in cartilage and soft connective tissues. Proc Biol Sci. 1994;258(1352):195-200.

42. Gibson GJ, Bearman CH, Flint MH. The immunoperoxidase localization of type X collagen in chick cartilage and lung. Coll Relat Res. 1986;6(2):163-84.

43. Bonen DK, Schmid TM. Elevated extracellular calcium concentrations induce type X collagen synthesis in chondrocyte cultures. J Cell Biol. 1991;115(4):1171-8.

44. Gannon JM, Walker G, Fischer M, Carpenter R, Thompson RC, Oegema TR. Localization of type X collagen in canine growth plate and adult canine articular cartilage. J Orthop Res. 1991;9(4):485-94.

45. Aigner T, Stöve J. Collagens--major component of the physiological cartilage matrix, major target of cartilage degeneration, major tool in cartilage repair. Adv Drug Deliv Rev. 2003;55(12):1569-93.

46. Yanagishita M. Function of proteoglycans in the extracellular matrix. Acta pathologica japonica. 1993;43(6):283-93.

47. Kiani C, Chen L, Wu YJ, Yee AJ, Yang BB. Structure and function of aggrecan. Cell Res. 2002;12(1):19-32.

48. Bock HC, Michaeli P, Bode C, Schultz W, Kresse H, Herken R, et al. The small proteoglycans decorin and biglycan in human articular cartilage of late-stage osteoarthritis. Osteoarthritis Cartilage. 2001;9(7):654-63.

49. Knudson CB, Knudson W. Cartilage proteoglycans. Semin Cell Dev Biol. 2001;12(2):69-78.

50. Bidanset DJ, Guidry C, Rosenberg LC, Choi HU, Timpl R, Hook M. Binding of the proteoglycan decorin to collagen type VI. J Biol Chem. 1992;267(8):5250-6.

51. Chen FH, Herndon ME, Patel N, Hecht JT, Tuan RS, Lawler J. Interaction of cartilage oligomeric matrix protein/thrombospondin 5 with aggrecan. J Biol Chem. 2007;282(34):24591-8.

52. Svensson L, Oldberg A, Heinegård D. Collagen binding proteins. Osteoarthritis Cartilage. 2001;9 Suppl A:S23-8.

53. Miosge N, Flachsbart K, Goetz W, Schultz W, Kresse H, Herken R. Light and electron microscopical immunohistochemical localization of the small proteoglycan core proteins decorin and biglycan in human knee joint cartilage. The Histochemical Journal. 1994;26(12):939-45.

54. Klatt AR, Becker A-KA, Neacsu CD, Paulsson M, Wagener R. The matrilins: modulators of extracellular matrix assembly. The international journal of biochemistry & cell biology. 2011;43(3):320-30.

55. Acharya C, Yik JH, Kishore A, Van Dinh V, Di Cesare PE, Haudenschild DR. Cartilage oligomeric matrix protein and its binding partners in the cartilage extracellular matrix: interaction, regulation and role in chondrogenesis. Matrix Biol. 2014;37:102-11.

56. Mann HH, Özbek S, Engel J, Paulsson M, Wagener R. Interactions between the cartilage oligomeric matrix protein and matrilins Implications for matrix assembly and the pathogenesis of chondrodysplasias. Journal of Biological Chemistry. 2004;279(24):25294-8.

57. Jayasuriya CT, Goldring MB, Terek R, Chen Q. Matrilin-3 Induction of IL-1 receptor antagonist Is required for up-regulating collagen II and aggrecan and down-

regulating ADAMTS-5 gene expression. Arthritis research & therapy. 2012;14(5):R197.

58. Klatt AR, Klinger G, Paul-Klausch B, Kühn G, Renno JH, Wagener R, et al. Matrilin-3 activates the expression of osteoarthritis-associated genes in primary human chondrocytes. FEBS letters. 2009;583(22):3611-7.

59. Vincourt J-B, Etienne S, Grossin L, Cottet J, Bantsimba-Malanda C, Netter P, et al. Matrilin-3 switches from anti-to pro-anabolic upon integration to the extracellular matrix. Matrix Biology. 2012;31(5):290-8.

60. van der Weyden L, Wei L, Luo J, Yang X, Birk DE, Adams DJ, et al. Functional knockout of the matrilin-3 gene causes premature chondrocyte maturation to hypertrophy and increases bone mineral density and osteoarthritis. Am J Pathol. 2006;169(2):515-27.

61. Ko Y, Kobbe B, Nicolae C, Miosge N, Paulsson M, Wagener R, et al. Matrilin-3 is dispensable for mouse skeletal growth and development. Mol Cell Biol. 2004;24(4):1691-9.

62. Armstrong LC, Bornstein P. Thrombospondins 1 and 2 function as inhibitors of angiogenesis. Matrix Biol. 2003;22(1):63-71.

63. Lawler J. The functions of thrombospondin-1 and-2. Curr Opin Cell Biol. 2000;12(5):634-40.

64. Simantov R, Febbraio M, Silverstein RL. The antiangiogenic effect of thrombospondin-2 is mediated by CD36 and modulated by histidine-rich glycoprotein. Matrix Biol. 2005;24(1):27-34.

65. Volpert OV, Tolsma SS, Pellerin S, Feige JJ, Chen H, Mosher DF, et al. Inhibition of angiogenesis by thrombospondin-2. Biochem Biophys Res Commun. 1995;217(1):326-32.

66. Lawler J. Thrombospondin-1 as an endogenous inhibitor of angiogenesis and tumor growth. J Cell Mol Med. 2002;6(1):1-12.

67. Tan K, Lawler J. The interaction of Thrombospondins with extracellular matrix proteins. J Cell Commun Signal. 2009;3(3-4):177-87.

68. Stenina-Adognravi O, Plow EF. Thrombospondin-4 in tissue remodeling. Matrix Biol. 2019;75-76:300-13.

69. Müller G, Michel A, Altenburg E. COMP (cartilage oligomeric matrix protein) is synthesized in ligament, tendon, meniscus, and articular cartilage. Connect Tissue Res. 1998;39(4):233-44.

70. Stenina OI, Topol EJ, Plow EF. Thrombospondins, their polymorphisms, and cardiovascular disease. Arterioscler Thromb Vasc Biol. 2007;27(9):1886-94.

71. Södersten F, Ekman S, Schmitz M, Paulsson M, Zaucke F. Thrombospondin-4 and cartilage oligomeric matrix protein form heterooligomers in equine tendon. Connect Tissue Res. 2006;47(2):85-91.

72. Pfander D, Cramer T, Deuerling D, Weseloh G, Swoboda B. Expression of thrombospondin-1 and its receptor CD36 in human osteoarthritic cartilage. Ann Rheum Dis. 2000;59(6):448-54.

73. DiCesare PE, Mörgelin M, Mann K, Paulsson M. Cartilage oligomeric matrix protein and thrombospondin 1. Purification from articular cartilage, electron microscopic structure, and chondrocyte binding. Eur J Biochem. 1994;223(3):927-37.

74. Iruela-Arispe ML, Liska DJ, Sage EH, Bornstein P. Differential expression of thrombospondin 1, 2, and 3 during murine development. Dev Dyn. 1993;197(1):40-56.

75. Kyriakides TR, Zhu YH, Yang Z, Bornstein P. The distribution of the matricellular protein thrombospondin 2 in tissues of embryonic and adult mice. J Histochem Cytochem. 1998;46(9):1007-15.

76. Hankenson KD, Hormuzdi SG, Meganck JA, Bornstein P. Mice with a disruption of the thrombospondin 3 gene differ in geometric and biomechanical properties of bone and have accelerated development of the femoral head. Mol Cell Biol. 2005;25(13):5599-606.

77. Hedbom E, Antonsson P, Hjerpe A, Aeschlimann D, Paulsson M, Rosa-Pimentel E, et al. Cartilage matrix proteins. An acidic oligomeric protein (COMP) detected only in cartilage. J Biol Chem. 1992;267(9):6132-6.

78. Efimov VP, Lustig A, Engel J. The thrombospondin-like chains of cartilage oligomeric matrix protein are assembled by a five-stranded alpha-helical bundle between residues 20 and 83. FEBS Lett. 1994;341(1):54-8.

79. Koelling S, Clauditz TS, Kaste M, Miosge N. Cartilage oligomeric matrix protein is involved in human limb development and in the pathogenesis of osteoarthritis. Arthritis Res Ther. 2006;8(3):R56.

80. Rosenberg K, Olsson H, Mörgelin M, Heinegård D. Cartilage oligomeric matrix protein shows high affinity zinc-dependent interaction with triple helical collagen. J Biol Chem. 1998;273(32):20397-403.

81. Thur J, Rosenberg K, Nitsche DP, Pihlajamaa T, Ala-Kokko L, Heinegård D, et al. Mutations in cartilage oligomeric matrix protein causing pseudoachondroplasia and multiple epiphyseal dysplasia affect binding of calcium and collagen I, II, and IX. J Biol Chem. 2001;276(9):6083-92.

82. Holden P, Meadows RS, Chapman KL, Grant ME, Kadler KE, Briggs MD. Cartilage oligomeric matrix protein interacts with type IX collagen, and disruptions to these interactions identify a pathogenetic mechanism in a bone dysplasia family. J Biol Chem. 2001;276(8):6046-55.

83. Di Cesare PE, Chen FS, Moergelin M, Carlson CS, Leslie MP, Perris R, et al. Matrix-matrix interaction of cartilage oligomeric matrix protein and fibronectin. Matrix Biol. 2002;21(5):461-70.

84. Schulz JN, Nüchel J, Niehoff A, Bloch W, Schönborn K, Hayashi S, et al. COMP-assisted collagen secretion--a novel intracellular function required for fibrosis. J Cell Sci. 2016;129(4):706-16.

85. Halász K, Kassner A, Mörgelin M, Heinegård D. COMP acts as a catalyst in collagen fibrillogenesis. J Biol Chem. 2007;282(43):31166-73.

86. Chen FH, Thomas AO, Hecht JT, Goldring MB, Lawler J. Cartilage oligomeric matrix protein/thrombospondin 5 supports chondrocyte attachment through interaction with integrins. J Biol Chem. 2005;280(38):32655-61.

87. Haudenschild DR, Hong E, Yik JH, Chromy B, Mörgelin M, Snow KD, et al. Enhanced activity of transforming growth factor β1 (TGF-β1) bound to cartilage oligomeric matrix protein. J Biol Chem. 2011;286(50):43250-8.

88. Ishida K, Acharya C, Christiansen BA, Yik JH, DiCesare PE, Haudenschild DR. Cartilage oligomeric matrix protein enhances osteogenesis by directly binding and activating bone morphogenetic protein-2. Bone. 2013;55(1):23-35.

89. Grimaud E, Heymann D, Rédini F. Recent advances in TGF-beta effects on chondrocyte metabolism. Potential therapeutic roles of TGF-beta in cartilage disorders. Cytokine Growth Factor Rev. 2002;13(3):241-57.

90. Zhu Y, Tao H, Jin C, Liu Y, Lu X, Hu X, et al. Transforming growth factor-β1 induces type II collagen and aggrecan expression via activation of extracellular signal-regulated kinase 1/2 and Smad2/3 signaling pathways. Mol Med Rep. 2015;12(4):5573-9.

91. Recklies AD, Baillargeon L, White C. Regulation of cartilage oligomeric matrix protein synthesis in human synovial cells and articular chondrocytes. Arthritis Rheum. 1998;41(6):997-1006.

92. Svensson L, Aszódi A, Heinegård D, Hunziker EB, Reinholt FP, Fässler R, et al. Cartilage oligomeric matrix protein-deficient mice have normal skeletal development. Mol Cell Biol. 2002;22(12):4366-71.

93. Cohn DH, Briggs MD, King LM, Rimoin DL, Wilcox WR, Lachman RS, et al. Mutations in the cartilage oligomeric matrix protein (COMP) gene in pseudoachondroplasia and multiple epiphyseal dysplasia. Ann N Y Acad Sci. 1996;785:188-94.

94. Briggs MD, Mortier GR, Cole WG, King LM, Golik SS, Bonaventure J, et al. Diverse mutations in the gene for cartilage oligomeric matrix protein in the pseudoachondroplasia-multiple epiphyseal dysplasia disease spectrum. Am J Hum Genet. 1998;62(2):311-9.

95. Briggs MD, Hoffman SM, King LM, Olsen AS, Mohrenweiser H, Leroy JG, et al. Pseudoachondroplasia and multiple epiphyseal dysplasia due to mutations in the cartilage oligomeric matrix protein gene. Nat Genet. 1995;10(3):330-6.

96. Jackson GC, Mittaz-Crettol L, Taylor JA, Mortier GR, Spranger J, Zabel B, et al. Pseudoachondroplasia and multiple epiphyseal dysplasia: a 7-year comprehensive analysis of the known disease genes identify novel and recurrent mutations and provides an accurate assessment of their relative contribution. Hum Mutat. 2012;33(1):144-57.

97. Chen H, Deere M, Hecht JT, Lawler J. Cartilage oligomeric matrix protein is a calcium-binding protein, and a mutation in its type 3 repeats causes conformational changes. J Biol Chem. 2000;275(34):26538-44.

98. Hashimoto Y, Tomiyama T, Yamano Y, Mori H. Mutation (D472Y) in the type 3 repeat domain of cartilage oligomeric matrix protein affects its early vesicle trafficking in endoplasmic reticulum and induces apoptosis. Am J Pathol. 2003;163(1):101-10.

99. Hecht JT, Montufar-Solis D, Decker G, Lawler J, Daniels K, Duke PJ. Retention of cartilage oligomeric matrix protein (COMP) and cell death in redifferentiated pseudoachondroplasia chondrocytes. Matrix Biol. 1998;17(8-9):625-33.

100. Hecht JT, Hayes E, Haynes R, Cole WG. COMP mutations, chondrocyte function and cartilage matrix. Matrix Biol. 2005;23(8):525-33.

101. Schmitz M, Becker A, Schmitz A, Weirich C, Paulsson M, Zaucke F, et al. Disruption of extracellular matrix structure may cause pseudoachondroplasia phenotypes in the absence of impaired cartilage oligomeric matrix protein secretion. J Biol Chem. 2006;281(43):32587-95.

102. Lawler J, McHenry K, Duquette M, Derick L. Characterization of human thrombospondin-4. J Biol Chem. 1995;270(6):2809-14.

103. Narouz-Ott L, Maurer P, Nitsche DP, Smyth N, Paulsson M. Thrombospondin-4 binds specifically to both collagenous and non-collagenous extracellular matrix proteins via its C-terminal domains. J Biol Chem. 2000;275(47):37110-7.

104. Södersten F, Ekman S, Niehoff A, Zaucke F, Heinegård D, Hultenby K. Ultrastructural immunolocalization of cartilage oligomeric matrix protein, thrombospondin-4, and collagen fibril size in rodent achilles tendon in relation to exercise. Connect Tissue Res. 2007;48(5):254-62.

105. Muppala S, Xiao R, Krukovets I, Verbovetsky D, Yendamuri R, Habib N, et al. Thrombospondin-4 mediates TGF-β-induced angiogenesis. Oncogene. 2017;36(36):5189-98.

106. Muppala S, Frolova E, Xiao R, Krukovets I, Yoon S, Hoppe G, et al. Proangiogenic Properties of Thrombospondin-4. Arterioscler Thromb Vasc Biol. 2015;35(9):1975-86.

107. Adams JC, Lawler J. Cell-type specific adhesive interactions of skeletal myoblasts with thrombospondin-1. Mol Biol Cell. 1994;5(4):423-37.

108. Frolova EG, Sopko N, Blech L, Popovic ZB, Li J, Vasanji A, et al. Thrombospondin-4 regulates fibrosis and remodeling of the myocardium in response to pressure overload. FASEB J. 2012;26(6):2363-73.

109. Frolova EG, Drazba J, Krukovets I, Kostenko V, Blech L, Harry C, et al. Control of organization and function of muscle and tendon by thrombospondin-4. Matrix Biol. 2014;37:35-48.

110. Jeschke A, Bonitz M, Simon M, Peters S, Baum W, Schett G, et al. Deficiency of Thrombospondin-4 in Mice Does Not Affect Skeletal Growth or Bone Mass Acquisition, but Causes a Transient Reduction of Articular Cartilage Thickness. PLoS One. 2015;10(12):e0144272.

111. Frolova EG, Pluskota E, Krukovets I, Burke T, Drumm C, Smith JD, et al. Thrombospondin-4 regulates vascular inflammation and atherogenesis. Circ Res. 2010;107(11):1313-25.

112. Mustonen E, Aro J, Puhakka J, Ilves M, Soini Y, Leskinen H, et al. Thrombospondin-4 expression is rapidly upregulated by cardiac overload. Biochem Biophys Res Commun. 2008;373(2):186-91.

113. Rysä J, Leskinen H, Ilves M, Ruskoaho H. Distinct upregulation of extracellular matrix genes in transition from hypertrophy to hypertensive heart failure. Hypertension. 2005;45(5):927-33.

114. Tan FL, Moravec CS, Li J, Apperson-Hansen C, McCarthy PM, Young JB, et al. The gene expression fingerprint of human heart failure. Proc Natl Acad Sci U S A. 2002;99(17):11387-92.

115. Palao T, Medzikovic L, Rippe C, Wanga S, Al-Mardini C, van Weert A, et al. Thrombospondin-4 mediates cardiovascular remodelling in angiotensin II-induced hypertension. Cardiovasc Pathol. 2018;35:12-9.

116. Qian W, Li N, Cao Q, Fan J. Thrombospondin-4 critically controls transforming growth factor β1 induced hypertrophic scar formation. J Cell Physiol. 2018;234(1):731-9.

117. Chen YW, Zhao P, Borup R, Hoffman EP. Expression profiling in the muscular dystrophies: identification of novel aspects of molecular pathophysiology. J Cell Biol. 2000;151(6):1321-36.

118. Park J, Yu YP, Zhou CY, Li KW, Wang D, Chang E, et al. Central Mechanisms Mediating Thrombospondin-4-induced Pain States. J Biol Chem. 2016;291(25):13335-48.

119. Park JF, Yu YP, Gong N, Trinh VN, Luo ZD. The EGF-LIKE domain of thrombospondin-4 is a key determinant in the development of pain states due to increased excitatory synaptogenesis. J Biol Chem. 2018;293(42):16453-63.

120. Greco SA, Chia J, Inglis KJ, Cozzi SJ, Ramsnes I, Buttenshaw RL, et al. Thrombospondin-4 is a putative tumour-suppressor gene in colorectal cancer that exhibits age-related methylation. BMC Cancer. 2010;10:494.

121. Kuroda K, Yashiro M, Sera T, Yamamoto Y, Kushitani Y, Sugimoto A, et al. The clinicopathological significance of Thrombospondin-4 expression in the tumor microenvironment of gastric cancer. PLoS One. 2019;14(11):e0224727.

122. McCart Reed AE, Song S, Kutasovic JR, Reid LE, Valle JM, Vargas AC, et al. Thrombospondin-4 expression is activated during the stromal response to invasive breast cancer. Virchows Arch. 2013;463(4):535-45.

123. Liu J, Cheng G, Yang H, Deng X, Qin C, Hua L, et al. Reciprocal regulation of long noncoding RNAs THBS4-003 and THBS4 control migration and invasion in prostate cancer cell lines. Mol Med Rep. 2016;14(2):1451-8.

124. Ruthard J, Hermes G, Hartmann U, Sengle G, Pongratz G, Ostendorf B, et al. Identification of antibodies against extracellular matrix proteins in human osteoarthritis. Biochem Biophys Res Commun. 2018;503(3):1273-7.

125. Kuttapitiya A, Assi L, Laing K, Hing C, Mitchell P, Whitley G, et al. Microarray analysis of bone marrow lesions in osteoarthritis demonstrates upregulation of genes implicated in osteochondral turnover, neurogenesis and inflammation. Ann Rheum Dis. 2017;76(10):1764-73.

126. van der Kraan PM, Blaney Davidson EN, Blom A, van den Berg WB. TGF-beta signaling in chondrocyte terminal differentiation and osteoarthritis: modulation and integration of signaling pathways through receptor-Smads. Osteoarthritis Cartilage. 2009;17(12):1539-45.

127. Blaney Davidson EN, Remst DF, Vitters EL, van Beuningen HM, Blom AB, Goumans MJ, et al. Increase in ALK1/ALK5 ratio as a cause for elevated MMP-13

expression in osteoarthritis in humans and mice. J Immunol. 2009;182(12):7937-45.

128. Kim K-O, Sampson ER, Maynard RD, O'Keefe RJ, Chen D, Drissi H, et al. Ski inhibits TGF-β/phospho-Smad3 signaling and accelerates hypertrophic differentiation in chondrocytes. Journal of cellular biochemistry. 2012;113(6):2156-66.

129. Ferguson CM, Schwarz EM, Reynolds PR, Puzas JE, Rosier RN, O'Keefe RJ. Smad2 and 3 mediate transforming growth factor-β1-induced inhibition of chondrocyte maturation. Endocrinology. 2000;141(12):4728-35.

130. Lian C, Wang X, Qiu X, Wu Z, Gao B, Liu L, et al. Collagen type II suppresses articular chondrocyte hypertrophy and osteoarthritis progression by promoting integrin β1-SMAD1 interaction. Bone Res. 2019;7:8.

131. Zhu Y, Gu J, Zhu T, Jin C, Hu X, Wang X. Crosstalk between Smad2/3 and specific isoforms of ERK in TGF-β1-induced TIMP-3 expression in rat chondrocytes. J Cell Mol Med. 2017;21(9):1781-90.

132. Wang X, Zhu Y, Tao H, Jin C, Liu Y, Lu X, et al. Interaction of ERK1/2 and Smad2/3 signaling pathways in TGF-β1-induced TIMP-3 expression in rat chondrocytes. Arch Biochem Biophys. 2014;564:229-36.

133. Watanabe H, de Caestecker MP, Yamada Y. Transcriptional cross-talk between Smad, ERK1/2, and p38 mitogen-activated protein kinase pathways regulates transforming growth factor-beta-induced aggrecan gene expression in chondrogenic ATDC5 cells. J Biol Chem. 2001;276(17):14466-73.

134. Yang X, Chen L, Xu X, Li C, Huang C, Deng CX. TGF-beta/Smad3 signals repress chondrocyte hypertrophic differentiation and are required for maintaining articular cartilage. J Cell Biol. 2001;153(1):35-46.

135. Retting KN, Song B, Yoon BS, Lyons KM. BMP canonical Smad signaling through Smad1 and Smad5 is required for endochondral bone formation. Development. 2009;136(7):1093-104.

136. Chen Z, Yue SX, Zhou G, Greenfield EM, Murakami S. ERK1 and ERK2 regulate chondrocyte terminal differentiation during endochondral bone formation. J Bone Miner Res. 2015;30(5):765-74.

137. Shakibaei M, Schulze-Tanzil G, de Souza P, John T, Rahmanzadeh M, Rahmanzadeh R, et al. Inhibition of mitogen-activated protein kinase kinase induces apoptosis of human chondrocytes. J Biol Chem. 2001;276(16):13289-94.
138. Hunter W. Of the structure and disease of articulating cartilages. 1743. Clin Orthop Relat Res. 1995(317):3-6.
139. Østerås N, Risberg MA, Kvien TK, Engebretsen L, Nordsletten L, Bruusgaard D, et al. Hand, hip and knee osteoarthritis in a Norwegian population-based study--the MUST protocol. BMC Musculoskelet Disord. 2013;14:201.
140. Hunter DJ, Bierma-Zeinstra S. Osteoarthritis. Lancet. 2019;393(10182):1745-59.
141. Mobasheri A, Batt M. An update on the pathophysiology of osteoarthritis. Ann Phys Rehabil Med. 2016;59(5-6):333-9.
142. Loeser RF, Goldring SR, Scanzello CR, Goldring MB. Osteoarthritis: a disease of the joint as an organ. Arthritis Rheum. 2012;64(6):1697-707.
143. Ivirico JLE, Bhattacharjee M, Kuyinu E, Nair LS, Laurencin CT. Regenerative Engineering for Knee Osteoarthritis Treatment: Biomaterials and Cell-Based Technologies. 2017.
144. Srikanth VK, Fryer JL, Zhai G, Winzenberg TM, Hosmer D, Jones G. A meta-analysis of sex differences prevalence, incidence and severity of osteoarthritis. Osteoarthritis Cartilage. 2005;13(9):769-81.
145. O'Connor MI. Sex differences in osteoarthritis of the hip and knee. J Am Acad Orthop Surg. 2007;15 Suppl 1:S22-5.
146. Hame SL, Alexander RA. Knee osteoarthritis in women. Curr Rev Musculoskelet Med. 2013;6(2):182-7.
147. Zhang S, Wang J, Ji H, Jia H, Guan D. Interaction between GDF5 gene polymorphisms and environment factors increased the risk of knee osteoarthritis: a case-control study. Biosci Rep. 2019;39(2).
148. Hui W, Cao Z, Wang X, Zhu J. Association of matrix Gla protein polymorphism and knee osteoarthritis in a chinese population. Biosci Rep. 2019;39(1).
149. Lee AS, Ellman MB, Yan D, Kroin JS, Cole BJ, van Wijnen AJ, et al. A current review of molecular mechanisms regarding osteoarthritis and pain. Gene. 2013;527(2):440-7.

150. van der Kraan PM, Goumans MJ, Blaney Davidson E, ten Dijke P. Age-dependent alteration of TGF-β signalling in osteoarthritis. Cell Tissue Res. 2012;347(1):257-65.

151. Fava R, Olsen N, Keski-Oja J, Moses H, Pincus T. Active and latent forms of transforming growth factor beta activity in synovial effusions. J Exp Med. 1989;169(1):291-6.

152. Miosge N, Hartmann M, Maelicke C, Herken R. Expression of collagen type I and type II in consecutive stages of human osteoarthritis. Histochem Cell Biol. 2004;122(3):229-36.

153. Goldwasser M, Astley T, van der Rest M, Glorieux FH. Analysis of the type of collagen present in osteoarthritic human cartilage. Clin Orthop Relat Res. 1982(167):296-302.

154. Pullig O, Weseloh G, Klatt AR, Wagener R, Swoboda B. Matrilin-3 in human articular cartilage: increased expression in osteoarthritis. Osteoarthritis Cartilage. 2002;10(4):253-63.

155. Sofat N. Analysing the role of endogenous matrix molecules in the development of osteoarthritis. Int J Exp Pathol. 2009;90(5):463-79.

156. Grimmer C, Balbus N, Lang U, Aigner T, Cramer T, Müller L, et al. Regulation of type II collagen synthesis during osteoarthritis by prolyl-4-hydroxylases: possible influence of low oxygen levels. Am J Pathol. 2006;169(2):491-502.

157. Lippiello L, Hall D, Mankin HJ. Collagen synthesis in normal and osteoarthritic human cartilage. J Clin Invest. 1977;59(4):593-600.

158. Kirsch T, Swoboda B, Nah H. Activation of annexin II and V expression, terminal differentiation, mineralization and apoptosis in human osteoarthritic cartilage. Osteoarthritis Cartilage. 2000;8(4):294-302.

159. von der Mark K, Frischholz S, Aigner T, Beier F, Belke J, Erdmann S, et al. Upregulation of type X collagen expression in osteoarthritic cartilage. Acta Orthop Scand Suppl. 1995;266:125-9.

160. Girkontaite I, Frischholz S, Lammi P, Wagner K, Swoboda B, Aigner T, et al. Immunolocalization of type X collagen in normal fetal and adult osteoarthritic cartilage with monoclonal antibodies. Matrix Biol. 1996;15(4):231-8.

161. Goldring MB, Marcu KB. Cartilage homeostasis in health and rheumatic diseases. Arthritis Res Ther. 2009;11(3):224.

162. Aigner T, Zien A, Gehrsitz A, Gebhard PM, McKenna L. Anabolic and catabolic gene expression pattern analysis in normal versus osteoarthritic cartilage using complementary DNA-array technology. Arthritis Rheum. 2001;44(12):2777-89.

163. Mort JS, Geng Y, Fisher WD, Roughley PJ. Aggrecan heterogeneity in articular cartilage from patients with osteoarthritis. BMC Musculoskelet Disord. 2016;17:89.

164. Karsdal MA, Madsen SH, Christiansen C, Henriksen K, Fosang AJ, Sondergaard BC. Cartilage degradation is fully reversible in the presence of aggrecanase but not matrix metalloproteinase activity. Arthritis Res Ther. 2008;10(3):R63.

165. Diab M. The role of type IX collagen in osteoarthritis and rheumatoid arthritis. Orthop Rev. 1993;22(2):165-70.

166. Klatt AR, Paul-Klausch B, Klinger G, Kühn G, Renno JH, Banerjee M, et al. A critical role for collagen II in cartilage matrix degradation: collagen II induces pro-inflammatory cytokines and MMPs in primary human chondrocytes. J Orthop Res. 2009;27(1):65-70.

167. Homandberg GA, Hui F, Wen C, Purple C, Bewsey K, Koepp H, et al. Fibronectin-fragment-induced cartilage chondrolysis is associated with release of catabolic cytokines. Biochem J. 1997;321 (Pt 3):751-7.

168. Ding L, Guo D, Homandberg GA. Fibronectin fragments mediate matrix metalloproteinase upregulation and cartilage damage through proline rich tyrosine kinase 2, c-src, NF-kappaB and protein kinase Cdelta. Osteoarthritis Cartilage. 2009;17(10):1385-92.

169. Xia M, Zhu Y. Fibronectin fragment activation of ERK increasing integrin α_5 and β_1 subunit expression to degenerate nucleus pulposus cells. J Orthop Res. 2011;29(4):556-61.

170. Suri S, Gill SE, Massena de Camin S, Wilson D, McWilliams DF, Walsh DA. Neurovascular invasion at the osteochondral junction and in osteophytes in osteoarthritis. Ann Rheum Dis. 2007;66(11):1423-8.

171. Hashimoto S, Creighton-Achermann L, Takahashi K, Amiel D, Coutts RD, Lotz M. Development and regulation of osteophyte formation during experimental osteoarthritis. Osteoarthritis Cartilage. 2002;10(3):180-7.

172. Enomoto H, Inoki I, Komiya K, Shiomi T, Ikeda E, Obata K, et al. Vascular endothelial growth factor isoforms and their receptors are expressed in human osteoarthritic cartilage. Am J Pathol. 2003;162(1):171-81.

173. Pfander D, Körtje D, Zimmermann R, Weseloh G, Kirsch T, Gesslein M, et al. Vascular endothelial growth factor in articular cartilage of healthy and osteoarthritic human knee joints. Ann Rheum Dis. 2001;60(11):1070-3.

174. Liu J, Dai J, Wang Y, Lai S, Wang S. Significance of new blood vessels in the pathogenesis of temporomandibular joint osteoarthritis. Exp Ther Med. 2017;13(5):2325-31.

175. Bonnet CS, Walsh DA. Osteoarthritis, angiogenesis and inflammation. Rheumatology (Oxford). 2005;44(1):7-16.

176. KELLGREN JH, LAWRENCE JS. Radiological assessment of osteo-arthrosis. Ann Rheum Dis. 1957;16(4):494-502.

177. Abadie E, Ethgen D, Avouac B, Bouvenot G, Branco J, Bruyere O, et al. Recommendations for the use of new methods to assess the efficacy of disease-modifying drugs in the treatment of osteoarthritis. Osteoarthritis Cartilage. 2004;12(4):263-8.

178. Roemer FW, Crema MD, Trattnig S, Guermazi A. Advances in imaging of osteoarthritis and cartilage. Radiology. 2011;260(2):332-54.

179. Heinegård D, Inerot S, Wieslander J, Lindblad G. A method for the quantification of cartilage proteoglycan structures liberated to the synovial fluid during developing degenerative joint disease. Scand J Clin Lab Invest. 1985;45(5):421-7.

180. Clark AG, Jordan JM, Vilim V, Renner JB, Dragomir AD, Luta G, et al. Serum cartilage oligomeric matrix protein reflects osteoarthritis presence and severity: the Johnston County Osteoarthritis Project. Arthritis Rheum. 1999;42(11):2356-64.

181. Garnero P, Ayral X, Rousseau JC, Christgau S, Sandell LJ, Dougados M, et al. Uncoupling of type II collagen synthesis and degradation predicts progression of

joint damage in patients with knee osteoarthritis. Arthritis Rheum. 2002;46(10):2613-24.

182. Reijman M, Hazes JM, Bierma-Zeinstra SM, Koes BW, Christgau S, Christiansen C, et al. A new marker for osteoarthritis: cross-sectional and longitudinal approach. Arthritis Rheum. 2004;50(8):2471-8.

183. Lohmander LS, Atley LM, Pietka TA, Eyre DR. The release of crosslinked peptides from type II collagen into human synovial fluid is increased soon after joint injury and in osteoarthritis. Arthritis Rheum. 2003;48(11):3130-9.

184. Flannery CR, Lark MW, Sandy JD. Identification of a stromelysin cleavage site within the interglobular domain of human aggrecan. Evidence for proteolysis at this site in vivo in human articular cartilage. J Biol Chem. 1992;267(2):1008-14.

185. Lark MW, Bayne EK, Flanagan J, Harper CF, Hoerrner LA, Hutchinson NI, et al. Aggrecan degradation in human cartilage. Evidence for both matrix metalloproteinase and aggrecanase activity in normal, osteoarthritic, and rheumatoid joints. J Clin Invest. 1997;100(1):93-106.

186. Sandy JD. A contentious issue finds some clarity: on the independent and complementary roles of aggrecanase activity and MMP activity in human joint aggrecanolysis. Osteoarthritis Cartilage. 14. England2006. p. 95-100.

187. Struglics A, Larsson S, Pratta MA, Kumar S, Lark MW, Lohmander LS. Human osteoarthritis synovial fluid and joint cartilage contain both aggrecanase- and matrix metalloproteinase-generated aggrecan fragments. Osteoarthritis Cartilage. 14. England2006. p. 101-13.

188. Germaschewski FM, Matheny CJ, Larkin J, Liu F, Thomas LR, Saunders JS, et al. Quantitation OF ARGS aggrecan fragments in synovial fluid, serum and urine from osteoarthritis patients. Osteoarthritis Cartilage. 22. England: 2014 Osteoarthritis Research Society International. Published by Elsevier Ltd; 2014. p. 690-7.

189. Hunter DJ, Li J, LaValley M, Bauer DC, Nevitt M, DeGroot J, et al. Cartilage markers and their association with cartilage loss on magnetic resonance imaging in knee osteoarthritis: the Boston Osteoarthritis Knee Study. Arthritis Res Ther. 2007;9(5):R108.

190. Mundermann A, Dyrby CO, Andriacchi TP, King KB. Serum concentration of cartilage oligomeric matrix protein (COMP) is sensitive to physiological cyclic loading in healthy adults. Osteoarthritis Cartilage. 13. England2005. p. 34-8.

191. Neidhart M, Muller-Ladner U, Frey W, Bosserhoff AK, Colombani PC, Frey-Rindova P, et al. Increased serum levels of non-collagenous matrix proteins (cartilage oligomeric matrix protein and melanoma inhibitory activity) in marathon runners. Osteoarthritis Cartilage. 8. England2000. p. 222-9.

192. Hesselstrand R, Kassner A, Heinegard D, Saxne T. COMP: a candidate molecule in the pathogenesis of systemic sclerosis with a potential as a disease marker. Ann Rheum Dis. 67. England2008. p. 1242-8.

193. Norman GL, Gatselis NK, Shums Z, Liaskos C, Bogdanos DP, Koukoulis GK, et al. Cartilage oligomeric matrix protein: A novel non-invasive marker for assessing cirrhosis and risk of hepatocellular carcinoma. World J Hepatol. 2015;7(14):1875-83.

194. Zachou K, Gabeta S, Shums Z, Gatselis NK, Koukoulis GK, Norman GL, et al. COMP serum levels: A new non-invasive biomarker of liver fibrosis in patients with chronic viral hepatitis. Eur J Intern Med. 38. Netherlands: 2017 European Federation of Internal Medicine. Published by Elsevier B.V; 2017. p. 83-8.

195. Englund E, Bartoschek M, Reitsma B, Jacobsson L, Escudero-Esparza A, Orimo A, et al. Cartilage oligomeric matrix protein contributes to the development and metastasis of breast cancer. Oncogene. 35. England2016. p. 5585-96.

196. Liu TT, Liu XS, Zhang M, Liu XN, Zhu FX, Zhu FM, et al. Cartilage oligomeric matrix protein is a prognostic factor and biomarker of colon cancer and promotes cell proliferation by activating the Akt pathway. J Cancer Res Clin Oncol. 144. Germany2018. p. 1049-63.

197. Zheng C, Li X, Ren Y, Yin Z, Zhou B. Coexisting EGFR and TP53 Mutations in Lung Adenocarcinoma Patients Are Associated With COMP and ITGB8 Upregulation and Poor Prognosis. Front Mol Biosci. 2020;7:30.

198. Ahrman E, Lorenzo P, Holmgren K, Grodzinsky AJ, Dahlberg LE, Saxne T, et al. Novel cartilage oligomeric matrix protein (COMP) neoepitopes identified in synovial fluids from patients with joint diseases using affinity chromatography and mass spectrometry. J Biol Chem. 2014;289(30):20908-16.

199. Lorenzo P, Aspberg A, Saxne T, Onnerfjord P. Quantification of cartilage oligomeric matrix protein (COMP) and a COMP neoepitope in synovial fluid of patients with different joint disorders by novel automated assays. Osteoarthritis Cartilage. 25. England: 2017 Osteoarthritis Research Society International. Published by Elsevier Ltd; 2017. p. 1436-42.

200. Chimutengwende-Gordon M, Donaldson J, Bentley G. Current solutions for the treatment of chronic articular cartilage defects in the knee. EFORT Open Rev. 2020;5(3):156-63.

201. Bartlett W, Skinner JA, Gooding CR, Carrington RW, Flanagan AM, Briggs TW, et al. Autologous chondrocyte implantation versus matrix-induced autologous chondrocyte implantation for osteochondral defects of the knee: a prospective, randomised study. J Bone Joint Surg Br. 2005;87(5):640-5.

202. Anders S, Schaumburger J, Schubert T, Grifka J, Behrens P. [Matrix-associated autologous chondrocyte transplantation (MACT). Minimally invasive technique in the knee]. Oper Orthop Traumatol. 2008;20(3):208-19.

203. Schulze-Tanzil G. Activation and dedifferentiation of chondrocytes: implications in cartilage injury and repair. Ann Anat. 2009;191(4):325-38.

204. Klatt AR, Nitsche DP, Kobbe B, Mörgelin M, Paulsson M, Wagener R. Molecular structure and tissue distribution of matrilin-3, a filament-forming extracellular matrix protein expressed during skeletal development. J Biol Chem. 2000;275(6):3999-4006.

205. Maly K, Schaible I, Riegger J, Brenner RE, Meurer A, Zaucke F. The Expression of Thrombospondin-4 Correlates with Disease Severity in Osteoarthritic Knee Cartilage. Int J Mol Sci. 2019;20(2).

206. Dunkle ET, Zaucke F, Clegg DO. Thrombospondin-4 and matrix three-dimensionality in axon outgrowth and adhesion in the developing retina. Exp Eye Res. 2007;84(4):707-17.

207. Büchele G, Günther KP, Brenner H, Puhl W, Stürmer T, Rothenbacher D, et al. Osteoarthritis-patterns, cardio-metabolic risk factors and risk of all-cause mortality: 20 years follow-up in patients after hip or knee replacement. Sci Rep. 2018;8(1):5253.

208. Pritzker KP, Gay S, Jimenez SA, Ostergaard K, Pelletier JP, Revell PA, et al. Osteoarthritis cartilage histopathology: grading and staging. Osteoarthritis Cartilage. 2006;14(1):13-29.

209. Meissner P, Pick H, Kulangara A, Chatellard P, Friedrich K, Wurm FM. Transient gene expression: recombinant protein production with suspension-adapted HEK293-EBNA cells. Biotechnol Bioeng. 2001;75(2):197-203.

210. Yates JL, Warren N, Sugden B. Stable replication of plasmids derived from Epstein-Barr virus in various mammalian cells. Nature. 1985;313(6005):812-5.

211. Kohfeldt E, Maurer P, Vannahme C, Timpl R. Properties of the extracellular calcium binding module of the proteoglycan testican. FEBS Lett. 1997;414(3):557-61.

212. Holden P, Keene DR, Lunstrum GP, Bächinger HP, Horton WA. Secretion of cartilage oligomeric matrix protein is affected by the signal peptide. J Biol Chem. 2005;280(17):17172-9.

213. Kanigicherla D, Gummadova J, McKenzie EA, Roberts SA, Harris S, Nikam M, et al. Anti-PLA2R antibodies measured by ELISA predict long-term outcome in a prevalent population of patients with idiopathic membranous nephropathy. Kidney Int. 2013;83(5):940-8.

214. Laemmli UK. Cleavage of structural proteins during the assembly of the head of bacteriophage T4. Nature. 1970;227(5259):680-5.

215. Mishima Y, Lotz M. Chemotaxis of human articular chondrocytes and mesenchymal stem cells. J Orthop Res. 2008;26(10):1407-12.

216. Daheshia M, Yao JQ. The interleukin 1beta pathway in the pathogenesis of osteoarthritis. J Rheumatol. 2008;35(12):2306-12.

217. Kempson GE. Relationship between the tensile properties of articular cartilage from the human knee and age. Ann Rheum Dis. 1982;41(5):508-11.

218. Cingolani OH, Kirk JA, Seo K, Koitabashi N, Lee DI, Ramirez-Correa G, et al. Thrombospondin-4 is required for stretch-mediated contractility augmentation in cardiac muscle. Circ Res. 2011;109(12):1410-4.

219. Islam A, Mbimba T, Younesi M, Akkus O. Effects of substrate stiffness on the tenoinduction of human mesenchymal stem cells. Acta Biomater. 2017;58:244-53.

220. Brachvogel B, Zaucke F, Dave K, Norris EL, Stermann J, Dayakli M, et al. Comparative proteomic analysis of normal and collagen IX null mouse cartilage reveals altered extracellular matrix composition and novel components of the collagen IX interactome. J Biol Chem. 2013;288(19):13481-92.

221. Groma G, Xin W, Grskovic I, Niehoff A, Brachvogel B, Paulsson M, et al. Abnormal bone quality in cartilage oligomeric matrix protein and matrilin 3 double-deficient mice caused by increased tissue inhibitor of metalloproteinases 3 deposition and delayed aggrecan degradation. Arthritis Rheum. 2012;64(8):2644-54.

222. Kuznetsova SA, Issa P, Perruccio EM, Zeng B, Sipes JM, Ward Y, et al. Versican-thrombospondin-1 binding in vitro and colocalization in microfibrils induced by inflammation on vascular smooth muscle cells. J Cell Sci. 2006;119(Pt 21):4499-509.

223. Aigner T, Zhu Y, Chansky HH, Matsen FA, Maloney WJ, Sandell LJ. Reexpression of type IIA procollagen by adult articular chondrocytes in osteoarthritic cartilage. Arthritis Rheum. 1999;42(7):1443-50.

224. Schminke B, Frese J, Bode C, Goldring MB, Miosge N. Laminins and Nidogens in the Pericellular Matrix of Chondrocytes: Their Role in Osteoarthritis and Chondrogenic Differentiation. Am J Pathol. 2016;186(2):410-8.

225. Kruegel J, Sadowski B, Miosge N. Nidogen-1 and nidogen-2 in healthy human cartilage and in late-stage osteoarthritis cartilage. Arthritis Rheum. 2008;58(5):1422-32.

226. Huwe LW, Brown WE, Hu JC, Athanasiou KA. Characterization of costal cartilage and its suitability as a cell source for articular cartilage tissue engineering. J Tissue Eng Regen Med. 2018;12(5):1163-76.

227. Schook LB, Collares TV, Darfour-Oduro KA, De AK, Rund LA, Schachtschneider KM, et al. Unraveling the swine genome: implications for human health. Annu Rev Anim Biosci. 2015;3:219-44.

228. Macfadyen MA, Daniel Z, Kelly S, Parr T, Brameld JM, Murton AJ, et al. The commercial pig as a model of spontaneously-occurring osteoarthritis. BMC Musculoskelet Disord. 2019;20(1):70.

229. Guilak F, Nims RJ, Dicks A, Wu CL, Meulenbelt I. Osteoarthritis as a disease of the cartilage pericellular matrix. Matrix Biol. 2018;71-72:40-50.

230. Lotz MK, Otsuki S, Grogan SP, Sah R, Terkeltaub R, D'Lima D. Cartilage cell clusters. Arthritis Rheum. 2010;62(8):2206-18.

231. Rothwell AG, Bentley G. Chondrocyte multiplication in osteoarthritic articular cartilage. J Bone Joint Surg Br. 1973;55(3):588-94.

232. Hirotani H, Ito T. Chondrocyte mitosis in the articular cartilage of femoral heads with various diseases. Acta Orthop Scand. 1975;46(6):979-86.

233. Kouri JB, Jiménez SA, Quintero M, Chico A. Ultrastructural study of chondrocytes from fibrillated and non-fibrillated human osteoarthritic cartilage. Osteoarthritis Cartilage. 1996;4(2):111-25.

234. Henson FM, Bowe EA, Davies ME. Promotion of the intrinsic damage-repair response in articular cartilage by fibroblastic growth factor-2. Osteoarthritis Cartilage. 2005;13(6):537-44.

235. Seol D, McCabe DJ, Choe H, Zheng H, Yu Y, Jang K, et al. Chondrogenic progenitor cells respond to cartilage injury. Arthritis Rheum. 2012;64(11):3626-37.

236. Koelling S, Kruegel J, Irmer M, Path JR, Sadowski B, Miro X, et al. Migratory chondrogenic progenitor cells from repair tissue during the later stages of human osteoarthritis. Cell Stem Cell. 2009;4(4):324-35.

237. Loeser RF. Integrins and chondrocyte-matrix interactions in articular cartilage. Matrix Biol. 2014;39:11-6.

238. Tian J, Zhang FJ, Lei GH. Role of integrins and their ligands in osteoarthritic cartilage. Rheumatol Int. 2015;35(5):787-98.

239. Tiwari A, Jung JJ, Inamdar SM, Brown CO, Goel A, Choudhury A. Endothelial cell migration on fibronectin is regulated by syntaxin 6-mediated alpha5beta1 integrin recycling. J Biol Chem. 2011;286(42):36749-61.

240. Thelen K, Kedar V, Panicker AK, Schmid RS, Midkiff BR, Maness PF. The neural cell adhesion molecule L1 potentiates integrin-dependent cell migration to extracellular matrix proteins. J Neurosci. 2002;22(12):4918-31.

241. Wang Q, Onuma K, Liu C, Wong H, Bloom MS, Elliott EE, et al. Dysregulated integrin αVβ3 and CD47 signaling promotes joint inflammation, cartilage breakdown, and progression of osteoarthritis. JCI Insight. 2019;4(18).

242. Forsyth CB, Pulai J, Loeser RF. Fibronectin fragments and blocking antibodies to alpha2beta1 and alpha5beta1 integrins stimulate mitogen-activated protein kinase signaling and increase collagenase 3 (matrix metalloproteinase 13) production by human articular chondrocytes. Arthritis Rheum. 2002;46(9):2368-76.

243. Ostergaard K, Salter DM, Petersen J, Bendtzen K, Hvolris J, Andersen CB. Expression of alpha and beta subunits of the integrin superfamily in articular cartilage from macroscopically normal and osteoarthritic human femoral heads. Ann Rheum Dis. 1998;57(5):303-8.

244. Almonte-Becerril M, Costell M, Kouri JB. Changes in the integrins expression are related with the osteoarthritis severity in an experimental animal model in rats. J Orthop Res. 2014;32(9):1161-6.

245. Subramanian A, Schilling TF. Thrombospondin-4 controls matrix assembly during development and repair of myotendinous junctions. Elife. 2014;3.

246. Li Q, Wang C, Wang Y, Sun L, Liu Z, Wang L, et al. HSCs-derived COMP drives hepatocellular carcinoma progression by activating MEK/ERK and PI3K/AKT signaling pathways. J Exp Clin Cancer Res. 2018;37(1):231.

247. Caron MM, Janssen MP, Peeters L, Haudenschild DR, Cremers A, Surtel DA, et al. Aggrecan and COMP improve periosteal chondrogenesis by delaying chondrocyte hypertrophic maturation. Frontiers in Bioengineering and Biotechnology. 2020;8:1036.

248. Du Y, Wang Y, Wang L, Liu B, Tian Q, Liu CJ, et al. Cartilage oligomeric matrix protein inhibits vascular smooth muscle calcification by interacting with bone morphogenetic protein-2. Circ Res. 2011;108(8):917-28.

249. Gordon MK, Gerecke DR, Dublet B, van der Rest M, Olsen BR. Type XII collagen. A large multidomain molecule with partial homology to type IX collagen. J Biol Chem. 1989;264(33):19772-8.

250. Vranka J, Mokashi A, Keene DR, Tufa S, Corson G, Sussman M, et al. Selective intracellular retention of extracellular matrix proteins and chaperones associated with pseudoachondroplasia. Matrix Biol. 2001;20(7):439-50.

251. Zaucke F, Dinser R, Maurer P, Paulsson M. Cartilage oligomeric matrix protein (COMP) and collagen IX are sensitive markers for the differentiation state of articular primary chondrocytes. Biochem J. 2001;358(Pt 1):17-24.

252. Darling EM, Pritchett PE, Evans BA, Superfine R, Zauscher S, Guilak F. Mechanical properties and gene expression of chondrocytes on micropatterned substrates following dedifferentiation in monolayer. Cell Mol Bioeng. 2009;2(3):395-404.

253. Lynch JM, Maillet M, Vanhoutte D, Schloemer A, Sargent MA, Blair NS, et al. A thrombospondin-dependent pathway for a protective ER stress response. Cell. 2012;149(6):1257-68.

254. Brody MJ, Vanhoutte D, Schips TG, Boyer JG, Bakshi CV, Sargent MA, et al. Defective Flux of Thrombospondin-4 through the Secretory Pathway Impairs Cardiomyocyte Membrane Stability and Causes Cardiomyopathy. Mol Cell Biol. 2018;38(14).

255. Rosini S, Pugh N, Bonna AM, Hulmes DJS, Farndale RW, Adams JC. Thrombospondin-1 promotes matrix homeostasis by interacting with collagen and lysyl oxidase precursors and collagen cross-linking sites. Sci Signal. 2018;11(532).

256. Gebauer JM, Köhler A, Dietmar H, Gompert M, Neundorf I, Zaucke F, et al. COMP and TSP-4 interact specifically with the novel GXKGHR motif only found in fibrillar collagens. Sci Rep. 2018;8(1):17187.

257. Magdaleno F, Arriazu E, Ruiz de Galarreta M, Chen Y, Ge X, Conde de la Rosa L, et al. Cartilage oligomeric matrix protein participates in the pathogenesis of liver fibrosis. J Hepatol. 2016;65(5):963-71.

258. Yang HJ, Ma SP, Ju F, Zhang YP, Li ZC, Zhang BB, et al. Thrombospondin-4 Promotes Neuronal Differentiation of NG2 Cells via the ERK/MAPK Pathway. J Mol Neurosci. 2016;60(4):517-24.

259. Wehner D, Tsarouchas TM, Michael A, Haase C, Weidinger G, Reimer MM, et al. Wnt signaling controls pro-regenerative Collagen XII in functional spinal cord regeneration in zebrafish. Nat Commun. 2017;8(1):126.

260. Koyama E, Shibukawa Y, Nagayama M, Sugito H, Young B, Yuasa T, et al. A distinct cohort of progenitor cells participates in synovial joint and articular cartilage formation during mouse limb skeletogenesis. Dev Biol. 2008;316(1):62-73.

261. Yasuhara R, Ohta Y, Yuasa T, Kondo N, Hoang T, Addya S, et al. Roles of β-catenin signaling in phenotypic expression and proliferation of articular cartilage superficial zone cells. Lab Invest. 2011;91(12):1739-52.

262. Usami Y, Gunawardena AT, Iwamoto M, Enomoto-Iwamoto M. Wnt signaling in cartilage development and diseases: lessons from animal studies. Lab Invest. 2016;96(2):186-96.

263. Zhou Y, Wang T, Hamilton JL, Chen D. Wnt/β-catenin Signaling in Osteoarthritis and in Other Forms of Arthritis. Curr Rheumatol Rep. 2017;19(9):53.

264. Lei S, Dubeykovskiy A, Chakladar A, Wojtukiewicz L, Wang TC. The murine gastrin promoter is synergistically activated by transforming growth factor-beta/Smad and Wnt signaling pathways. J Biol Chem. 2004;279(41):42492-502.

265. Annes JP, Chen Y, Munger JS, Rifkin DB. Integrin alphaVbeta6-mediated activation of latent TGF-beta requires the latent TGF-beta binding protein-1. J Cell Biol. 2004;165(5):723-34.

266. Murphy-Ullrich JE, Poczatek M. Activation of latent TGF-beta by thrombospondin-1: mechanisms and physiology. Cytokine Growth Factor Rev. 2000;11(1-2):59-69.

267. Haywood L, Walsh DA. Vasculature of the normal and arthritic synovial joint. Histol Histopathol. 2001;16(1):277-84.

268. Kim HJ, Lee YH, Kim CK. Changes in serum cartilage oligomeric matrix protein (COMP), plasma CPK and plasma hs-CRP in relation to running distance in a marathon (42.195 km) and an ultra-marathon (200 km) race. Eur J Appl Physiol. 2009;105(5):765-70.

269. Skiöldebrand E, Ekman S, Mattsson Hultén L, Svala E, Björkman K, Lindahl A, et al. Cartilage oligomeric matrix protein neoepitope in the synovial fluid of horses with acute lameness: A new biomarker for the early stages of osteoarthritis. Equine Vet J. 2017;49(5):662-7.

270. Zeng GQ, Chen AB, Li W, Song JH, Gao CY. High MMP-1, MMP-2, and MMP-9 protein levels in osteoarthritis. Genet Mol Res. 2015;14(4):14811-22.

271. Liu CJ. The role of ADAMTS-7 and ADAMTS-12 in the pathogenesis of arthritis. Nat Clin Pract Rheumatol. 2009;5(1):38-45.

272. Ganu V, Goldberg R, Peppard J, Rediske J, Melton R, Hu SI, et al. Inhibition of interleukin-1alpha-induced cartilage oligomeric matrix protein degradation in bovine articular cartilage by matrix metalloproteinase inhibitors: potential role for matrix metalloproteinases in the generation of cartilage oligomeric matrix protein fragments in arthritic synovial fluid. Arthritis Rheum. 1998;41(12):2143-51.

273. Liu CJ, Kong W, Xu K, Luan Y, Ilalov K, Sehgal B, et al. ADAMTS-12 associates with and degrades cartilage oligomeric matrix protein. J Biol Chem. 2006;281(23):15800-8.

274. Liu CJ, Kong W, Ilalov K, Yu S, Xu K, Prazak L, et al. ADAMTS-7: a metalloproteinase that directly binds to and degrades cartilage oligomeric matrix protein. FASEB J. 2006;20(7):988-90.

275. Klatt AR, Klinger G, Paul-Klausch B, Kühn G, Renno JH, Wagener R, et al. Matrilin-3 activates the expression of osteoarthritis-associated genes in primary human chondrocytes. FEBS Lett. 2009;583(22):3611-7.

276. Ma B, Leijten JC, Wu L, Kip M, van Blitterswijk CA, Post JN, et al. Gene expression profiling of dedifferentiated human articular chondrocytes in monolayer culture. Osteoarthritis Cartilage. 2013;21(4):599-603.

277. Benya PD, Padilla SR, Nimni ME. Independent regulation of collagen types by chondrocytes during the loss of differentiated function in culture. Cell. 1978;15(4):1313-21.

278. Bonaventure J, Kadhom N, Cohen-Solal L, Ng KH, Bourguignon J, Lasselin C, et al. Reexpression of cartilage-specific genes by dedifferentiated human articular chondrocytes cultured in alginate beads. Exp Cell Res. 1994;212(1):97-104.

279. Liu H, Lee YW, Dean MF. Re-expression of differentiated proteoglycan phenotype by dedifferentiated human chondrocytes during culture in alginate beads. Biochim Biophys Acta. 1998;1425(3):505-15.

280. Mandl EW, Jahr H, Koevoet JL, van Leeuwen JP, Weinans H, Verhaar JA, et al. Fibroblast growth factor-2 in serum-free medium is a potent mitogen and reduces dedifferentiation of human ear chondrocytes in monolayer culture. Matrix Biol. 2004;23(4):231-41.

281. Mandl EW, van der Veen SW, Verhaar JA, van Osch GJ. Multiplication of human chondrocytes with low seeding densities accelerates cell yield without losing redifferentiation capacity. Tissue Eng. 2004;10(1-2):109-18.

282. Watt FM. Effect of seeding density on stability of the differentiated phenotype of pig articular chondrocytes in culture. J Cell Sci. 1988;89 (Pt 3):373-8.

283. Ellman MB, Yan D, Ahmadinia K, Chen D, An HS, Im HJ. Fibroblast growth factor control of cartilage homeostasis. J Cell Biochem. 2013;114(4):735-42.

284. Murphy CM, Haugh MG, O'Brien FJ. The effect of mean pore size on cell attachment, proliferation and migration in collagen-glycosaminoglycan scaffolds for bone tissue engineering. Biomaterials. 31. Netherlands2010. p. 461-6.

285. O'Brien FJ, Harley BA, Yannas IV, Gibson LJ. The effect of pore size on cell adhesion in collagen-GAG scaffolds. Biomaterials. 26. Netherlands2005. p. 433-41.

286. Engler AJ, Sen S, Sweeney HL, Discher DE. Matrix elasticity directs stem cell lineage specification. Cell. 126. United States2006. p. 677-89.

287. Murphy CM, Matsiko A, Haugh MG, Gleeson JP, O'Brien FJ. Mesenchymal stem cell fate is regulated by the composition and mechanical properties of collagen-glycosaminoglycan scaffolds. J Mech Behav Biomed Mater. 11. Netherlands: 2011 Elsevier Ltd; 2012. p. 53-62.

6. Supplement

6.1. COMP and TSP-4 are involved in the cell associated matrix formation

To better estimate the amount of matrix integrated collagens, proteoglycans and adaptor-proteins, the areas of positive staining was analysed with Fiji – ImageJ and statistically evaluated in **Supp.1**.

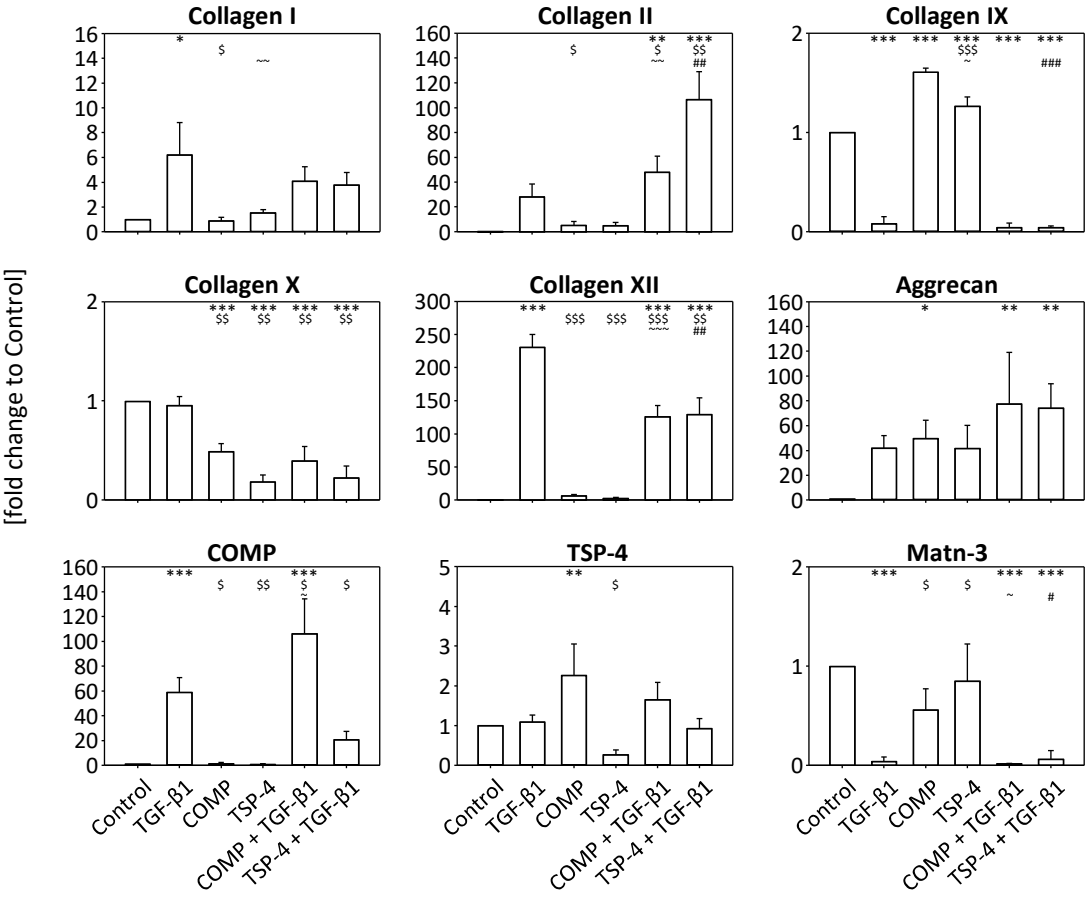

Supplement 1: The effects of COMP and TSP-4 on ECM formation
Chondrocytes were stimulated with COMP (10 µg/ml) or TSP-4 (10 µg/ml) and in combination with TGF-β1 (0.5 ng/ml) for 7 days. ECM proteins were detected by immunofluorescence staining in the cell-associated matrix at day 10. Positively stained areas were analysed and fold change to control represented. Each bar shows the mean + SD and significance ($p \leq 0.05$*, $p \leq 0.01$** and $p \leq 0.001$***) was analysed with the Friedman test and either the Tuckey or Dunnett's post-hoc test. Asterisks* indicate significance to unstimulated control, the dollar$ to TGF-β1, the wave~ to COMP and the rhombus# to TSP-4. (n = 3)

6.2. Collagen IX and Matn-3 are predominantly co-localised in a cell-associated matrix

Collagen IX and Matn-3 levels were dramatically reduced in cultures treated with TGF-β1 alone and in combination with COMP or TSP-4. To investigate if the anchorage of both proteins may partially depend on the other, immunofluorescence double staining was performed and co-localisation evaluated. Matn-3 was predominantly co-localised with collagen IX. However, collagen IX was also observable in the absence of Matn-3. (**Supp.2**)

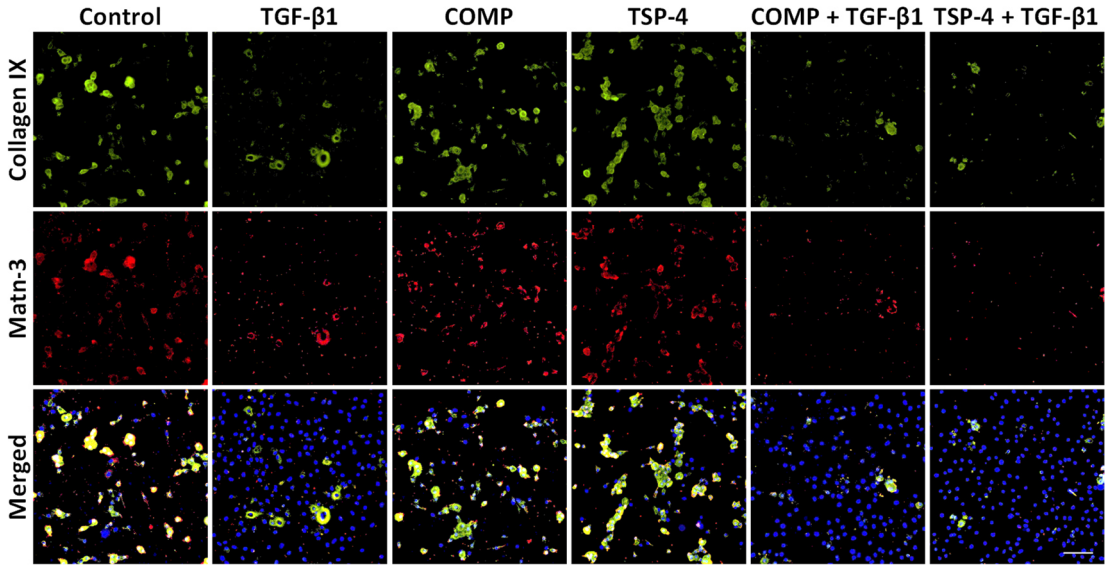

Supplement 2: Co-localisation of collagen IX and Matn-3
Chondrocytes were stimulated with COMP (10 µg/ml) or TSP-4 (10 µg/ml) for 7 days. Immunofluorescence staining of collagen IX (green), Matn-3 (red) and nuclei (blue). The merged images show co-localisation of collagen IX and Matn-3 (yellow). Unstimulated cells were used as a control. (n = 3); scale bar = 100 µm.

6.3. COMP and TSP-4 did not increase the protein amount of VEGF

A hallmark of late-stage OA is the invasion of blood vessels into the cartilage (1, 2), by so far unknown mechanisms. However, it is speculated that the increased expression of VEGF in OA (3, 4) could promote this event. On gene level, COMP and TSP-4 had no significant effect on *VEGF* expression. However, TGF-β1 increased the *VEGF* expression in chondrocytes and addition of COMP and TSP-4 could further increase this level (**Fig.3.12** and **Fig.3.13**).

To investigate if COMP and TSP-4 can contribute to cartilage vascularisation in OA by modulating VEGF protein synthesis, chondrocytes were stimulated with 10 µg/ml COMP or TSP-4 alone and in combination with 0.5 ng/ml TGF-β1 for 7 days. The amount

of intracellular VEGF was determined by immunofluorescence staining (**Supp.3**) as well as soluble VEGF by immunoblot analysis. The amount of cell associated VEGF was highest in the control and significantly reduced by stimulation with COMP ($p = 0.008$) and tendentially reduced with TSP-4 ($p = 0.052$). TGF-β1 ($p = 0.004$) alone and in combination with COMP ($p = 0.004$) or TSP-4 ($p = 0.002$) also reduced the level of VEGF compared to the control. No soluble VEGF could be detected in the supernatant (data not shown).

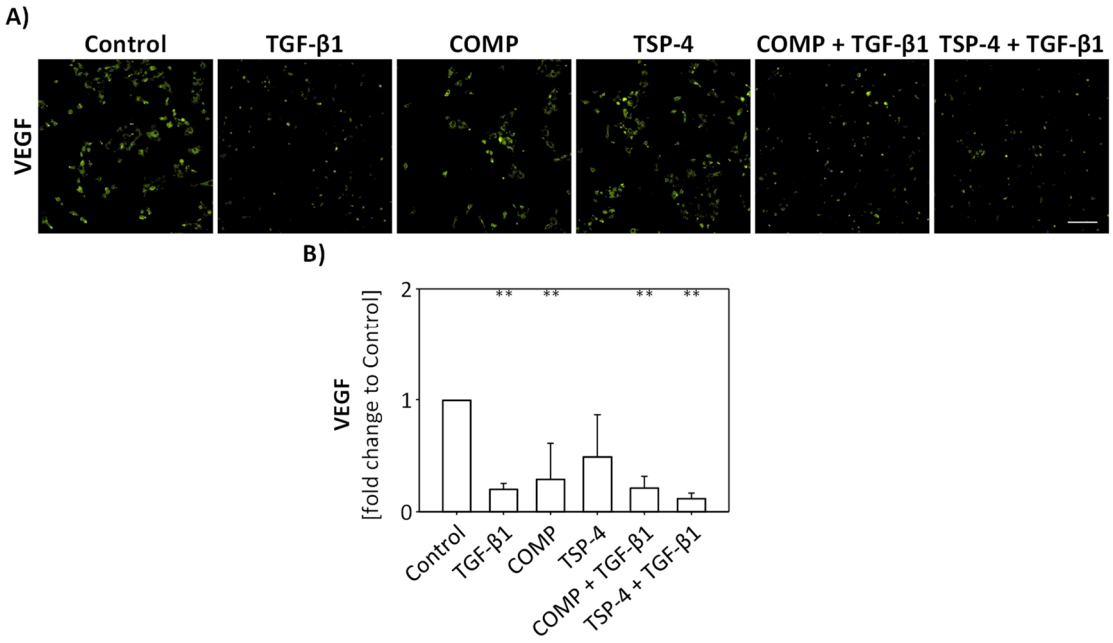

Supplement 3: COMP and TSP-4 induced collagen matrix formation and secretion
Chondrocytes were stimulated with COMP (10 µg/ml) or TSP-4 (10 µg/ml) and in combination with TGF-β1 (0.5 ng/ml) for 7 days. **A**) Immunofluorescence staining of VEGF at day 10. **B**) Statistical representation of positively stained areas. Each bar shows the mean + SD and significance ($p \leq 0.01$**) was analysed with the Friedman test and either the Tuckey or Dunnett's post-hoc test. Asterisks* indicate significance to control. Unstimulated cells were used as a control. (n = 3); scale bar = 100 µm

COMP and TSP-4 did not regulate *VEGF* gene expression but reduced its protein level, suggesting a rather anti-angiogenic potential of both proteins in articular cartilage. In OA, also the underlying bone is affected and represent the origin of blood vessels, invading the cartilage in later OA stages. To test the general effects of COMP and TSP-4 on vascularisation, their potential to modulate migration, proliferation and tube formation capacity of HUVECs were analysed. These experiments were performed in cooperation with the Erasmus MC in Holland, part of the Marie-Curie ITN CarBon.

6.4. TSP-4 but not COMP could attract HUVECs

The migratory capacity of HUVECs was investigated via the transwell system. As attractants, 10 µg/ml COMP or TSP-4 were added to the lower compartment and HUVECs in the upper compartment were allowed to migrate for 10 h.

TSP-4 ($p = 0.007$) but not COMP ($p = 0.581$) could attract HUVECs (**Supp.4.A, B**). This data shows just the opposite compared to chondrocytes.

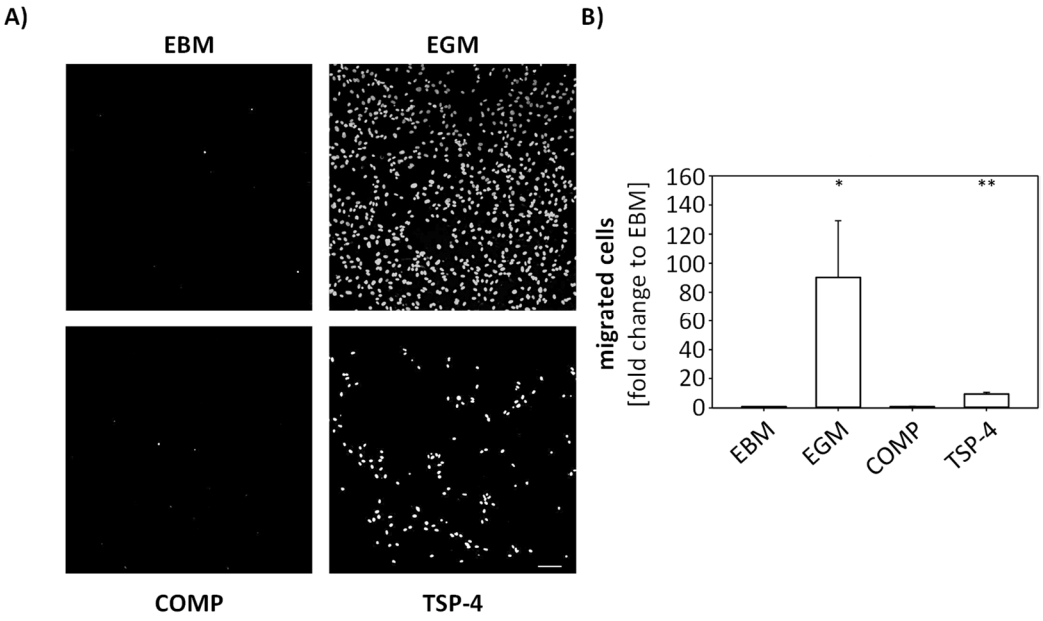

Supplement 4: The effects of COMP and TSP-4 on HUVEC migration
HUVECs were attracted with COMP (10 µg/ml) or TSP-4 (10 µg/ml) in a transwell system for 10 h. **A**) Representative images of migrated HUVECs stained with DAPI (red). **B**) Migrated cells were counted and statistically evaluated. Each bar shows the mean + SD and significance to EBM ($p < 0.05$*, $p < 0.01$**) was analysed with the Friedman test and Tuckey post-hoc test. EBM was used as a negative and EGM as a positive control. (n = 3); scale bar = 100 µm.

6.5. Neither, TSP-4 nor COMP did effect HUVEC proliferation

To investigate the contribution of COMP and TSP-4 in neovascularisation, also their potential to induce HUVEC proliferation was investigated.

Therefore, HUVECs were stimulated with 10 µg/ml COMP or TSP-4 for 24 h and the number of proliferated cells counted. None of the proteins could induce HUVEC proliferation (**Supp.5**).

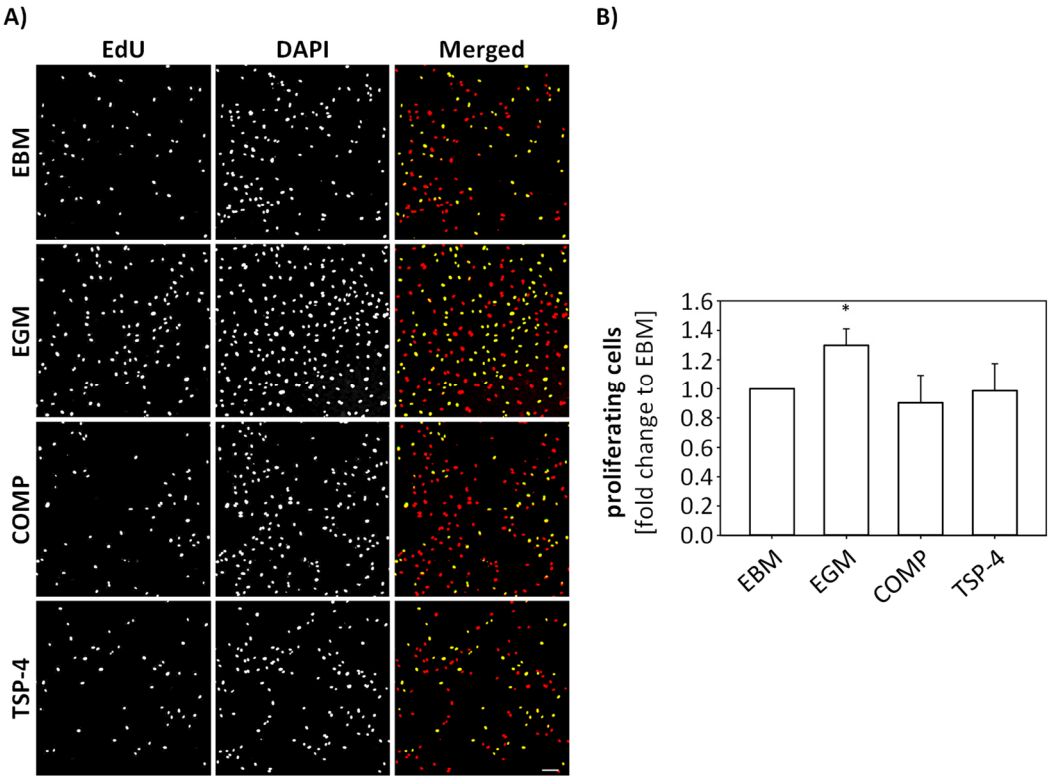

Supplement 5: The effects of COMP and TSP-4 on HUVEC proliferation
HUVECs were stimulated with 10 µg/ml COMP or TSP-4 and their proliferation rate measured after 24 h. **A**) Proliferating cells were labelled with EdU and the nuclei of all cells stained with DAPI. The merged pictures show the overlap of proliferating (yellow) and non-proliferating (red) cells. **B**) The ratio of proliferating cells was calculated and statistically evaluated. Each bar shows the mean + SD and significance to EBM ($p < 0.05$*) was analysed with the paired t-test. EBM was used as a negative and EGM as a positive control. (n = 3); scale bar = 100 µm

6.6. Neither, TSP-4 nor COMP did effect HUVEC tube formation

To test if TSP-4 or COMP can induce the tube formation of attracted cells, HUVECs were seeded onto a Geltrex™ matrix and stimulated with 10 µg/ml COMP or TSP-4 for 24 h. The tube formation was observed after 6 h and 24 h (**Supp.6.A**) as well as the length of the formed tubes (**Supp.6.B**) and the number of junctions (**Supp.6.C**) measured after 24 h. Neither COMP nor TSP-4 could modulate the tube formation of HUVECs.

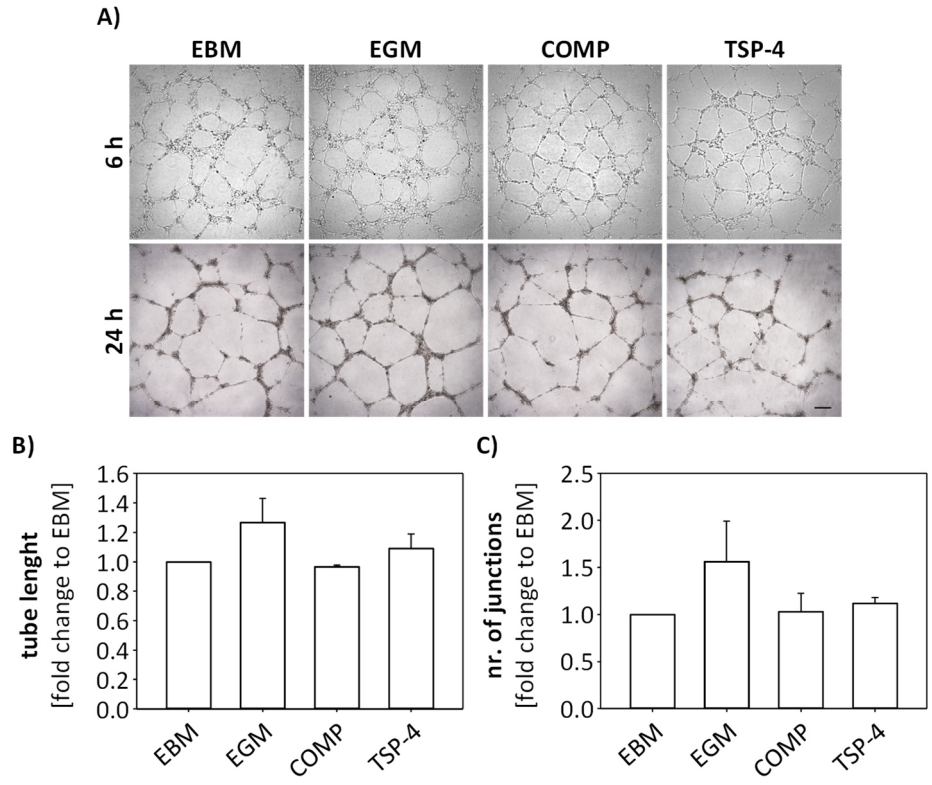

Supplement 6: The effects of COMP and TSP-4 on HUVEC tube formation
HUVECs were stimulated with 10 µg/ml COMP or TSP-4 and the tube formation measured after 6 h and 24 h. **A**) Representative pictures showing the tube formation after 6 h and 24 h. The tube length (**B**) and the number of junctions (**C**) were calculated and statistically evaluated. Each bar shows the mean + SD and significance to EBM ($p < 0.05$*) was analysed with the paired t-test. EBM was used as a negative and EGM as a positive control. (n = 3); scale bar = 100 µm

TSP-4 but not COMP has the potential to attract HUVECs. Therefore, TSP-4 might be involved in processes of vascular invasion in OA cartilage. Although, neither proliferation nor the tube formation could be modulated by TSP-4, suggesting an insignificant role in angiogenesis. Besides, COMP and TSP-4 had a negative effect of on VEGF levels, the main regulator of angiogenesis, in chondrocytes, indicating a rather protective effect of the articular cartilage from vascular invasion.

6.7. Supplementary references

1. Suri S, Gill SE, Massena de Camin S, Wilson D, McWilliams DF, Walsh DA. Neurovascular invasion at the osteochondral junction and in osteophytes in osteoarthritis. Ann Rheum Dis. 2007;66(11):1423-8.
2. Hashimoto S, Creighton-Achermann L, Takahashi K, Amiel D, Coutts RD, Lotz M. Development and regulation of osteophyte formation during experimental osteoarthritis. Osteoarthritis Cartilage. 2002;10(3):180-7.
3. Enomoto H, Inoki I, Komiya K, Shiomi T, Ikeda E, Obata K, et al. Vascular endothelial growth factor isoforms and their receptors are expressed in human osteoarthritic cartilage. Am J Pathol. 2003;162(1):171-81.
4. Pfander D, Körtje D, Zimmermann R, Weseloh G, Kirsch T, Gesslein M, et al. Vascular endothelial growth factor in articular cartilage of healthy and osteoarthritic human knee joints. Ann Rheum Dis. 2001;60(11):1070-3.

Schriftliche Erklärung

Ich erkläre ehrenwörtlich, dass ich die dem Fachbereich Medizin der Johann Wolfgang Goethe-Universität Frankfurt am Main zur Prüfung eingereichte Thesis mit dem Titel

“Functional roles of COMP and TSP-4 in articular cartilage and their relevance in osteoarthritis”

in der orthopädischen Universitätsklinik Friedrichsheim, Dr. Rolf M. Schwiete Forschungsbereich für Arthrose

unter Betreuung und Anleitung von Prof. Dr. Andrea Meurer mit Unterstützung durch Prof. Dr. Frank Zaucke ohne sonstige Hilfe selbst durchgeführt und bei der Abfassung der Arbeit keine anderen als die in der Thesis angeführten Hilfsmittel benutzt habe.

Darüber hinaus versichere ich, nicht die Hilfe einer kommerziellen Promotionsvermittlung in Anspruch genommen zu haben.

Ich habe bisher an keiner in- oder ausländischen Universität ein Gesuch um Zulassung zur Promotion oder zu einem PhD-Verfahren eingereicht. Die vorliegende Arbeit wurde bisher nicht als Thesis oder Dissertation eingereicht.

Die Grundsätze der Johann Wolfgang Goethe-Universität Frankfurt am Main zur Sicherung guter wissenschaftlicher Praxis in ihrer gültigen Form liegen mir vor und wurden bei der wissenschaftlichen Arbeit eingehalten.

Vorliegende Ergebnisse der Arbeit wurden (oder werden) in folgendem Publikationsorgan veröffentlicht:

Maly K, Schaible I, Riegger J, Brenner RE, Meurer A, Zaucke F. The Expression of Thrombospondin-4 Correlates with Disease Severity in Osteoarthritic Knee Cartilage. Int J Mol Sci. 2019;20(2).

Frankfurt, 25.11.2020
(Ort, Datum)

(Unterschrift)